THEORETICAL ANALYSIS OF THE GUARD RING
TECHNIQUE IN IMPEDANCE PNEUMOGRAPHY

by

LIONEL J. D'LUNA

B. Tech, Indian Institute of Technology, Bombay, INDIA, 1973

—————————————

A MASTER'S THESIS

submitted in partial fulfillment of the

requirements for the degree
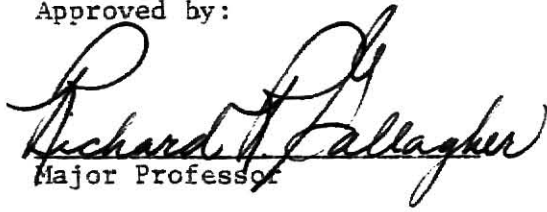
MASTER OF SCIENCE

Department of Electrical Engineering

KANSAS STATE UNIVERSITY
Manhattan, Kansas

1977

Approved by:

Major Professor

To my sisters Lorrayne, Lynette and Lubelle.

TABLE OF CONTENTS

LIST OF FIGURES

LIST OF FIGURES (Continued)

I. INTRODUCTION

Impedance pneumography is a technique used to study breathing patterns and lung function by means of impedance measurements across the thorax. During respiration the impedance across the thorax changes for a variety of reasons. Air entering and leaving the lungs changes the resistivity of the medium; expansion and contraction of the thoracic wall muscles changes the resistivity of muscle fibers, and blood circulating in the capillaries in the lungs causes variations in their resistivities. Additionally, the thorax contains complicated distributions of bone, fat and membrane. The thoracic wall is highly conductive compared with the other tissues of the thorax other than the heart.

Impedance measurements are made by placing electrodes on the surface of the thorax and measuring the impedance between them during respiration. The impedance is expressed as the ratio of the voltage applied to the current that flows between the electrodes. There are several methods used to make impedance measurements: the two-electrode technique, the four-electrode technique, and the three-electrode or guard ring technique. All these techniques are described by Cooley [1] and shown in Fig. 1.1. The two- and four-electrode techniques have disadvantages of low current penetration and large thoracic wall impedance effects [1]. In order to make significant studies of respiration, current penetration of the lung must be achieved. The guard ring technique is used to focus the current from the central impedance measuring electrode through the lung tissue so that the measurement of the impedance can be restricted to only a central core of tissue [2].

Guard Electrode
Buffer Amp.

Three-Electrode

Two-Electrode
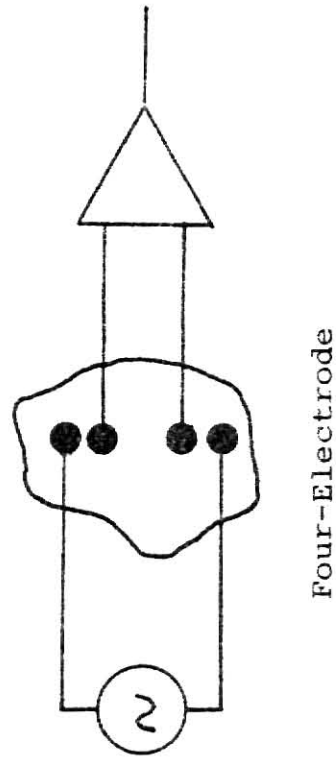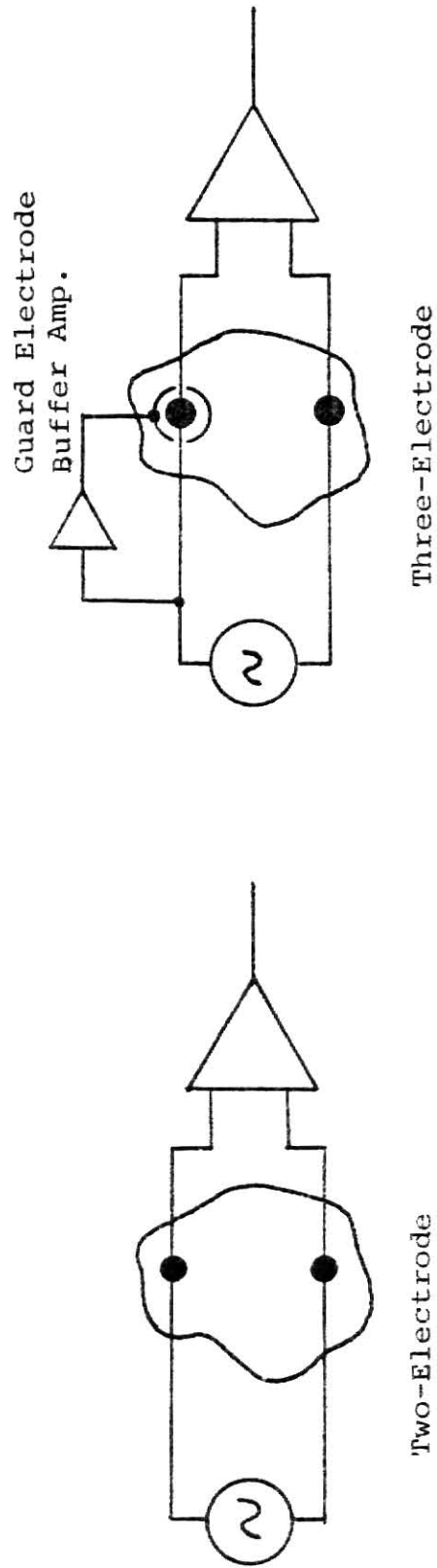
Four-Electrode

Figure 1.1. Impedance Recording Techniques.

It is the objective of this research effort to investigate the current pathways arising in guard ring electrode systems. The impedance pneumograph described by Schmalzel et al. [3] uses the guard ring technique to inject a constant current from the central electrode. The ratio of the potential developed between the central electrode and the reference electrode and the constant current is the impedance of the pathway through which the constant current flows.

This research effort uses a highly simplified modeling approach to analyze the current pathways. Initially the thorax is represented by an infinite layer of a homogeneous medium of finite thickness. The solution of the field problem is then extended to a 2-layered configuration with different conductivities representing the thoracic wall and the remaining thoracic tissue. Parameter variations pertaining to electrode dimensions and relative potentials between the central electrode and the guard ring are also investigated.

II. SINGLE-LAYER MODEL

Electrostatic Analysis: The single-layer model is shown in Fig. 2.1. The medium consists of an infinite layer of thickness d and conductivity σ. The reference electrode is an infinite ground plane. This represents a worst case condition as a finite size reference electrode will channel the current through a smaller core. This will be discussed later. The potential on the center electrode is V_e and that on the guard ring is V_g. The impedance pneumograph [3] injects a constant current through, and detects the potential on, the center electrode. However, from a field equation point of view, it is simpler to keep the potential on the center electrode constant and detect the current injected. It will be shown that the two approaches are equivalent.

The field equation to be solved is Laplace's equation

$$\nabla^2 V = 0 \qquad (2.1)$$

where V is the potential at any point in the region. Assuming cylindrical coordinates (r, θ, z) Laplace's equation can be rewritten as

$$\frac{1}{r} \frac{\partial}{\partial r} \left(r \frac{\partial V}{\partial r} \right) + \frac{1}{r^2} \frac{\partial^2 V}{\partial \theta^2} + \frac{\partial^2 V}{\partial z^2} = 0 . \qquad (2.2)$$

Due to axial symmetry about the axis of the center electrode, variations of potential with θ are nil and hence $\partial^2 V / \partial \theta^2 = 0$. Laplace's equation then reduces to

$$\frac{1}{r} \frac{\partial}{\partial r} \left(r \frac{\partial V}{\partial r} \right) + \frac{\partial^2 V}{\partial z^2} = 0 . \qquad (2.3)$$

The solution to the above equation is the potential at any point in the region under consideration, which is shown in Fig. 2.1b.

(a)
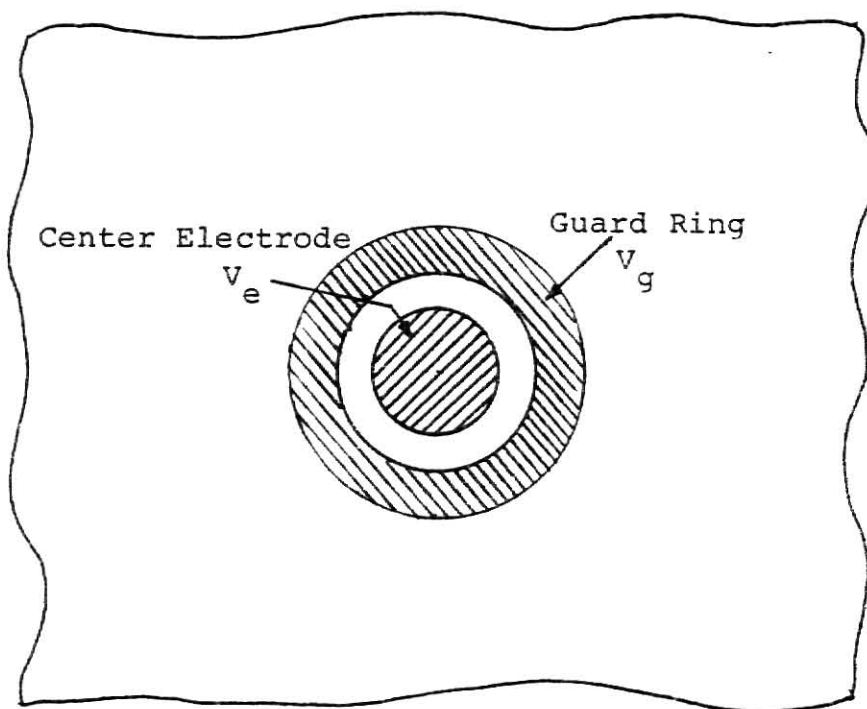
Bottom View
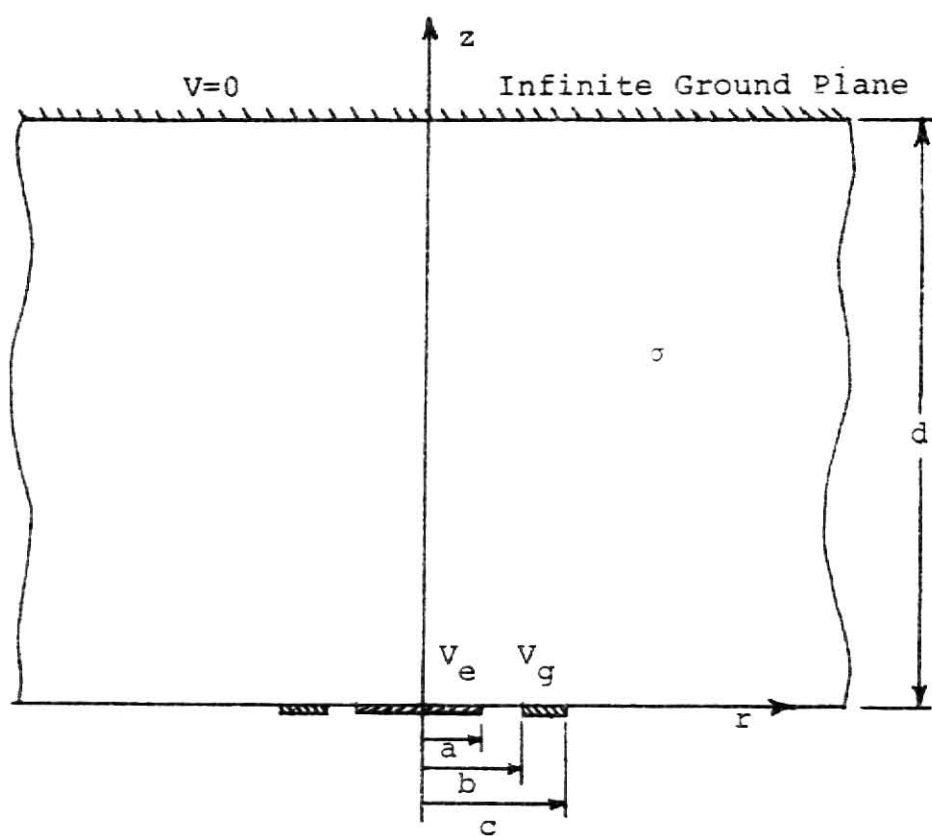
(b) Cross-Section

Figure 2.1. Single-Layer Model.

The boundary conditions which must be imposed are

$$V = 0 \qquad \text{at} \qquad z = d \qquad \text{(all } r\text{)} \tag{2.4}$$

$$V = V_e \qquad \text{at} \qquad z = 0 \qquad (0 \le r < a) \tag{2.5}$$

$$V = V_g \qquad \text{at} \qquad z = 0 \qquad (b < r < c) \tag{2.6}$$

$$\frac{\partial V}{\partial z} = 0 \qquad \text{at} \qquad z = 0 \qquad (a < r < b, \quad c < r < \infty) \; . \tag{2.7}$$

The last condition arises from the fact that current flowing normal to the boundary at z = 0 outside the electrodes is zero. The Fourier-Bessel integral representation of the solution for the potential in the medium is

$$V(r,z) = \int_0^\infty \frac{A'(u)}{u} e^{-uz} J_0(ur)du + \int_0^\infty \frac{B'(u)}{u} e^{uz} J_0(ur)du \tag{2.8}$$

where $A'(u)$ and $B'(u)$ are unknown functions to be determined from the boundary conditions and J_0 is the zero-order Bessel function of the first kind [4-6].

From Eq. (2.4), $V(r,d) = 0$. Therefore,

$$\frac{A'(u)}{u} e^{-ud} + \frac{B'(u)}{u} e^{ud} = 0$$

or

$$B'(u) = -\frac{A'(u)e^{-ud}}{e^{ud}} \; . \tag{2.9}$$

Substituting Eq. (2.9) into Eq. (2.8), yields

$$V(r,z) = \int_0^\infty \frac{A'(u)}{u} e^{-uz} J_0(ur)du + \int_0^\infty - \frac{A'(u)}{u} \frac{e^{-ud}}{e^{ud}} e^{uz} J_0(ur)du$$

$$= \int_0^\infty \frac{A'(u)}{u} [\frac{e^{ud-uz} - e^{-ud+uz}}{e^{ud}}] J_0(ur)du \; . \tag{2.10}$$

Now let

$$A'(u) = \frac{A(u)}{1 + e^{-2ud}} \; . \tag{2.11}$$

Substituting Eq. (2.11) into Eq. (2.10), it follows that

$$V(r,z) = \int_0^\infty \frac{A(u)}{u(1 + e^{-2ud})} \left[\frac{e^{ud-uz} - e^{-(ud-uz)}}{e^{ud}}\right] J_0(ur)du$$

or

$$V(r,z) = \int_0^\infty \frac{A(u)}{u} \frac{\sinh u(d-z)}{\cosh ud} J_0(ur)du \quad . \tag{2.12}$$

It is clear that Eq. (2.12) satisfies the boundary condition in Eq. (2.4), i.e., $V(r,d) = 0$.

The unknown function $A(u)$ must be determined from the remaining boundary conditions. From the condition in Eq. (2.5)

$$V(r,0) = V_e \qquad (0 \le r < a). \tag{2.13}$$

Substituting Eq. (2.13) in Eq. (2.12),

$$\int_0^\infty \frac{A(u)}{u} \tanh(ud)J_0(ur)du = V_e \qquad (0 \le r < a) \quad . \tag{2.14}$$

From the condition in Eq. (2.6),

$$V(r,0) = V_g \qquad\qquad (b < r < c) \quad . \tag{2.15}$$

Substituting Eq. (2.15) in Eq. (2.12),

$$\int_0^\infty \frac{A(u)}{u} \tanh(ud)J_0(ur)du = V_g \qquad (b < r < c) \quad . \tag{2.16}$$

Now from Eq. (2.12),

$$\frac{\partial V(r,z)}{\partial z} = \frac{\partial}{\partial z} \int_0^\infty \frac{A(u)}{u} \frac{\sinh u (d-z)}{\cosh ud} J_0(ur)du \quad .$$

Interchanging the order of differentiation and integration yields

$$\frac{\partial V(r,z)}{\partial z} = \int_0^\infty - A(u) \frac{\cosh u(d-z)}{\cosh ud} J_0(ur)du \quad . \tag{2.17}$$

From the condition in Eq. (2.7) for $a < r < b$

$$\frac{\partial V(r,0)}{\partial z} = 0 \qquad (a < r < b) \ . \qquad (2.18)$$

Substituting Eq. (2.18) into Eq. (2.17) yields

$$\int_0^\infty -A(u)J_0(ur)du = 0 \qquad (a < r < b) \ . \qquad (2.19)$$

Equation (2.18) also applies to the region $c < r < \infty$ by virtue of the condition in Eq. (2.7), so that

$$\int_0^\infty -A(u)J_0(ur)du = 0 \qquad (c < r < \infty) \ . \qquad (2.20)$$

Equations (2.14), (2.16), (2.19) and (2.20) are four integral equations that must be solved to obtain the function $A(u)$.

In order to transform the quadruple integral equations into the form described by Kiyono, et al. [8] and Cooke [9], Eqs. (2.14) and (2.16) are rewritten as

$$\int_0^\infty \frac{A(u)}{u} [1 + h(u)]J_0(ur)du = V_e \qquad (0 \le r < a) \qquad (2.21)$$

and

$$\int_0^\infty \frac{A(u)}{u} [1 + h(u)]J_0(ur)du = V_g \qquad (b < r < c) \qquad (2.22)$$

where $\qquad h(u) = \tanh(ud) - 1 \ . \qquad (2.23)$

The set of quadruple integral equations to be solved are Eqs. (2.19)-(2.22). Summarizing these:

$$\int_0^\infty \frac{A(u)}{u}[1 + h(u)]J_0(ur)du = V_e \qquad (0 \leq r < a)$$

$$\int_0^\infty A(u)J_0(ur)du = 0 \qquad (a < r < b)$$

$$\int_0^\infty \frac{A(u)}{u}[1 + h(u)]J_0(ur)du = V_g \qquad (b < r < c) \qquad (2.24)$$

$$\int_0^\infty A(u)J_0(ur)du = 0 \qquad (r > c) .$$

The solution of these quadruple integral equations is treated in Chapter III.

III. THE SOLUTION OF QUADRUPLE INTEGRAL EQUATIONS

The treatment in this chapter follows that of Kiyono and Shimasaki [8] and includes the relevant details. In this chapter the quadruple integral equations (2.24) are analytically reduced to numerically solvable forms since a closed form solution cannot be obtained. They are reduced to a pair of Fredholm integral equations.

Reproduced here for convenience, the set of Eq. (2.24) is

$$\int_0^\infty \frac{A(u)}{u} [1 + h(u)] J_0(ur) du = V_e \qquad (0 \le r < a) \qquad (3.1)$$

$$\int_0^\infty A(u) J_0(ur) du = 0 \qquad (a < r < b) \qquad (3.2)$$

$$\int_0^\infty \frac{A(u)}{u} [1 + h(u)] J_0(ur) du = V_g \qquad (b < r < c) \qquad (3.3)$$

$$\int_0^\infty A(u) J_0(ur) du = 0 \qquad (r > c) . \qquad (3.4)$$

Equations (3.1) and (3.3) correspond to potentials on the electrodes where as Eqs. (3.2) and (3.4) correspond to the derivative conditions in the regions between and beyond the electrodes.

It is convenient to define a potential function f(r) and a derivative function g(r) as follows:

$$\int_0^\infty \frac{A(u)}{u} [1 + h(u)] J_0(ur) du = f(r) \qquad (3.5)$$

$$\int_0^\infty A(u) J_0(ur) du = g(r) . \qquad (3.6)$$

f(r) and g(r) are split into four functions for the four regions as follows:

$$f(r) = f_1(r) \quad \text{and} \quad g(r) = g_1(r) \qquad (0 \leq r < a) \qquad (3.7)$$

$$f(r) = f_2(r) \quad \text{and} \quad g(r) = g_2(r) \qquad (a < r < b) \qquad (3.8)$$

$$f(r) = f_3(r) \quad \text{and} \quad g(r) = g_3(r) \qquad (b < r < c) \qquad (3.9)$$

$$f(r) = f_4(r) \quad \text{and} \quad g(r) = g_4(r) \qquad (c < r < \infty) \ . \qquad (3.10)$$

Now from Eqs. (3.1) and (3.3)

$$f_1(r) = V_e \quad \text{and} \quad f_3(r) = V_g \qquad (3.11)$$

and from Eqs. (3.2) and (3.4)

$$g_2(r) = 0 \quad \text{and} \quad g_4(r) = 0 \ . \qquad (3.12)$$

$f_2(r)$ and $f_4(r)$ are the unknown potentials in the regions $a < r < b$ and $c < r < \infty$, respectively. Similarly $g_1(r)$ and $g_3(r)$ are the unknown derivative functions in the regions $0 \leq r < a$ and $b < r < c$, respectively. Since interest is in the current distributions, and since the current density is proportional to the derivative (with respect to z) of the potential, the solution is constructed to yield $g_1(r)$ and $g_3(r)$. Equations (3.1)-(3.4) in terms of the functions f and g become

$$\int_0^\infty \frac{A(u)}{u} [1 + h(u)] J_0(ur) du = f_1(r) \qquad (0 \leq r < a) \qquad (3.13)$$

$$\int_0^\infty A(u) J_0(ur) du = 0 = g_2(r) \qquad (a < r < b) \qquad (3.14)$$

$$\int_0^\infty \frac{A(u)}{u} [1 + h(u)] J_0(ur) du = f_3(r) \qquad (b < r < c) \qquad (3.15)$$

$$\int_0^\infty A(u) J_0(ur) du = 0 = g_4(r) \qquad (c < r < \infty) \ . \qquad (3.16)$$

The technique used to reduce these quadruple integral equations is as follows: An expression is obtained for $A(u)$ in terms of the function $g(r)$ and this

expression is substituted in the equations involving f(r). The equations are then simplified to yield known forms, the solutions of which are given in Appendix A.

Applying the Hankel Inversion Theorem [7,10] to Eq. (3.6) yields

$$A(u) = u \int_0^\infty yg(y)J_0(uy)dy \ . \qquad (3.17)$$

Therefore,

$$A(u) = u \int_0^a yg_1(y)J_0(uy)dy + u \int_a^b yg_2(y)J_0(uy)dy + u \int_b^c yg_3(y)J_0(uy)dy$$

$$+ u \int_c^\infty yg_4(y)J_0(uy)dy \ . \qquad (3.18)$$

However, $g_2(y)$ and $g_4(y)$ are both zero by Eq. (3.12). Therefore,

$$A(u) = u \int_0^a yg_1(y)J_0(uy)dy + u \int_b^c yg_3(y)J_0(uy)dy \ . \qquad (3.19)$$

This expression for A(u) is used to simplify the equations involving f(r).

Expanding the left hand side of Eq. (3.5) yields

$$\int_0^\infty \frac{A(u)}{u} J_0(ur)du + \int_0^\infty \frac{A(u)}{u} h(u)J_0(ur)du = f(r) \ . \qquad (3.20)$$

Substituting for A(u) from Eq. (3.19) into the first term of Eq. (3.20)

$$\int_0^\infty \frac{A(u)}{u} J_0(ur)du = \int_0^\infty \left[\int_0^a yg_1(y)J_0(uy)dy + \int_b^c yg_3(y)J_0(uy)dy \right] J_0(ur)du \ .$$

$$(3.21)$$

Changing the order of integration on the right-hand side of Eq. (3.21), yields

$$\int_0^\infty \frac{A(u)}{u} J_0(ur)du = \int_0^a yg_1(y)dy \int_0^\infty J_0(ur)J_0(uy)du$$

$$+ \int_b^c yg_3(y)dy \int_0^\infty J_0(ur)J_0(uy)du \ . \qquad (3.22)$$

Defining $L(r,y)$ as

$$L(r,y) = \int_0^\infty J_0(ur)J_0(uy)du \qquad (3.23)$$

and noting that Noble [11] has shown that

$$L(r,y) = \frac{2}{\pi} \int_0^{\min(r,y)} \frac{ds}{(r^2-s^2)^{1/2}(y^2-s^2)^{1/2}} \quad , \qquad (3.24)$$

Eq. (3.22) becomes

$$\int_0^\infty \frac{A(u)}{u} J_0(ur)du = \int_0^a yg_1(y)L(r,y)dy + \int_b^c yg_3(y)L(r,y)dy \quad . \qquad (3.25)$$

Each of the terms on the right-hand side of Eq. (3.25) is simplified

separately. Using Eq. (3.24) in the first term on the right of Eq. (3.25)

yields

$$\int_0^a yg_1(y)L(r,y)dy = \int_0^a yg_1(y)\left[\frac{2}{\pi}\int_0^{\min(r,y)} \frac{ds}{(r^2-s^2)^{1/2}(y^2-s^2)^{1/2}}\right] dy \quad .$$

$$(3.26)$$

Note the general result

$$\int_a^b dy \int_0^{\min(r,y)} ds = \int_a^r ds \int_s^b dy + \int_0^a ds \int_a^b dy \qquad (3.27)$$

for the field of integration shown in Fig. 3.1 [7]. The first term pertains

to the shaded region above the dotted line and the second term pertains to

the shaded region below the dotted line. Applying the result (3.27) to Eq.

(3.26) where the field of integration, $0 \le r < a$, is shown in Fig. 3.2

$$\int_0^a yg_1(y)L(r,y)dy = \frac{2}{\pi} \int_0^r \frac{ds}{(r^2-s^2)^{1/2}} \int_s^a \frac{yg_1(y)dy}{(y^2-s^2)^{1/2}} \qquad (3.28)$$

since the range of y here is the shaded area $(0,a)$. Let

$$\int_s^a \frac{yg_1(y)dy}{(y^2-s^2)^{1/2}} = G_1(s) \quad . \qquad (3.29)$$
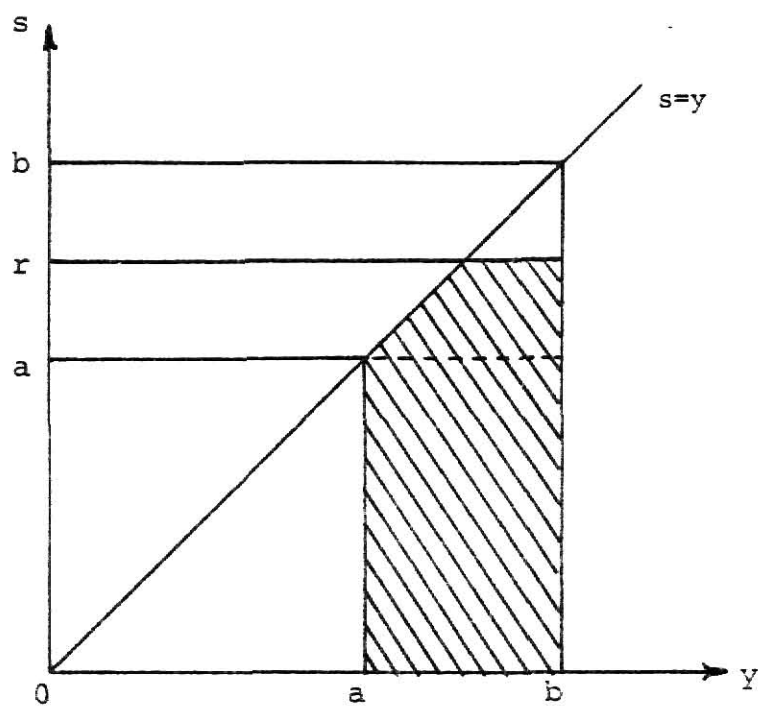
Figure 3.1. Field of Integration for Eq.(3.27).
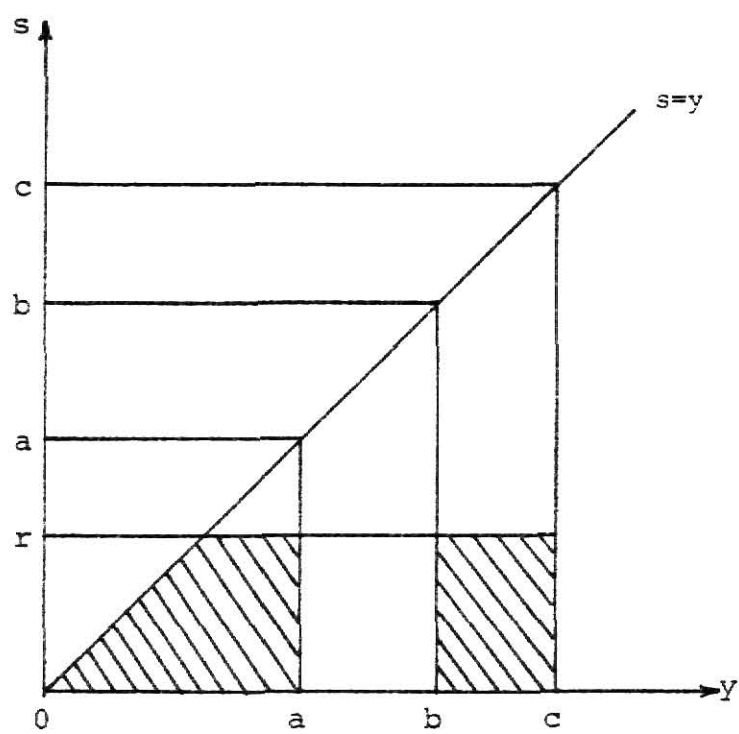
Figure 3.2. Field of Integration for the
Region 0≤r≤a.

Therefore Eq. (3.28) becomes

$$\int_0^a yg_1(y)L(r,y)dy = \frac{2}{\pi}\int_0^r \frac{G_1(s)ds}{(r^2-s^2)^{1/2}} \ . \tag{3.30}$$

Similarly, the second term on the right hand side of Eq. (3.25) becomes

$$\int_b^c yg_3(y)L(r,y)dy = \frac{2}{\pi}\int_b^c yg_3(y)dy \int_0^{\min(r,y)} \frac{ds}{(r^2-s^2)^{1/2}(y^2-s^2)^{1/2}} \ .$$

$$\tag{3.31}$$

Now the range of y is the (b,c) shaded area in Fig. 3.2. Again applying Eq. (3.27)

$$\int_b^c yg_3(y)L(r,y)dy = \frac{2}{\pi}\int_0^r \frac{ds}{(r^2-s^2)^{1/2}}\int_b^c \frac{yg_3(y)dy}{(y^2-s^2)^{1/2}} \ . \tag{3.32}$$

Let

$$\int_s^c \frac{yg_3(y)dy}{(y^2-s^2)^{1/2}} = G_3(s) \ . \tag{3.33}$$

From Appendix A the solutions to the integral equations (3.29) and (3.33) are

$$yg_1(y) = -\frac{2}{\pi}\frac{d}{dy}\int_y^a \frac{sG_1(s)ds}{(s^2-y^2)^{1/2}} \tag{3.34}$$

and

$$yg_3(y) = -\frac{2}{\pi}\frac{d}{dy}\int_y^c \frac{sG_3(s)ds}{(s^2-y^2)^{1/2}} \ . \tag{3.35}$$

Substituting Eq. (3.35) into Eq. (3.32)

$$\int_b^c yg_3(y)L(r,y)dy = \frac{2}{\pi}\int_0^r \frac{ds}{(r^2-s^2)^{1/2}}\int_b^c \frac{1}{(y^2-s^2)^{1/2}}\left[-\frac{2}{\pi}\frac{d}{dy}\int_y^c \frac{tG_3(t)dt}{(t^2-y^2)^{1/2}}\right]dy$$

$$\tag{3.36}$$

$$= (\frac{2}{\pi})^2\int_0^r \frac{ds}{(r^2-s^2)^{1/2}}\int_b^c \frac{t(b^2-s^2)^{1/2}}{(t^2-s^2)(t^2-b^2)^{1/2}}G_3(t)\ dt$$

$$\tag{3.37}$$

as shown in Appendix B.

Substituting Eq. (3.30) and Eq. (3.37) into Eq. (3.25) yields

$$\int_0^\infty \frac{A(u)}{u} J_0(ur)du = \frac{2}{\pi} \int_0^r \frac{G_1(s)ds}{(r^2-s^2)^{1/2}} + (\frac{2}{\pi})^2 \int_0^r \frac{ds}{(r^2-s^2)^{1/2}}$$

$$\cdot \int_b^c \frac{t(b^2-s^2)^{1/2}}{(t^2-s^2)(t^2-b^2)^{1/2}} G_3(t)dt \qquad (0 \leq r < a) \ . \qquad (3.38)$$

Now substituting for A(u) from Eq. (3.19), the second term of Eq. (3.20) becomes

$$\int_0^\infty \frac{A(u)}{u} h(u)J_0(ur)du = \int_0^\infty \left[\int_0^a yg_1(y)J_0(uy)dy + \int_b^c yg_3(y)J_0(uy)dy \right] h(u)J_0(ur)du$$

$$= \int_0^\infty h(u)J_0(ur)du \int_0^a yg_1(y)J_0(uy)dy + \int_0^\infty h(u)J_0(ur)du$$

$$\cdot \int_b^c yg_3(y)J_0(uy)dy \ . \qquad (3.39)$$

Define the quantity I(t,u,a) by

$$I(t,u,a) = \frac{d}{dt} \int_a^t \frac{yJ_0(yu)dy}{(t^2-y^2)^{1/2}} \ . \qquad (3.40)$$

From Appendix A the solution to this integral equation is

$$\frac{2}{\pi} \int_a^y \frac{I(t,u,a)}{(y^2-t^2)^{1/2}} dt = J_0(yu) \ . \qquad (3.41)$$

Using Eq. (3.41)

$$\int_0^a yg_1(y)J_0(uy)dy = \frac{2}{\pi} \int_0^a yg_1(y)dy \int_0^y \frac{I(t,u,0)}{(y^2-t^2)^{1/2}} dt \ .$$

The region of integration is shown in Fig. 3.3. Interchanging the order of integration and inserting appropriate limits yields

$$\int_0^a yg_1(y)J_0(uy)dy = \frac{2}{\pi} \int_0^a I(t,u,0)dt \int_t^a \frac{yg_1(y)dy}{(y^2-t^2)^{1/2}}$$
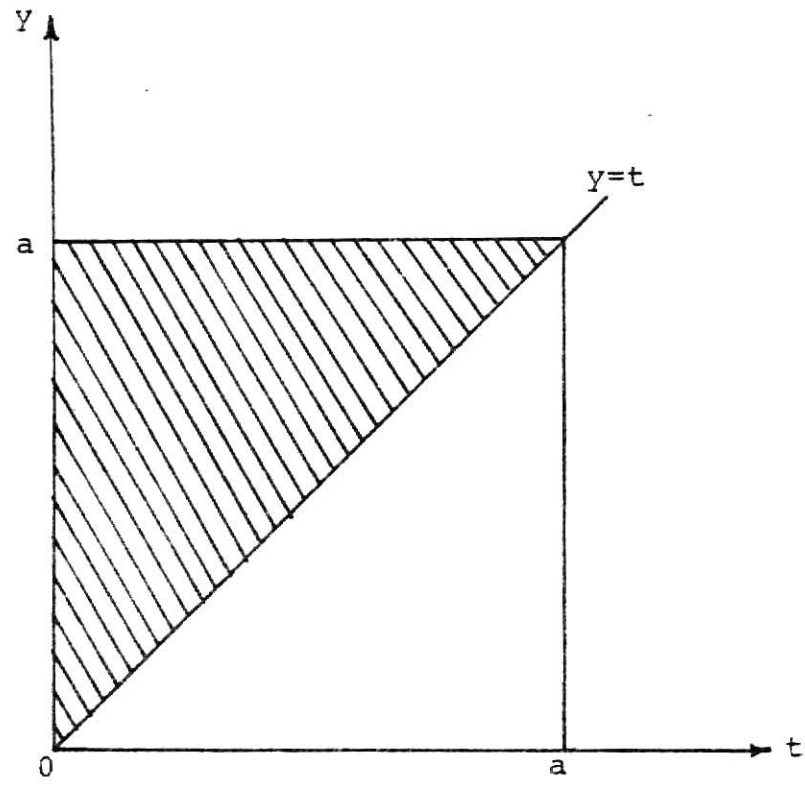
Figure 3.3. Field of Integration for Eq.(3.42).
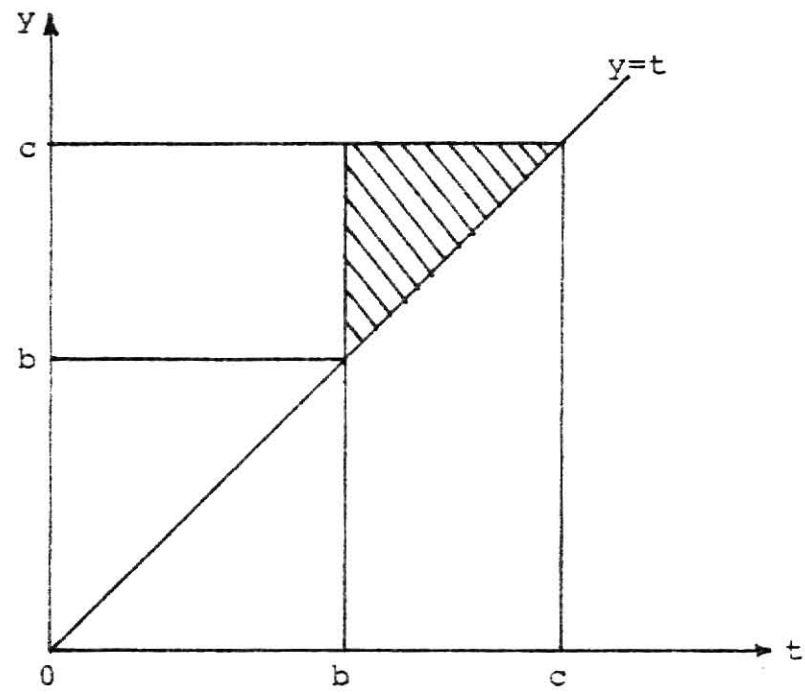
Figure 3.4 . Field of Integration for Eq.(3.43).

$$= \frac{2}{\pi} \int_0^a I(t,u,0)G_1(t)dt \qquad (3.42)$$

by Eq. (3.29). Similarly,

$$\int_b^c yg_3(y)J_0(uy)dy = \frac{2}{\pi} \int_b^c yg_3(y)dy \int_b^y \frac{I(t,u,b)}{(y^2-t^2)^{1/2}} dt . \qquad (3.43)$$

The region of integration is shown in Fig. 3.4. Again interchanging the order of integration and inserting the appropriate limits yields

$$\int_b^c yg_3(y)J_0(uy)dy = \frac{2}{\pi} \int_b^c I(t,u,b)dt \int_t^c \frac{yg_3(y)dy}{(y^2-t^2)^{1/2}}$$

$$= \frac{2}{\pi} \int_b^c I(t,u,b)G_3(t)dt . \qquad (3.44)$$

Substituting Eqs. (3.42) and (3.44), Eq. (3.39) becomes

$$\int_0^\infty \frac{A(u)}{u} h(u)J_0(ur)du = \frac{2}{\pi} \int_0^\infty h(u)J_0(ur)du \int_0^a G_1(t)I(t,u,0)dt$$

$$+ \frac{2}{\pi} \int_0^\infty h(u)J_0(ur)du \int_b^c G_3(t)I(t,u,b)dt . \qquad (3.45)$$

Equation (3.38) is developed for the region $0 \le r < a$ and Eq. (3.45) holds for all r. The left-hand sides of Eqs. (3.38) and (3.45) are the terms on the left-hand side of the first integral equation (3.13). Substituting from Eqs. (3.38) and (3.45) into Eq. (3.13) yields

$$\frac{2}{\pi} \int_0^r \frac{G_1(s)ds}{(r^2-s^2)^{1/2}} + (\frac{2}{\pi})^2 \int_0^r \frac{ds}{(r^2-s^2)^{1/2}} \int_b^c \frac{t(b^2-s^2)^{1/2}}{(t^2-s^2)(t^2-b^2)^{1/2}} G_3(t)dt = M(r)$$

$$(0 \le r < a) \qquad (3.46)$$

where

$$M(r) = f_1(r) - \frac{2}{\pi} \int_0^\infty h(u)J_0(ur)du \int_0^a G_1(t)I(t,u,0)dt$$

$$- \frac{2}{\pi} \int_0^\infty h(u)J_0(ur)du \int_b^c G_3(t)I(t,u,b)dt . \qquad (3.47)$$

Rewriting Eq. (3.46)

$$\frac{2}{\pi} \int_0^r \frac{ds}{(r^2-s^2)^{1/2}} \left\{ G_1(s) + \frac{2}{\pi} \int_b^c \frac{t(b^2-s^2)^{1/2}}{(t^2-s^2)(t^2-b^2)^{1/2}} G_3(t)dt \right\} = M(r)$$

$$(0 \leq r < a) . \qquad (3.48)$$

This is a known form of integral equation. Referring to Appendix A, Eq. (3.48) is an integral equation of the type (A.8); hence the solution is of the form (A.9). Therefore,

$$G_1(s) + \frac{2}{\pi} \int_b^c \frac{t(b^2-s^2)^{1/2}}{(t^2-s^2)(t^2-b^2)^{1/2}} G_3(t)dt = \frac{d}{ds} \int_0^s \frac{rM(r)dr}{(s^2-r^2)^{1/2}}$$

$$(0 \leq s < a) . \qquad (3.49)$$

Substituting for $M(r)$ from Eq. (3.47)

$$\frac{d}{ds} \int_0^s \frac{rM(r)dr}{(s^2-r^2)^{1/2}} = \frac{d}{ds} \int_0^s \frac{rf_1(r)dr}{(s^2-r^2)^{1/2}} - \frac{2}{\pi} \frac{d}{ds} \int_0^s \frac{rdr}{(s^2-r^2)^{1/2}} \int_0^\infty h(u)J_0(ur)du$$

$$\cdot \int_0^a G_1(t)I(t,u,0)dt - \frac{2}{\pi} \frac{d}{ds} \int_0^s \frac{rdr}{(s^2-r^2)^{1/2}} \int_0^\infty h(u)J_0(ur)du$$

$$\cdot \int_b^c G_3(t)I(t,u,b)dt .$$

Interchanging orders of integration

$$\frac{d}{ds} \int_0^s \frac{rM(r)dr}{(s^2-r^2)^{1/2}} = \frac{d}{ds} \int_0^s \frac{rf_1(r)dr}{(s^2-r^2)^{1/2}} - \int_0^a G_1(t)dt \frac{2}{\pi} \int_0^\infty h(u)I(t,u,0)du$$

$$\cdot \frac{d}{ds} \int_0^s \frac{rJ_0(ur)dr}{(s^2-r^2)^{1/2}} - \int_b^c G_3(t)dt \cdot \frac{2}{\pi} \int_0^\infty h(u)I(t,u,b)du$$

$$\cdot \frac{d}{ds} \int_0^s \frac{rJ_0(ur)dr}{(s^2-r^2)^{1/2}} .$$

Using Eq. (3.40) yields

$$\frac{d}{ds} \int_0^s \frac{rM(r)dr}{(s^2-r^2)^{1/2}} = \frac{d}{ds} \int_0^s \frac{rf_1(r)dr}{(s^2-r^2)^{1/2}} - \int_0^a G_1(t)dt \cdot \frac{2}{\pi} \int_0^\infty h(u)I(t,u,0)I(s,u,0)du$$

$$- \int_b^c G_3(t)dt \cdot \frac{2}{\pi} \int_0^\infty h(u)I(t,u,b)I(s,u,0)du . \tag{3.50}$$

Substituting Eq. (3.50) into Eq. (3.49),

$$G_1(s) + \int_0^a G_1(t)dt \cdot \frac{2}{\pi} \int_0^\infty h(u)I(s,u,0)I(t,u,0)du + \int_b^c G_3(t)dt \left[\frac{2}{\pi} \frac{t(b^2-s^2)^{1/2}}{(t^2-s^2)(t^2-b^2)^{1/2}}\right.$$

$$\left. + \frac{2}{\pi} \int_0^\infty h(u)I(t,u,b)I(s,u,0)du\right] = \frac{d}{ds} \int_0^s \frac{rf_1(r)dr}{(s^2-r^2)^{1/2}}$$

$$(0 \leq s < a) . \tag{3.51}$$

Now let

$$K_{11}(s,t) = \frac{2}{\pi} \int_0^\infty h(u)I(s,u,0)I(t,u,0)du \tag{3.52}$$

and

$$K_{13}(s,t) = \frac{2}{\pi} \frac{t(b^2-s^2)^{1/2}}{(t^2-s^2)(t^2-b^2)^{1/2}} + \frac{2}{\pi} \int_0^\infty h(u)I(s,u,0)I(t,u,b)du . \tag{3.53}$$

Therefore, Eq. (3.51) becomes

$$G_1(s) + \int_0^a K_{11}(s,t)G_1(t)dt + \int_b^c K_{13}(s,t)G_3(t)dt = \frac{d}{ds} \int_0^s \frac{rf_1(r)dr}{(s^2-r^2)^{1/2}}$$

$$(0 \leq s < a) . \tag{3.54}$$

This is the first Fredholm integral equation.

So far Eqs. (3.13), (3.14) and (3.16) have been used. The next step is to use Eq. (3.15). The simplifications (3.20)-(3.25) still hold but the region now is $b < r < c$. Beginning from Eq. (3.26)

$$\int_0^a yg_1(y)L(r,y)dy = \int_0^a yg_1(y) \left[\frac{2}{\pi} \int_0^{\min(r,y)} \frac{ds}{(r^2-s^2)^{1/2}(y^2-s^2)^{1/2}}\right]dy .$$

$$\tag{3.55}$$

Applying the result (3.27) to Eq. (3.55) where the field of integration, $b < r < c$, is shown in Fig. 3.5 yields

$$\int_0^a y g_1(y) L(r,y) dy = \frac{2}{\pi} \int_0^a \frac{ds}{(r^2-s^2)^{1/2}} \int_s^a \frac{y g_1(y) dy}{(y^2-s^2)^{1/2}} \;,$$

since the range of y here is the shaded area $(0,a)$.

Substituting from Eq. (3.29)

$$\int_0^a y g_1(y) L(r,y) dy = \frac{2}{\pi} \int_0^a \frac{G_1(s) ds}{(r^2-s^2)^{1/2}} \tag{3.56}$$

Similarly Eq. (3.31) becomes

$$\int_b^c y g_3(y) L(r,y) dy = \int_b^c y g_3(y) \left[\frac{2}{\pi} \int_0^{\min(r,y)} \frac{ds}{(r^2-s^2)^{1/2}(y^2-s^2)^{1/2}} \right] dy \;.$$

$$\tag{3.57}$$

Now the range of y is the (b,c) shaded area in Fig. 3.5. Again applying Eq. (3.27) to Eq. (3.57)

$$\int_b^c y g_3(y) L(r,y) dy = \frac{2}{\pi} \int_b^r \frac{ds}{(r^2-s^2)^{1/2}} \int_s^c \frac{y g_3(y) dy}{(y^2-s^2)^{1/2}}$$

$$+ \frac{2}{\pi} \int_0^b \frac{ds}{(r^2-s^2)^{1/2}} \int_b^c \frac{y g_3(y) dy}{(y^2-s^2)^{1/2}} \;.$$

Using Eq. (3.33)

$$\int_b^c y g_3(y) L(r,y) dy = \frac{2}{\pi} \int_b^r \frac{G_3(s) ds}{(r^2-s^2)^{1/2}} + \frac{2}{\pi} \int_0^b \frac{ds}{(r^2-s^2)^{1/2}}$$

$$\cdot \int_b^c \frac{y g_3(y) dy}{(y^2-s^2)^{1/2}} \;. \tag{3.58}$$

Substituting Eqs. (3.56) and (3.58) into Eq. (3.25) yields
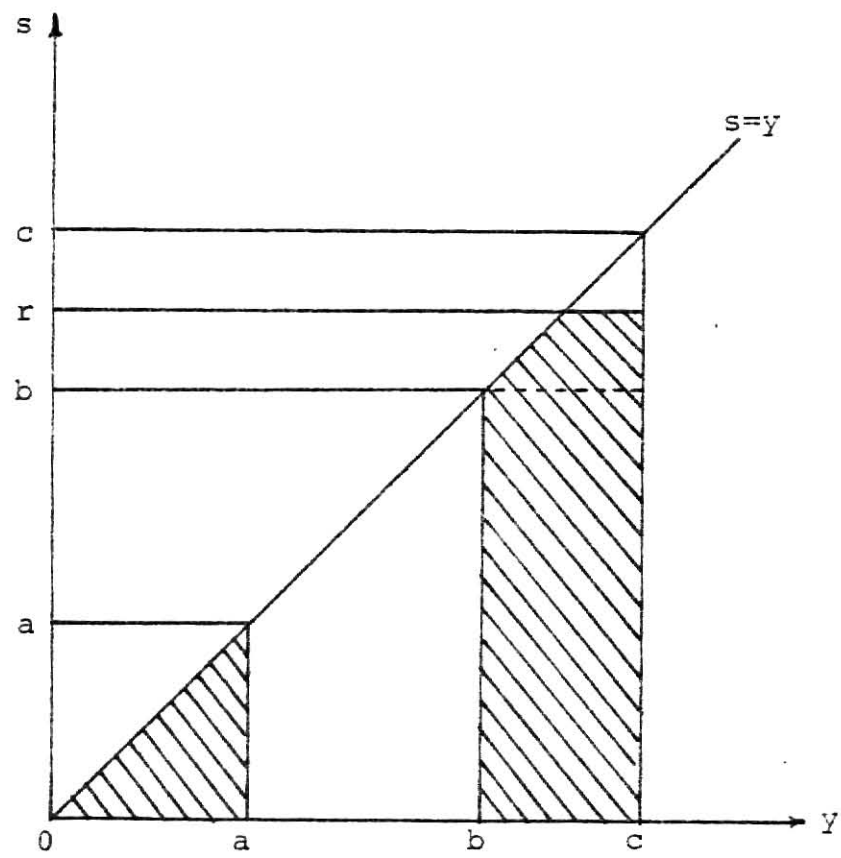
Figure 3.5.Field of Integration for the
Region b<r<c .

$$\int_0^\infty \frac{A(u)}{u} J_0(ur)du = \frac{2}{\pi} \int_0^a \frac{G_1(s)ds}{(r^2-s^2)^{1/2}} + \frac{2}{\pi} \int_b^r \frac{G_3(s)ds}{(r^2-s^2)^{1/2}}$$

$$+ \frac{2}{\pi} \int_0^b \frac{ds}{(r^2-s^2)^{1/2}} \int_b^c \frac{yg_3(y)dy}{(y^2-s^2)^{1/2}} \quad (b < r < c). \quad (3.59)$$

The left-hand sides of Eqs. (3.59) and (3.45) are the terms on the left-hand side of the integral equation (3.15). Substituting Eqs. (3.59) and (3.45) into Eq. (3.15) yields

$$\frac{2}{\pi} \int_0^a \frac{G_1(s)ds}{(r^2-s^2)^{1/2}} + \frac{2}{\pi} \int_b^r \frac{G_3(s)ds}{(r^2-s^2)^{1/2}} + \frac{2}{\pi} \int_0^b \frac{ds}{(r^2-s^2)^{1/2}} \int_b^c \frac{yg_3(y)dy}{(y^2-s^2)^{1/2}}$$

$$+ \frac{2}{\pi} \int_0^\infty h(u)J_0(ur)du \int_0^a G_1(t)I(t,u,0)dt + \frac{2}{\pi} \int_0^\infty h(u)J_0(ur)du$$

$$\cdot \int_b^c G_3(t)I(t,u,b)dt = f_3(r) \quad\quad (b < r < c) . \quad (3.60)$$

Rearranging to obtain a known form of integral equation

$$\frac{2}{\pi} \int_b^r \frac{G_3(s)ds}{(r^2-s^2)^{1/2}} = N(r) \quad\quad (b < r < c) \quad (3.61)$$

where with a change of variable to avoid confusion

$$N(r) = f_3(r) - \frac{2}{\pi} \int_0^a \frac{G_1(t)dt}{(r^2-t^2)^{1/2}} - \frac{2}{\pi} \int_0^b \frac{dt}{(r^2-t^2)^{1/2}} \int_b^c \frac{yg_3(y)dy}{(y^2-t^2)^{1/2}}$$

$$- \frac{2}{\pi} \int_0^a G_1(t)dt \int_0^\infty h(u)I(t,u,0)J_0(ur)du$$

$$- \frac{2}{\pi} \int_b^c G_3(t)dt \int_0^\infty h(u)I(t,u,b)J_0(ur)du . \quad (3.62)$$

Referring to Appendix A, Eq. (3.61) is an integral equation of the type (A.8), hence the solution is of the form (A.9). Therefore,

$$G_3(s) = \frac{d}{ds} \int_b^s \frac{rN(r)dr}{(s^2-r^2)^{1/2}} \quad\quad (b < s < c) . \quad (3.63)$$

Substituting for $N(r)$ from Eq. (3.62)

$$\frac{d}{ds}\int_b^s \frac{rN(r)dr}{(s^2-r^2)^{1/2}} = \frac{d}{ds}\int_b^s \frac{rf_3(r)dr}{(s^2-r^2)^{1/2}} - \frac{2}{\pi}\frac{d}{ds}\int_b^s \frac{rdr}{(s^2-r^2)^{1/2}}\int_0^a \frac{G_1(t)dt}{(r^2-t^2)^{1/2}}$$

$$- \frac{2}{\pi}\frac{d}{ds}\int_b^s \frac{rdr}{(s^2-r^2)^{1/2}}\int_0^b \frac{dt}{(r^2-t^2)^{1/2}}\int_b^c \frac{yg_3(y)dy}{(y^2-t^2)^{1/2}}$$

$$- \frac{2}{\pi}\frac{d}{ds}\int_b^s \frac{rdr}{(s^2-r^2)^{1/2}}\int_0^a G_1(t)dt\int_0^\infty h(u)I(t,u,0)J_0(ur)du$$

$$- \frac{2}{\pi}\frac{d}{ds}\int_b^s \frac{rdr}{(s^2-r^2)^{1/2}}\int_b^c G_3(t)dt\int_0^\infty h(u)I(t,u,b)J_0(ur)du \ . \quad (3.64)$$

Simplifying term by term, the second term on the right-hand side of Eq.

(3.64) is

$$- \frac{2}{\pi}\frac{d}{ds}\int_b^s \frac{rdr}{(s^2-r^2)^{1/2}}\int_0^a \frac{G_1(t)dt}{(r^2-t^2)^{1/2}} = - \frac{2}{\pi}\int_0^a G_1(t)dt \cdot \frac{d}{ds}\int_b^s \frac{rdr}{(s^2-r^2)^{1/2}(r^2-t^2)^{1/2}}$$

$$= - \frac{2}{\pi}\int_0^a \frac{G_1(t)s(b^2-t^2)^{1/2}}{(s^2-t^2)(s^2-b^2)^{1/2}}\ dt \quad (3.65)$$

as shown in Appendix B. The third term on the right-hand side of Eq. (3.64)

is

$$- \frac{2}{\pi}\frac{d}{ds}\int_b^s \frac{rdr}{(s^2-r^2)^{1/2}}\int_0^b \frac{dt}{(r^2-t^2)^{1/2}}\int_b^c \frac{yg_3(y)dy}{(y^2-t^2)^{1/2}}$$

$$= - (\frac{2}{\pi})^2\int_b^c G_3(t)dt\ \frac{ts}{(t^2-b^2)^{1/2}(s^2-b^2)^{1/2}}\int_0^b \frac{(b^2-x^2)}{(t^2-x^2)(s^2-x^2)}\ dx$$

$$(3.66)$$

as shown in Appendix B. The fourth term on the right-hand side of Eq.

(3.64) is

$$- \frac{2}{\pi} \frac{d}{ds} \int_b^s \frac{rdr}{(s^2-r^2)^{1/2}} \int_0^a G_1(t)dt \int_0^\infty h(u)I(t,u,0)J_0(ur)du \ .$$

$$= - \frac{2}{\pi} \int_0^a G_1(t)dt \int_0^\infty h(u)I(t,u,0)du \cdot \frac{d}{ds} \int_b^s \frac{rJ_0(ur)dr}{(s^2-r^2)^{1/2}}$$

$$= - \frac{2}{\pi} \int_0^a G_1(t)dt \int_0^\infty h(u)I(t,u,0)I(s,u,b)du \qquad (3.67)$$

by Eq. (3.40). Similarly rearranging and again using Eq. (3.40), the fifth term on the right-hand side of Eq. (3.64) is

$$- \frac{2}{\pi} \frac{d}{ds} \int_b^s \frac{rdr}{(s^2-r^2)^{1/2}} \int_b^c G_3(t)dt \int_0^\infty h(u)I(t,u,b)J_0(ur)du$$

$$= - \frac{2}{\pi} \int_b^c G_3(t)dt \int_0^\infty h(u)I(t,u,b)I(s,u,b)du \ . \qquad (3.68)$$

Substituting Eqs. (3.65)-(3.68) into Eq. (3.64), Eq. (3.63) becomes

$$G_3(s) = \frac{d}{ds} \int_b^s \frac{rf_3(r)dr}{(s^2-r^2)^{1/2}} - \int_0^a G_1(t) \left\{ \frac{2}{\pi} \frac{s(b^2-t^2)^{1/2}}{(s^2-t^2)(s^2-b^2)^{1/2}} \right\} dt$$

$$- \int_b^c G_3(t) \left\{ \left(\frac{2}{\pi}\right)^2 \frac{ts}{(t^2-b^2)^{1/2}(s^2-b^2)^{1/2}} \int_0^b \frac{b^2-x^2}{(t^2-x^2)(s^2-x^2)} dx \right\} dt$$

$$- \int_0^a G_1(t) \left\{ \frac{2}{\pi} \int_0^\infty h(u)I(t,u,0)I(s,u,b)du \right\} dt$$

$$- \int_b^c G_3(t) \left\{ \frac{2}{\pi} \int_0^\infty h(u)I(t,u,b)I(s,u,b)du \right\} dt \qquad (b < s < c) \ .$$

$$(3.69)$$

Rearranging,

$$G_3(s) + \int_0^a G_1(t)dt \left[\frac{2}{\pi} \frac{s(b^2-t^2)^{1/2}}{(s^2-t^2)(s^2-b^2)^{1/2}} + \frac{2}{\pi} \int_0^\infty h(u)I(t,u,0)I(s,u,b)du \right]$$

$$+ \int_b^c G_3(t)dt \left[(\frac{2}{\pi})^2 \frac{ts}{(t^2-b^2)^{1/2}(s^2-b^2)^{1/2}} \int_0^b \frac{b^2-x^2}{(t^2-x^2)(s^2-x^2)} dx \right.$$

$$\left. + \frac{2}{\pi} \int_0^\infty h(u)I(t,u,b)I(s,u,b)du \right] = \frac{d}{ds} \int_b^s \frac{rf_3(r)dr}{(s^2-r^2)^{1/2}}$$

$$(b < s < c) \ . \qquad (3.70)$$

Let

$$K_{31}(s,t) = \frac{2}{\pi} \frac{s(b^2-t^2)^{1/2}}{(s^2-t^2)(s^2-b^2)^{1/2}} + \frac{2}{\pi} \int_0^\infty h(u)I(t,u,0)I(s,u,b)du \qquad (3.71)$$

and

$$K_{33}(s,t) = (\frac{2}{\pi})^2 \frac{ts}{(t^2-b^2)^{1/2}(s^2-b^2)^{1/2}} \int_0^b \frac{b^2-x^2}{(t^2-x^2)(s^2-x^2)} dx$$

$$+ \frac{2}{\pi} \int_0^\infty h(u)I(t,u,b)I(s,u,b)du \ . \qquad (3.72)$$

Substituting Eqs. (3.71) and (3.72) into Eq. (3.70) yields

$$G_3(s) + \int_0^a K_{31}(s,t)G_1(t)dt + \int_b^c K_{33}(s,t)G_3(t)dt = \frac{d}{ds} \int_b^s \frac{rf_3(r)dr}{(s^2-r^2)^{1/2}}$$

$$(b < s < c) \ . \qquad (3.73)$$

This is the second Fredholm integral equation. Thus the quadruple integral equations (3.13)-(3.16) have been reduced to a pair of Fredholm integral equations (3.54) and (3.73). These Fredholm integral equations cannot be analytically solved for the functions $G_1(s)$ and $G_3(s)$; hence they will be resolved using numerical methods discussed in Chapter IV.

IV. NUMERICAL METHODS

To recapitulate, the pair of Fredholm Integral equations that must be solved are

$$G_1(s) + \int_0^a K_{11}(s,t)G_1(t)dt + \int_b^c K_{13}(s,t)G_3(t)dt = \frac{d}{ds} \int_0^s \frac{rf_1(r)dr}{(s^2-r^2)^{1/2}}$$

$$(0 \leq s < a) \qquad (4.1)$$

and

$$G_3(s) + \int_0^a K_{31}(s,t)G_1(t)dt + \int_b^c K_{33}(s,t)G_3(t)dt = \frac{d}{ds} \int_b^s \frac{rf_3(r)dr}{(s^2-r^2)^{1/2}}$$

$$(b < s < c) \qquad (4.2)$$

where the kernels are:

$$K_{11}(s,t) = \frac{2}{\pi} \int_0^\infty h(u)I(s,u,0)I(t,u,0)du \ , \qquad (4.3)$$

$$K_{13}(s,t) = \frac{2}{\pi} \frac{t(b^2-s^2)^{1/2}}{(t^2-s^2)(t^2-b^2)^{1/2}} + \frac{2}{\pi} \int_0^\infty h(u)I(s,u,0)I(t,u,b)du \ , \qquad (4.4)$$

$$K_{31}(s,t) = \frac{2}{\pi} \frac{s(b^2-t^2)^{1/2}}{(s^2-t^2)(s^2-b^2)^{1/2}} + \frac{2}{\pi} \int_0^\infty h(u)I(t,u,0)I(s,u,b)du \ , \qquad (4.5)$$

$$K_{33}(s,t) = \left(\frac{2}{\pi}\right)^2 \frac{ts}{(t^2-b^2)^{1/2}(s^2-b^2)^{1/2}} \int_0^b \frac{b^2-x^2}{(t^2-x^2)(s^2-x^2)} dx$$

$$+ \frac{2}{\pi} \int_0^\infty h(u)I(t,u,b)I(s,u,b)du \ . \qquad (4.6)$$

The kernels are now further simplified. By Eq. (3.40)

$$I(t,u,b) = \frac{d}{dt} \int_b^t \frac{yJ_0(yu)dy}{(t^2-y^2)^{1/2}} \ . \qquad (4.7)$$

Therefore,

$$I(t,u,0) = \frac{d}{dt} \int_0^t \frac{yJ_0(yu)dy}{(t^2-y^2)^{1/2}} \ . \qquad (4.8)$$

By Watson [14]

$$I(t,u,0) = \frac{d}{dt} \left[\sqrt{\frac{\pi t}{2u}} \, J_{1/2}(ut) \right] . \qquad (4.9)$$

Now

$$J_{1/2}(ut) = \sqrt{\frac{2}{\pi ut}} \, \sin(ut) . \qquad (4.10)$$

Substituting Eq. (4.10) into Eq. (4.9)

$$\begin{aligned} I(t,u,0) &= \frac{d}{dt} \left[\sqrt{\frac{\pi t}{2u}} \, \sqrt{\frac{2}{\pi ut}} \, \sin(ut) \right] \\ &= \frac{d}{dt} \frac{\sin(ut)}{u} \\ &= \cos(ut) . \end{aligned} \qquad (4.11)$$

Using Eq. (4.11) in Eq. (4.3) yields

$$K_{11}(s,t) = \frac{2}{\pi} \int_0^\infty h(u)\cos(su)\cos(tu)\,du . \qquad (4.12)$$

Similarly Eq. (4.4) becomes

$$K_{13}(s,t) = \frac{2}{\pi} \frac{t(b^2-s^2)^{1/2}}{(t^2-s^2)(t^2-b^2)^{1/2}} + \frac{2}{\pi} \int_0^\infty h(u)I(t,u,b)\cos(su)\,du \qquad (4.13)$$

and Eq. (4.5) becomes

$$K_{31}(s,t) = \frac{2}{\pi} \frac{s(b^2-t^2)^{1/2}}{(s^2-t^2)(s^2-b^2)^{1/2}} + \frac{2}{\pi} \int_0^\infty h(u)I(s,u,b)\cos(tu)\,du . \qquad (4.14)$$

The first term on the right hand side of Eq. (4.6) can be simplified as follows:

$$(\frac{2}{\pi})^2 \frac{ts}{(t^2-b^2)^{1/2}(s^2-b^2)^{1/2}} \int_0^b \frac{b^2-x^2}{(t^2-x^2)(s^2-x^2)}\,dx$$

$$= (\frac{2}{\pi})^2 \frac{ts}{(t^2-b^2)^{1/2}(s^2-b^2)^{1/2}} \left[\frac{s^2-b^2}{s^2-t^2} \int_0^b \frac{dx}{s^2-x^2} - \frac{t^2-b^2}{s^2-t^2} \int_0^b \frac{dx}{t^2-x^2} \right] .$$

From standard tables

$$(\frac{2}{\pi})^2 \frac{ts}{(t^2-b^2)^{1/2}(s^2-b^2)^{1/2}} \int_0^b \frac{b^2-x^2}{(t^2-x^2)(s^2-x^2)} dx$$

$$= (\frac{2}{\pi})^2 \frac{ts}{(t^2-b^2)^{1/2}(s^2-b^2)^{1/2}} \left[\frac{s^2-b^2}{s^2-t^2} \left(\frac{1}{2s} \log \frac{s+x}{s-x} \Big|_0^b \right) \right.$$

$$\left. - \frac{t^2-b^2}{s^2-t^2} \left(\frac{1}{2t} \log \frac{t+x}{t-x} \Big|_0^b \right) \right]$$

$$= \frac{2}{\pi^2} \frac{1}{(s^2-t^2)} \left\{ t \sqrt{\frac{s^2-b^2}{t^2-b^2}} \log \frac{s+b}{s-b} - s \sqrt{\frac{t^2-b^2}{s^2-b^2}} \log \frac{t+b}{t-b} \right\} . \qquad (4.15)$$

Using Eq. (4.15), Eq. (4.6) becomes

$$K_{33}(s,t) = \frac{2}{\pi^2} \frac{1}{s^2-t^2} \left\{ t \sqrt{\frac{s^2-b^2}{t^2-b^2}} \log \frac{s+b}{s-b} - s \sqrt{\frac{t^2-b^2}{s^2-b^2}} \log \frac{t+b}{t-b} \right\}$$

$$+ \frac{2}{\pi} \int_0^\infty h(u) I(t,u,b) I(s,u,b) du . \qquad (4.16)$$

The integral equations (4.1) and (4.2) may be reduced to a set of simultaneous linear equations by using the Legendre-Gauss quadrature formulae. The following discussion relates to the quadrature formulae [15,16].

Integrals of the form $\int_a^b f(x)dx$ can be approximated by the formula

$$\int_a^b f(x)dx \simeq \sum_{i=1}^n A_i f(x_i) \qquad (4.17)$$

where the x_i's are the points or nodes and A_i's are the weights or coefficients of the formula. If $f(x)$ is a polynomial then n points and coefficients can be found to make Eq. (4.17) exact for all polynomials of degree $\leq 2n-1$. These points and coefficients are tabulated for the interval $-1 \leq x \leq +1$. They are computed using Legendre polynomials [16].

Nodes and coefficients on the intervals (a,b) can be calculated from the tabulated values on the interval (-1,+1) by suitable transformations.

$$\int_a^b f(t)dt \approx \sum_{i=1}^{n} A_i f(t_i) \ . \tag{4.18}$$

The integral $\int_a^b f(t)dt$ must be converted to the form $\int_{-1}^{1} f(x)dx$.

Let

$$t = px + q \tag{4.19}$$

Substituting at the upper limit t=b and x=1, and at the lower limit t=a and x=-1, yields

$$b = p + q$$

$$a = -p + q \ .$$

$$\therefore \quad p = \frac{b-a}{2} \quad \text{and} \quad q = \frac{b+a}{2} \ .$$

Equation (4.19) then becomes

$$t = \frac{(b+a) + (b-a)x}{2} \tag{4.20}$$

and

$$dt = \frac{b-a}{2} \cdot dx \ .$$

Therefore,

$$\int_a^b f(t)dt = \int_{-1}^{1} f[\frac{(b+a) + (b-a)x}{2}] \cdot \frac{b-a}{2} \ dx$$

$$= \int_{-1}^{1} g(x) \cdot \frac{b-a}{2} \cdot dx \tag{4.21}$$

where $\quad g(x) \equiv f(t)$.

By Eq. (4.17)

$$\int_{-1}^{1} g(x) \ dx \approx \sum_{i=1}^{n} A_i^* g(x_i)$$

where A_i^*'s are the coefficients from the tables for the interval (-1,+1) and the x_i's are the nodes for the same interval.

Therefore,

$$\int_{-1}^{1} g(x) \cdot (\frac{b-a}{2})dx \simeq \sum_{i=1}^{n} (\frac{b-a}{2})A_i^* \, g(x_i) \, . \tag{4.22}$$

Substituting Eqs. (4.18) and (4.22) into Eq. (4.21) yields

$$\sum_{i=1}^{n} A_i f(t_i) = \sum_{i=1}^{n} (\frac{b-a}{2})A_i^* g(x_i) = \sum_{i=1}^{n} (\frac{b-a}{2})A_i^* f(t_i)$$

Therefore the transformed weights A_i and nodes t_i are

$$A_i = (\frac{b-a}{2})A_i^* \quad \text{and} \quad t_i = \frac{(b+a) + (b-a)x_i}{2} \, . \tag{4.23}$$

The nodes of the Legendre-Gauss formula are symmetric about $x=0$ and the coefficients are all positive and have the same values on the $(-1,0)$ and $(0,+1)$ segments.

Integrals on the interval $(0,\infty)$ are approximated by the Laguerre-Gauss quadrature formula

$$\int_{0}^{\infty} e^{-x} f(x)dx \simeq \sum_{i=1}^{n} A_i f(x_i) \, . \tag{4.24}$$

The integrand must have an exponentially decaying envelope. If $f(x)$ is a slowly varying function then the Laguerre-Gauss formula is quite effective and 15 $\sim$ 20 points are sufficient. The nodes x_i and weights A_i of Eq. (4.24) are available from tables [16].

In order to diminish rounding errors, a suitable transformation has been suggested by Cooke [13].

For
$$b < s < c \, ,$$

let
$$s = b\sec\theta \, , \quad ds = b\sec^2\theta \, \sin\theta d\theta \quad \text{and} \quad 0 \le \theta \le \sec^{-1}(c/b) \tag{4.25}$$

$$H(\theta) = G_3(b\sec\theta)\sec^2\theta \tag{4.26}$$
and

$$F(\theta,u) = \sin\theta \, I(b\sec\theta,u,b) \, . \tag{4.27}$$

Now from Eq. (3.11), $f_1(r)$ and $f_3(r)$ on the right-hand sides of Eqs. (4.1) and (4.2) are equal to V_e and V_g respectively. Taking the right-hand side of Eq. (4.1)

$$\frac{d}{ds} \int_0^s \frac{rf_1(r)}{(s^2-r^2)^{1/2}}\, dr = \frac{d}{ds} \int_0^s \frac{rV_e}{(s^2-r^2)^{1/2}}\, dr$$

$$= V_e \frac{d}{ds} \left[-(s^2-r^2)^{1/2} \Big|_0^s \right]$$

$$= V_e \frac{d}{ds}\, (s)$$

$$= V_e\, . \tag{4.28}$$

Similarly the right-hand side of Eq. (4.2) becomes

$$\frac{d}{ds} \int_b^s \frac{rf_3(r)dr}{(s^2-r^2)^{1/2}} = \frac{d}{ds} \int_b^s \frac{rV_g}{(s^2-r^2)^{1/2}}\, dr$$

$$= V_g \frac{d}{ds} \left[-(s^2-r^2)^{1/2} \Big|_b^s \right]$$

$$= V_g \frac{d}{ds} \left[(s^2-b^2)^{1/2} \right]$$

$$= V_g \frac{s}{(s^2-b^2)^{1/2}}\, . \tag{4.29}$$

The Freholm integral equations and the kernels are now transformed according to Eqs. (4.25)-(4.27). Using the transformation (4.25) and Eq. (4.28) in Eq. (4.1) yields

$$G_1(s) + \int_0^a K_{11}(s,t)G_1(t)dt + \int_0^{\sec^{-1}(c/b)} K_{13}(s,b\sec\phi)G_3(b\sec\phi)b\sec^2\phi\sin\phi d\phi = V_e$$

$$(0 \le s < a)\, . \tag{4.30}$$

Let
$$T_{13}(s,\theta) = \sin\theta K_{13}(s,b\sec\theta)\, . \tag{4.31}$$

Using Eq. (4.13) in Eq. (4.31)

$$T_{13}(s,\theta) = \frac{2}{\pi} \frac{b\sec\theta(b^2-s^2)^{1/2}\sin\theta}{(b^2\sec^2\theta-s^2)(b^2\sec^2\theta-b^2)^{1/2}} + \frac{2}{\pi} \int_0^\infty h(u)I(b\sec\theta,u,b)\sin\theta\cos(su)\,du \ .$$

Using Eq. (4.27)

$$T_{13}(s,\theta) = \frac{2}{\pi} \frac{(b^2-s^2)^{1/2}}{(b^2\sec^2\theta-s^2)} + \frac{2}{\pi} \int_0^\infty h(u)F(\theta,u)\cos(su)\,du \qquad (4.32)$$

Using Eq. (4.31) and (4.26), Eq. (4.30) becomes

$$G_1(s) + \int_0^a K_{11}(s,t)G_1(t)dt + b\int_0^{\sec^{-1}(c/b)} T_{13}(s,\phi)H(\phi)d\phi = V_e \qquad (0 \le s < a) \ .$$

$$(4.33)$$

Similarly, using the transformation (4.25) and Eq. (4.29) in Eq. (4.2)
yields

$$G_3(b\sec\theta) + \int_0^a K_{31}(b\sec\theta,t)G_1(t)dt + \int_0^{\sec^{-1}(c/b)} K_{33}(b\sec\theta,b\sec\phi)G_3(b\sec\phi)$$

$$\cdot\, b\sec^2\phi\sin\phi d\phi = \frac{V_g\, b\sec\theta}{(b^2\sec^2\theta-b^2)^{1/2}} \qquad (0 \le \theta < \sec^{-1}(c/b)). \quad (4.34)$$

Multiplying by $\sin\theta$ and using Eq. (4.26)

$$\sin\theta\cos^2\theta\, H(\theta) + \int_0^a \sin\theta K_{31}(b\sec\theta,t)G_1(t)dt$$

$$+ \int_0^{\sec^{-1}(c/b)} b\sin\theta\sin\phi K_{33}(b\sec\theta,b\sec\phi)H(\phi)d\phi = V_g$$

$$(0 \le \theta < \sec^{-1}(c/b)). \quad (4.35)$$

Let
$$T_{31}(\theta,s) = \sin\theta K_{31}(b\sec\theta,s) \qquad (4.36)$$

From Eqs. (4.13) and (4.14) it is obvious that

$$K_{13}(s,t) = K_{31}(t,s) \ .$$

Therefore,

$$\sin\theta K_{13}(s, b\sec\theta) = \sin\theta K_{31}(b\sec\theta, s)$$

and hence from Eqs. (4.31) and (4.36)

$$T_{13}(s,\theta) = T_{31}(\theta,s) \ . \tag{4.37}$$

Let

$$T_{33}(\theta,\phi) = b\sin\theta\sin\phi K_{33}(b\sec\theta, b\sec\phi) \ . \tag{4.38}$$

Substituting Eq. (4.16) into Eq. (4.38) yields

$$T_{33}(\theta,\phi) = \frac{2}{\pi^2} \frac{b\sin\theta\sin\phi}{b^2(\sec^2\theta - \sec^2\phi)} \left\{ b\sec\phi \sqrt{\frac{\sec^2\theta - 1}{\sec^2\phi - 1}} \log\frac{\sec\theta + 1}{\sec\theta - 1} \right.$$

$$\left. - b\sec\theta \sqrt{\frac{\sec^2\phi - 1}{\sec^2\theta - 1}} \log\frac{\sec\phi + 1}{\sec\phi - 1} \right\}$$

$$+ \frac{2}{\pi} b \int_0^\infty h(u) I(b\sec\theta, u, b)\sin\theta \ I(b\sec\phi, u, b)\sin\phi \, du \ .$$

Using Eq. (4.27)

$$T_{33}(\theta,\phi) = \frac{2}{\pi^2} \frac{1}{\sec^2\theta - \sec^2\phi} \left\{ \sin^2\theta\sec\theta\log\frac{\cos^2\theta/2}{\sin^2\theta/2} - \sin^2\phi\sec\phi\log\frac{\cos^2\phi/2}{\sin^2\phi/2} \right\}$$

$$+ \frac{2}{\pi} b \int_0^\infty h(u) F(\theta, u) F(\phi, u) \, du$$

$$= \frac{4}{\pi^2} \frac{\sec\phi\sin^2\phi\log(\tan \phi/2) - \sec\theta\sin^2\theta\log(\tan \theta/2)}{\sec^2\theta - \sec^2\phi}$$

$$+ \frac{2}{\pi} b \int_0^\infty h(u) F(\theta, u) F(\phi, u) \, du \ . \tag{4.39}$$

When $\theta = \phi$ the first term on the right in Eq. (4.39) is an indeterminant form. Using L'Hospital's rule

$$T_{33}(\theta,\theta) = -\frac{4}{\pi^2}(1 - \frac{1}{2}\sin^2\theta)\cos\theta\log(\tan\theta/2) - \frac{2}{\pi^2}\cos^2\theta$$

$$+ \frac{2}{\pi} b \int_0^\infty h(u)F(\theta,u)F(\theta,u)du \qquad (4.40)$$

Substituting Eqs. (4.36) and (4.38) into Eq. (4.35) yields

$$\sin\theta\cos^2\theta \; H(\theta) + \int_0^a T_{31}(\theta,t)G_1(t)dt + \int_0^{\sec^{-1}(c/b)} T_{33}(\theta,\phi)H(\phi)d\phi = V_g$$

$$(0 \le \theta < \sec^{-1}(c/b)) \; . \qquad (4.41)$$

To compute the kernels T_{13}, T_{31} and T_{33}, $F(\theta,u)$ has to be evaluated.

As shown in Appendix C

$$F(\theta,u) = J_0(bu) - (bu)\tan\theta \int_0^\theta J_1(bu\;\sec\theta\cos\phi)d\phi \qquad (4.42)$$

Now the equations that have to be solved on a digital computer are:

$$G_1(s) + \int_0^a K_{11}(s,t)G_1(t)dt + b\int_0^{\sec^{-1}(c/b)} T_{13}(s,\phi)H(\phi)d\phi = V_e \qquad (0 \le s < a) \; ,$$

$$(4.43)$$

$$\sin\theta\cos^2\theta \; H(\theta) + \int_0^a T_{31}(\theta,t)G_1(t)dt + \int_0^{\sec^{-1}(c/b)} T_{33}(\theta,\phi)H(\phi)d\phi = V_g$$

$$(0 \le \theta < \sec^{-1}(c/b)) \; , \qquad (4.44)$$

$$K_{11}(s,t) = \frac{2}{\pi}\int_0^\infty h(u)\cos(su)\cos(tu)\;du \; , \qquad (4.45)$$

$$T_{13}(s,\theta) = T_{31}(\theta,s) = \frac{2}{\pi}\frac{(b^2-s^2)^{1/2}}{(b^2\sec^2\theta-s^2)} + \frac{2}{\pi}\int_0^\infty h(u)F(\theta,u)\cos(su)\;du \; ,$$

$$(4.46)$$

$$T_{33}(\theta,\phi) = \frac{4}{\pi^2}\frac{\sec\phi\sin^2\phi\log(\tan\phi/2) - \sec\theta\sin^2\theta\log(\tan\theta/2)}{\sec^2\theta - \sec^2\phi}$$

$$+ \frac{2}{\pi}b\int_0^\infty h(u)F(\theta,u)F(\phi,u)du \;, \tag{4.47}$$

$$T_{33}(\theta,\theta) = -\frac{4}{\pi^2}(1 - \frac{1}{2}\sin^2\theta)\cos\theta\log(\tan\theta/2) - \frac{2}{\pi^2}\cos^2\theta$$

$$+ \frac{2}{\pi}b\int_0^\infty h(u)F(\theta,u)F(\theta,u)du \;, \tag{4.48}$$

and

$$F(\theta,u) = J_0(bu) - (bu)\tan\theta\int_0^\theta J_1(bu\,\sec\theta\cos\phi)d\phi \;. \tag{4.49}$$

The 20-point Legendre-Gauss quadrature formula is used on the interval $(0,a)$ and the 15-point Legendre-Gauss quadrature formula is used on the interval $(0,\sec^{-1}(c/b))$.

Hence, Eqs. (4.43) and (4.44) are resolved into a set of 35 simultaneous equations. The function $G_1(s)$ is solved for 20 discrete values of s in the interval $(0,a)$ and the function $H(\theta)$ is solved for 15 discrete values of θ on the interval $(0,\sec^{-1}(c/b))$. The kernels of the Fredholm integral equations have $(0,\infty)$ integrals. These can be computed by the Laguerre-Gauss formulae as follows:

From Eq. (2.23)

$$h(u) = \tanh(ud) - 1$$

$$= \frac{e^{ud} - e^{-ud}}{e^{ud} + e^{-ud}} - 1$$

$$= \frac{-2e^{-2ud}}{1 + e^{-2ud}} \;. \tag{4.50}$$

In order to make the $(0,\infty)$ integrals in the form of Eq. (4.24), let

$$2ud = x \quad , \quad du = \frac{dx}{2d} \quad \text{and} \quad u = \frac{x}{2d} \quad . \tag{4.51}$$

Substituting in Eq. (4.50)

$$h(u)du = \frac{-2e^{-x}}{2d(1 + e^{-x})} \, dx$$

$$= \frac{-e^{-x}}{d(1 + e^{-x})} \, dx \quad . \tag{4.52}$$

Using the transformation (4.51) and Eq. (4.52) the kernels now become

$$K_{11}(s,t) = \frac{2}{\pi} \int_0^\infty e^{-x} \left(\frac{-1}{d(1+e^{-x})} \right) \cos\left(\frac{sx}{2d}\right) \cos\left(\frac{tx}{2d}\right) \cdot dx \quad , \tag{4.53}$$

$$T_{13}(s,\theta) = T_{31}(\theta,s) = \frac{2}{\pi} \frac{(b^2-s^2)^{1/2}}{(b^2\sec^2\theta-s^2)} + \frac{2}{\pi} \int_0^\infty e^{-x} \left(\frac{-1}{d(1+e^{-x})} \right) F\left(\theta,\frac{x}{2d}\right) \cos\left(\frac{sx}{2d}\right) dx \quad , \tag{4.54}$$

$$T_{33}(\theta,\phi) = \frac{4}{\pi^2} \frac{\sec\phi\sin^2\phi\log(\tan\phi/2) - \sec\theta\sin^2\theta\log(\tan\theta/2)}{\sec^2\theta - \sec^2\phi}$$

$$+ \frac{2}{\pi} b \int_0^\infty e^{-x} \left(\frac{-1}{d(1+e^{-x})} \right) F\left(\theta,\frac{x}{2d}\right) F\left(\phi,\frac{x}{2d}\right) dx \quad , \tag{4.55}$$

$$T_{33}(\theta,\theta) = -\frac{4}{\pi^2} \left(1 - \frac{1}{2}\sin^2\theta\right)\cos\theta\log(\tan\theta/2) - \frac{2}{\pi^2}\cos^2\theta$$

$$+ \frac{2}{\pi} b \int_0^\infty e^{-x} \left(\frac{-1}{d(1+e^{-x})} \right) F\left(\theta,\frac{x}{2d}\right) F\left(\theta,\frac{x}{2d}\right) dx \quad , \tag{4.56}$$

and

$$F\left(\theta,\frac{x}{2d}\right) = J_0\left(\frac{bx}{2d}\right) - \frac{bx}{2d}\tan\theta \int_0^\theta J_1\left(\frac{bx}{2d}\sec\theta\cos\phi\right)d\phi \quad . \tag{4.57}$$

The 24-point Laguerre-Gauss formula is used to evaluate the $(0,\infty)$ integrals. Writing Eqs. (4.43) and (4.44) in discrete form in order to solve them using the computer program in Appendix D yields

$$G_1(I) + \sum_{J=1}^{20} K_{11}(S(I),t(J))G_1(J)A(J) + b \sum_{K=1}^{15} T_{13}(S(I),\phi(K))H(K)W(K) = V_e$$

$$I = 1 \text{ to } 20 , \qquad (4.58)$$

$$\sin(\theta(I))\cos^2(\theta(I))H(I) + \sum_{J=1}^{20} T_{31}(\theta(I),t(J))G_1(J)A(J)$$

$$+ \sum_{K=1}^{15} T_{33}(\theta(I),\phi(K))H(K)W(K) = V_g \qquad I = 1 \text{ to } 15 \qquad (4.59)$$

where A and W are the weights of the 20-point and 15-point Legendre-Gauss formulae respectively,

$$S(I) = \frac{a}{2} (1 + X(I)) \qquad \text{where } X(I)\text{'s are the nodes of the 20-point formula,}$$

$$(4.60)$$

$$t(J) = \frac{a}{2} (1 + X(J)) \qquad \text{where } X(J)\text{'s are the nodes of the 20-point formula,}$$

$$(4.61)$$

$$\theta(I) = \frac{\sec^{-1}(c/b)}{2} (1 + Y(I)) \qquad \text{where } Y(I)\text{'s are the nodes of} \qquad (4.62)$$
$$\text{the 15-point formula,}$$

and

$$\phi(K) = \frac{\sec^{-1}(c/b)}{2} (1 + Y(K)) \qquad \text{where } Y(K)\text{'s are the nodes of} \qquad (4.63)$$
$$\text{the 15-point formula.}$$

From Eqs. (4.53)-(4.57)

$$K_{11}(S(I),t(J)) = \frac{2}{\pi} \sum_{L=1}^{24} \frac{-1}{d(1+e^{-X(L)})} \cos(\frac{S(I)X(L)}{2d})\cos(\frac{t(J)X(L)}{2d})P(L) \qquad (4.64)$$

where P(L)'s and X(L)'s are the weights and nodes of the 24-point Laguerre-Gauss formula,

$$T_{13}(S(I),\phi(K)) = T_{31}(\phi(K),S(I)) = \frac{2}{\pi} \frac{(b^2-S^2(I))^{1/2}}{(b^2 \sec^2(\phi(K)) - S^2(I))}$$

$$+ \frac{2}{\pi} \sum_{L=1}^{24} \frac{-1}{d(1+e^{-X(L)})} F(\phi(K), \frac{X(L)}{2d}) \cos(\frac{S(I)X(L)}{2d}) P(L) \ ,$$

$$(4.65)$$

$$T_{33}(\theta(I),\phi(K)) = \frac{4}{\pi^2} \frac{\sec(\phi(K))\sin^2(\phi(K))\log(\tan \phi(K)/2)}{\sec^2(\theta(I)) - \sec^2(\phi(K))}$$

$$- \frac{4}{\pi^2} \frac{\sec(\theta(I))\sin^2(\theta(I))\log(\tan \theta(I)/2)}{\sec^2(\theta(I)) - \sec^2(\phi(K))}$$

$$+ \frac{2}{\pi} b \sum_{L=1}^{24} \frac{-1}{d(1+e^{-X(L)})} F(\theta(I),\frac{X(L)}{2d}) F(\phi(K),\frac{X(L)}{2d}) P(L) \ ,$$

$$(4.66)$$

$$T_{33}(\theta(I),\theta(I)) = -\frac{4}{\pi^2}(1 - \frac{1}{2}\sin^2(\theta(I)))\cos(\theta(I))\log(\tan \theta(I)/2) - \frac{2}{\pi^2}\cos^2(\theta(I))$$

$$+ \frac{2}{\pi} b \sum_{L=1}^{24} \frac{-1}{d(1+e^{-X(L)})} F(\theta(I),\frac{X(L)}{2d}) F(\theta(I),\frac{X(L)}{2d}) P(L) \ ,$$

$$(4.67)$$

and

$$F(\theta(I),\frac{X(L)}{2d}) = J_0(\frac{bX(L)}{2d}) - \frac{bX(L)}{2d}\tan(\theta(I)) \sum_{M=1}^{15} J_1(\frac{bX(L)}{2d} \sec\theta(I)\cos\phi(M)) W(M)$$

$$(4.68)$$

where

$$\phi(M) = \frac{\theta(I)}{2} [1 + Y(M)] \qquad (4.69)$$

and $W(M)$ and $Y(M)$ are the weights and nodes of the 15 point Legendre-Gauss formula. The computer program in Appendix D is used to solve for the unknown functions $G_1(s)$ and $H(\theta)$.

Relationships to calculate the current are now derived. The electric field in the z direction is given by

$$E_z = - \frac{\partial V}{\partial z} \quad . \tag{4.70}$$

By Eq. (2.17)

$$\frac{\partial V}{\partial z} (r,z) = \int_0^\infty - A(u) \frac{\cosh u(d-z)}{\cosh ud} J_0(ur)du \quad . \tag{4.71}$$

In the z=0 plane at the position of the electrode and guard ring and by Eq. (3.6)

$$\frac{\partial V}{\partial z} (r,0) = \int_0^\infty - A(u)J_0(ur)du = -g(r). \tag{4.72}$$

Using Eq. (4.70) current density is given by

$$J_z = \sigma E_z = -\sigma \frac{\partial V(r,z)}{\partial z} \tag{4.73}$$

where σ = conductivity of the medium.

The current flowing in an annulus of radius r and width dr in any plane z = z is

$$dI = 2\pi r J_z dr$$

$$= -2\pi\sigma r \frac{\partial V(r,z)}{\partial z} dr \quad . \tag{4.74}$$

Hence, the total current flowing from the central electrode which is in the plane z=0 is

$$I_e = -2\pi\sigma \int_0^a r \frac{\partial V(r,0)}{\partial z} dr \quad .$$

Using Eq. (4.72)

$$I_e = 2\pi\sigma \int_0^a rg(r)dr \quad .$$

However, in the region $(0,a)$, $g(r) = g_1(r)$ by Eq. (3.7). Therefore,

$$I_e = 2\pi\sigma \int_0^a rg_1(r)dr \ . \tag{4.75}$$

Substituting Eq. (3.34) into Eq. (4.75) yields,

$$I_e = 2\pi\sigma \int_0^a \left[-\frac{2}{\pi} \frac{d}{dr} \int_r^a \frac{sG_1(s)ds}{(s^2-r^2)^{1/2}} \right] dr$$

$$= -4\sigma \int_0^a \left[\frac{d}{dr} \int_r^a \frac{sG_1(s)ds}{(s^2-r^2)^{1/2}} \right] dr \ . \tag{4.76}$$

Let

$$\int_r^a \frac{sG_1(s)ds}{(s^2-r^2)^{1/2}} = P(r) \quad .$$

Therefore,

$$\frac{d}{dr} \int_r^a \frac{sG_1(s)ds}{(s^2-r^2)^{1/2}} = P'(r) \ .$$

Substituting in Eq. (4.76)

$$I_e = -4\sigma \int_0^a P'(r)dr$$

$$= -4\sigma [P(r)]_0^a$$

$$= -4\sigma \left[\int_r^a \frac{sG_1(s)ds}{(s^2-r^2)^{1/2}} \right]_0^a$$

$$= 4\sigma \int_0^a G_1(s)ds \ . \tag{4.77}$$

Normalizing with respect to the conductivity σ

$$I_{eN} = \frac{I_e}{\sigma} = 4 \int_0^a G_1(s)ds \ . \tag{4.78}$$

Twenty discrete values of $G_1(s)$ have been computed. The normalized current flowing from the center electrode can be computed using the 20-point Legendre-Gauss formula.

$$I_{eN} = 4 \sum_{I=1}^{20} G_1(I)A(I) \qquad (4.79)$$

where $A(I)$'s are the weights.

Equation (4.79) is incorporated in the computer program in Appendix D. The total current supplied by the guard ring is similarly calculated. Analogous to Eq. (4.75)

$$I_g = 2\pi\sigma \int_b^c rg_3(r)dr \ . \qquad (4.80)$$

Substituting Eq. (3.35) for $rg_3(r)$ and simplifying in a manner similar to that used to obtain Eq. (4.77) yields

$$I_g = -4\sigma \left[\int_r^c \frac{sG_3(s)ds}{(s^2-r^2)^{1/2}} \right]_b^c \ .$$

Therefore,

$$I_g = 4\sigma \int_b^c \frac{sG_3(s)ds}{(s^2-b^2)^{1/2}} \ . \qquad (4.81)$$

Since the interval here is (b,c) the transformations of Eq. (4.25) and (4.26) are used. Therefore,

$$I_g = 4\sigma \int_0^{\sec^{-(c/b)}} \frac{b\sec\theta \, G_3(b\sec\theta)b\sec^2\theta\sin\theta d\theta}{(b^2\sec^2\theta - b^2)^{1/2}}$$

$$= 4\sigma b \int_0^{\sec^{-1}(c/b)} H(\theta)d\theta \ . \qquad (4.82)$$

Once again normalizing the guard ring current with respect to the conductivity σ yields

$$I_{gN} = \frac{I_g}{\sigma} = 4b \int_0^{\sec^{-1}(c/b)} H(\theta)d\theta \ . \qquad (4.83)$$

Fifteen discrete values of $H(\theta)$ have been computed. The normalized current supplied by the guard ring is computed by the 15-point Legendre-Gauss formula:

$$I_{gN} = 4b \sum_{I=1}^{15} H(I)W(I) \qquad (4.84)$$

where $W(I)$'s are the weights.

Equation (4.84) is incorporated in the computer program in Appendix D.

The impedance of the path through which the total center electrode current flows is given by

$$Z_N = \frac{V_e}{I_{eN}} \ . \qquad (4.85)$$

Note that the center electrode current, the guard ring current, and the impedance have been obtained without explicitly solving for the function $A(u)$ in Eqs. (3.1)-(3.4). As stated before, the purpose of this research effort is to establish the current pathways. This is done by computing the radius, R, through which the total center electrode current flows, at different planes ($0 \leq z \leq d$) in the layer.

From Eq. (4.74) the total current flowing within a radius R in any plane z=z is

$$I_z = -2\pi\sigma \int_0^R r \frac{\partial V(r,z)}{\partial z} dr \ . \qquad (4.86)$$

From Eq. (4.71)

$$\frac{\partial V(r,z)}{\partial z} = - \int_0^\infty A(u) \frac{\cosh u(d-z)}{\cosh ud} J_0(ur)du \ . \qquad (4.87)$$

To obtain the current flowing in the z=0 plane the function $A(u)$ is not explicitly required. However, for all other planes z=z the function $A(u)$ is needed to obtain $\partial V(r,z)/\partial z$. From Eq. (3.19)

$$\frac{A(u)}{u} = \int_0^a yg_1(y)J_0(uy)dy + \int_b^c yg_3(y)J_0(uy)dy \ . \tag{4.88}$$

By Eqs. (3.42) and (4.11)

$$\int_0^a yg_1(y)J_0(uy)dy = \frac{2}{\pi}\int_0^a G_1(t)I(t,u,0)dt$$

$$= \frac{2}{\pi}\int_0^a G_1(t)\cos(tu)dt \ . \tag{4.89}$$

Also, by Eq. (3.44) and the transformations (4.25)-(4.27)

$$\int_b^c yg_3(y)J_0(uy)dy = \frac{2}{\pi}\int_b^c I(t,u,b)G_3(t)dt$$

$$= \frac{2}{\pi}\int_0^{\sec^{-1}(c/b)} G_3(b\sec\theta)I(b\sec\theta,u,b)b\sec^2\theta\sin\theta d\theta$$

$$= \frac{2b}{\pi}\int_0^{\sec^{-1}(c/b)} H(\theta)F(\theta,u)d\theta \ . \tag{4.90}$$

Substituting Eqs. (4.89) and (4.90) into Eq. (4.88) yields,

$$\frac{A(u)}{u} = \frac{2}{\pi}\int_0^a G_1(t)\cos(tu)dt + \frac{2b}{\pi}\int_0^{\sec^{-1}(c/b)} H(\theta)F(\theta,u)d\theta \ . \tag{4.91}$$

Using the transformation $u = \frac{x}{2d}$ as in Eq. (4.51)

$$\frac{A(\frac{x}{2d})}{\frac{x}{2d}} = \frac{2}{\pi}\int_0^a G_1(t)\cos(\frac{tx}{2d})dt + \frac{2b}{\pi}\int_0^{\sec^{-1}(c/b)} H(\theta)F(\theta,\frac{x}{2d})d\theta \ .$$

Therefore,

$$\frac{A(\frac{x}{2d})}{x} = \frac{1}{2d} \left\{ \frac{2}{\pi} \int_0^a G_1(t) \cos(\frac{tx}{2d}) dt + \frac{2b}{\pi} \int_0^{\sec^{-1}(c/b)} H(\theta) F(\theta, \frac{x}{2d}) d\theta \right\} .$$

(4.92)

Returning to Eq. (4.87)

$$\frac{\partial V(r,z)}{\partial z} = - \int_0^\infty A(u) \frac{e^{u(d-z)} + e^{-u(d-z)}}{e^{ud} + e^{-ud}} J_0(ur) du$$

$$= - \int_0^\infty A(u) \frac{e^{-ud}(e^{2ud-uz} + e^{uz})}{e^{ud}(1 + e^{-2ud})} J_0(ur) du$$

$$= - \int_0^\infty A(u) \frac{e^{-2ud}(e^{2ud-uz} + e^{uz})}{(1 + e^{-2ud})} J_0(ur) du .$$

Using the transformation of Eq. (4.51) yields

$$\frac{\partial V(r,z)}{\partial z} = - \int_0^\infty \frac{A(\frac{x}{2d})}{2d} \frac{e^{-x}(e^{x - \frac{xz}{2d}} + e^{\frac{xz}{2d}})}{(1 + e^{-x})} J_0(\frac{rx}{2d}) dx .$$ (4.93)

Substituting Eq. (4.93), Eq. (4.86) becomes,

$$I_z = 2\pi \sigma \int_0^R r \left[\int_0^\infty \frac{A(\frac{x}{2d})}{2d} \frac{e^{-x}(e^{x - \frac{xz}{2d}} + e^{\frac{xz}{2d}})}{(1 + e^{-x})} J_0(\frac{rx}{2d}) dx \right] dr .$$

Interchanging the order of integration,

$$I_z = 2\pi \sigma \int_0^\infty e^{-x} \frac{A(\frac{x}{2d})}{2d} \frac{(e^{x - \frac{xz}{2d}} + e^{\frac{xz}{2d}})}{(1 + e^{-x})} dx \int_0^R r J_0(\frac{xr}{2d}) dr$$

$$= 2\pi \sigma \int_0^\infty e^{-x} \frac{A(\frac{x}{2d})}{2d} \frac{(e^{x - \frac{xz}{2d}} + e^{\frac{xz}{2d}})}{(1 + e^{-x})} dx \int_0^R (\frac{2d}{x})^2 \frac{xr}{2d} J_0(\frac{xr}{2d}) d(\frac{xr}{2d}) .$$

(4.94)

Let

$$\frac{xr}{2d} = q .$$

Therefore,

$$I_z = 2\pi\sigma \int_0^\infty e^{-x} \frac{A(\frac{x}{2d})}{2d} \frac{(e^{x-\frac{xz}{2d}} + e^{\frac{xz}{2d}})}{(1 + e^{-x})} dx \left(\frac{2d}{x}\right)^2 \int_0^{\frac{xR}{2d}} qJ_0(q)dq \ ,$$

from standard tables,

$$I_z = 2\pi\sigma \int_0^\infty e^{-x} \frac{A(\frac{x}{2d})}{2d} \frac{(e^{x-\frac{xz}{2d}} + e^{\frac{xz}{2d}})}{(1 + e^{-x})} dx \left(\frac{2d}{x}\right)^2 \left\{ qJ_1(q) \Big|_0^{\frac{xR}{2d}} \right\}$$

$$= 2\pi\sigma R \int_0^\infty e^{-x} \left\{ \frac{A(\frac{x}{2d})}{x} \frac{(e^{x-\frac{xz}{2d}} + e^{\frac{xz}{2d}})}{(1 + e^{-x})} J_1(\frac{xR}{2d}) \right\}dx \ . \tag{4.95}$$

The normalized current flowing through a radius, R, in any plane z=z is

$$I_{zN} = \frac{I_z}{\sigma} = 2\pi R \int_0^\infty e^{-x} \left\{ \frac{A(\frac{x}{2d})}{x} \left(\frac{e^{x-\frac{xz}{2d}} + e^{\frac{xz}{2d}}}{1 + e^{-x}}\right) J_1(\frac{xR}{2d}) \right\}dx \ . \tag{4.96}$$

This current is computed by the 24-point-Laguerre-Gauss quadrature formula. $\frac{A(\frac{x}{2d})}{x}$ is calculated at the 24 nodes, x_i, by Eq. (4.92).

It is difficult to solve Eq. (4.96) directly for the radius, R, through which the current $I_{zN} = I_{eN}$ flows. Hence the computer program in Appendix D is written to calculate I_{zN} at different discrete values of R and linear interpolation between the radii, for the current above and below I_{eN}, is carried out to solve for the radius through with the amount of current equal to the center electrode current flows.

Rewriting Eqs. (4.92) and (4.96) in the form of Eq. (4.24) yields

$$\frac{A(\frac{X(I)}{2d})}{X(I)} = \frac{1}{2d}\left[\frac{2}{\pi} \sum_{J=1}^{20} G_1(J)\cos(\frac{t(J)X(I)}{2d}) A(J) + \frac{2b}{\pi} \sum_{K=1}^{15} H(K)F(\theta(K),\frac{X(I)}{2d}) W(K)\right]$$

$$\tag{4.97}$$

where $t(J)$, $A(J)$, $\theta(K)$ and $W(K)$ are defined in Eqs. (4.58)-(4.63) and $X(I)$'s are the nodes of the 24-point Laguerre-Gauss quadrature formula which is used to evaluate Eq. (4.96). Also,

$$I_{zN} = 2\pi R \sum_{I=1}^{24} \frac{A(\frac{X(I)}{2d})}{X(I)} \left\{ \frac{e^{X(I) - \frac{X(I)z}{2d}} + e^{\frac{X(I)z}{2d}}}{1 + e^{-X(I)}} \right\} J_1\left\{\frac{X(I)R}{2d}\right\} P(I) \qquad (4.98)$$

where the $P(I)$'s are the weights of the Laguerre-Gauss quadrature formula. The computer program in Appendix D incorporates Eqs. (4.97) and (4.98). It must be noted that the function $F(\theta,\frac{x}{2d})$ is repeatedly required for the computation of the integrals and from Eqs. (4.57) and (4.68) since zero-order and first-order Bessel functions are involved, its computation takes considerable computer time. To increase the efficiency of the computer program $F(\theta,\frac{x}{2d})$ is first computed at the 15 points of θ on the interval $(0,\sec^{-1}(c/b))$ and the 24 points of x on the $(0,\infty)$ interval. These values are then used in routinely computing the kernels of the two Fredholm integral equations. Symmetry of the kernels $T_{13}(s,\theta) = T_{31}(\theta,s)$ is also utilized in increasing the efficiency of computation.

V. TWO-LAYER MODEL

The single layer model discussed in Chapter II obviously oversimplifies any representation of the thorax. However, the main purpose it serves is to set up the mechanics of solving quadruple integral equations which are basic to the formulation of the multi-layered representation. The model is now extended to two layers as shown in Fig. 5.1. The layer closest to the guarded electrode represents the thoracic wall and correspondingly has a higher conductivity σ_1 as compared to the rest of the tissue in the second layer, which has conductivity σ_2. Parameters pertaining to the first layer have subscript 1 and those pertaining to the second layer have subscript 2.

The boundary conditions pertaining to the model of Fig. 5.1 are:

$$V_2(r,d) = 0 \qquad \text{(all r)} \tag{5.1}$$

$$V_1(r,0) = V_e \qquad (0 \leq r < a) \tag{5.2}$$

$$V_1(r,0) = V_g \qquad (b < r < c) \tag{5.3}$$

$$\frac{\partial V_1(r,0)}{\partial z} = 0 \qquad (a < r < b) \quad \text{and} \quad (c < r < \infty) . \tag{5.4}$$

At the interface of the two layers the potentials are equal. Therefore,

$$V_1(r,\ell) = V_2(r,\ell) . \tag{5.5}$$

The currents flowing normal to the interface are equal also. Stating this condition in the form of Eq. (4.73)

$$\sigma_1 \frac{\partial V_1(r,\ell)}{\partial z} = \sigma_2 \frac{\partial V_2(r,\ell)}{\partial z} . \tag{5.6}$$

The field equation to be solved is again Laplace's Eq. (2.3). From the general form of the solution (Eq. (2.8)), applying condition (5.1), which

(a)
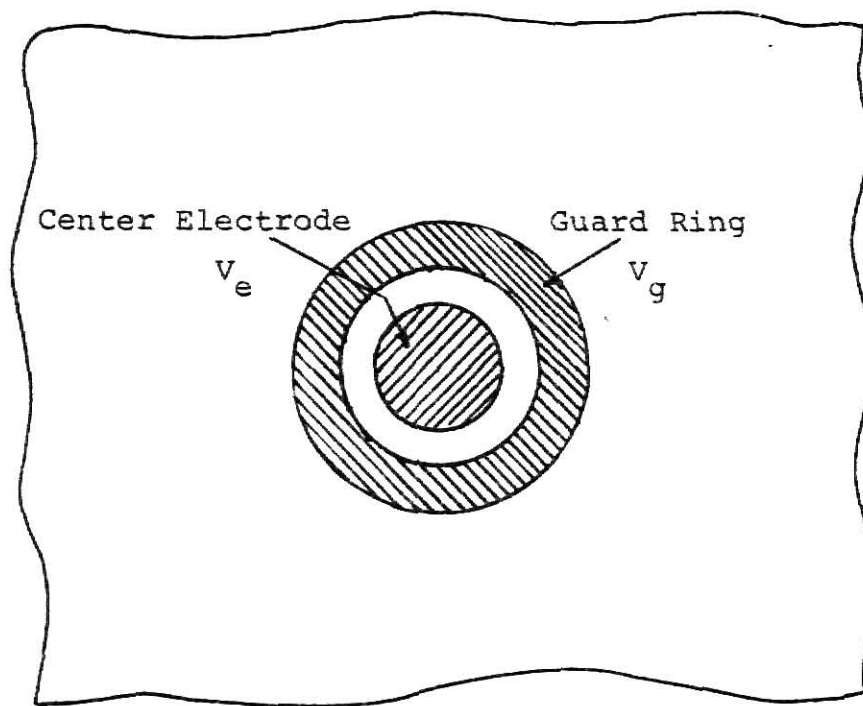
Bottom View
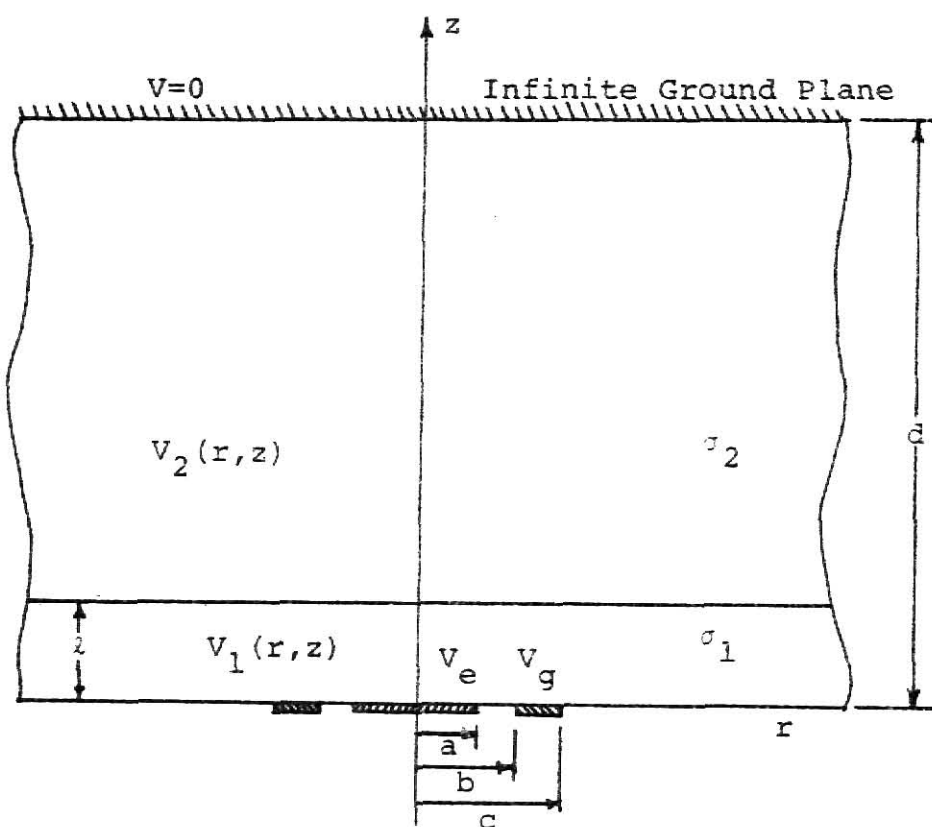
(b) Cross-Section

Figure 5.1. Two-Layer Model.

is the same as condition (2.4), the solution for $V_2(r,z)$ is the same as that in Eq. (2.12);

$$V_2(r,z) = \int_0^\infty \frac{A(u)}{u} \frac{\sinh u(d-z)}{\cosh ud} J_0(ur)du \qquad (5.7)$$

and
$$\frac{\partial V_2(r,z)}{\partial z} = \int_0^\infty -A(u) \frac{\cosh u(d-z)}{\cosh ud} J_0(ur)du \ . \qquad (5.8)$$

Eqs. (5.7) and (5.8) are used to obtain the potential and current distributions in the second layer. Again assuming the general solution of Eq. (2.8), and solving for the potential in the first layer,

$$V_1(r,z) = \int_0^\infty \frac{D'(u)}{u} e^{-uz} J_0(ur)du + \int_0^\infty \frac{E'(u)}{u} e^{uz} J_0(ur)du \ . \qquad (5.9)$$

Let $\qquad D'(u) = [\frac{B(u) - C(u)}{2}]e^{u\ell} \qquad$ and $\qquad E'(u) = [\frac{B(u) + C(u)}{2}]e^{-u\ell} \ .$

$$\qquad (5.10)$$

Therefore,

$$V_1(r,z) = \int_0^\infty \frac{B(u)}{u} \cosh u(z-\ell)J_0(ur)du + \int_0^\infty \frac{C(u)}{u} \sinh u(z-\ell)J_0(ur)du$$

$$\qquad (5.11)$$

and

$$\frac{\partial V_1(r,z)}{\partial z} = \int_0^\infty B(u)\sinh u(z-\ell)J_0(ur)du + \int_0^\infty C(u)\cosh u(z-\ell)J_0(ur)du \ .$$

$$\qquad (5.12)$$

Applying condition (5.5) to Eqs. (5.7) and (5.11) yields

$$\int_0^\infty \frac{A(u)}{u} \frac{\sinh u(d-\ell)}{\cosh ud} J_0(ur)du = \int_0^\infty \frac{B(u)}{u} J_0(ur)du \ .$$

Therefore,

$$B(u) = \frac{A(u)\sinh u(d-\ell)}{\cosh ud} \ . \tag{5.13}$$

Now applying conditions (5.6) to Eqs. (5.8) and (5.12) yields

$$\sigma_1 \int_0^\infty C(u) \, J_0(ur)du = \sigma_2 \int_0^\infty - A(u) \frac{\cosh u(d-\ell)}{\cosh ud} \, J_0(ur)du \ .$$

Therefore,

$$C(u) = - \frac{\sigma_2}{\sigma_1} \frac{A(u)\cosh u(d-\ell)}{\cosh ud} \ . \tag{5.14}$$

Substituting Eqs. (5.13) and (5.14), Eqs. (5.11) and (5.12) become

$$V_1(r,z) = \int_0^\infty \frac{A(u)}{u} \frac{\sinh u(d-\ell)}{\cosh ud} \cosh u(z-\ell)J_0(ur)du - \int_0^\infty \frac{\sigma_2}{\sigma_1} \frac{A(u)}{u} \frac{\cosh u(d-\ell)}{\cosh ud}$$

$$\cdot \sinh u(z-\ell)J_0(ur)du \ . \tag{5.15}$$

and

$$\frac{\partial V_1(r,z)}{\partial z} = \int_0^\infty A(u) \frac{\sinh u(d-\ell)}{\cosh ud} \sinh u(z-\ell)J_0(ur)du - \int_0^\infty \frac{\sigma_2}{\sigma_1} A(u) \frac{\cosh u(d-\ell)}{\cosh ud}$$

$$\cdot \cosh u(z-\ell)J_0(ur)du \ . \tag{5.16}$$

Equations (5.15) and (5.16) are used to obtain the potential and current distributions in the first layer. One the surface of the first layer.

$$V_1(r,0) = \int_0^\infty \frac{A(u)}{u} \left[\frac{\sinh u(d-\ell)\cosh u\ell}{\cosh ud} + \frac{\sigma_2}{\sigma_1} \frac{\cosh u(d-\ell)\sinh u\ell}{\cosh ud}\right] J_0(ur)du$$

$$\tag{5.17}$$

and

$$\frac{\partial V_1(r,0)}{\partial z} = \int_0^\infty \left[-A(u) \frac{\sinh u(d-\ell)\sinh u\ell}{\cosh ud} - \frac{\sigma_2}{\sigma_1} A(u) \frac{\cosh u(d-\ell)}{\cosh ud} \cosh u\ell\right]J_0(ur)du \ .$$

$$\tag{5.18}$$

A reasonable check for the correctness of Eqs. (5.17) and (5.18) can be made by making $\sigma_2 = \sigma_1$; in which case Eqs. (5.17) and (5.18) reduce to the form of Eqs. (2.14) and (2.19).

Let

$$\frac{A(u)}{\cosh ud} \left[-\sinh u(d-\ell)\sinh u\ell - \frac{\sigma_2}{\sigma_1} \cosh u(d-\ell)\cosh u\ell \right] = -D(u) \ . \quad (5.19)$$

Substituting Eq. (5.19), Eq. (5.18) becomes,

$$\frac{\partial V_1(r,0)}{\partial z} = \int_0^\infty -D(u)J_0(ur)du \qquad (5.20)$$

and Eq. (5.17) becomes

$$V_1(r,0) = \int_0^\infty \frac{D(u)}{u} [1 + h(u)]J_0(ur)du \ , \qquad (5.21)$$

where,

$$D(u)[1 + h(u)] = \frac{A(u)}{\cosh ud} \left[\sinh u(d-\ell)\cosh u\ell + \frac{\sigma_2}{\sigma_1} \cosh u(d-\ell)\sinh u\ell \right] \ .$$

$$(5.22)$$

Substituting for $D(u)$ from Eq. (5.19) and solving for $h(u)$ yields,

$$h(u) = \left[\frac{\sinh u(d-\ell)\cosh u\ell + \dfrac{\sigma_2}{\sigma_1} \cosh u(d-\ell)\sinh u\ell}{\sinh u(d-\ell)\sinh u\ell + \dfrac{\sigma_2}{\sigma_1} \cosh u(d-\ell)\cosh u\ell} \right] - 1 \ . \qquad (5.23)$$

Again if $\sigma_2 = \sigma_1$, $h(u) = \tanh(ud) - 1$ as in Eq. (2.23). The above manipulations are carried out so as to mold Eqs. (5.17) and (5.18) into the form of Eq. (2.24) which is readily solvable by the methods of Chapters III and IV. All other parameters are obtained by analogous methods too. From Eqs. (5.20) and (5.21) and the conditions (5.2)-(5.4)

$$\int_0^\infty \frac{D(u)}{u} [1 + h(u)]J_0(ur)du = f(r) \qquad (5.24)$$

and
$$\int_0^\infty D(u)J_0(ur)du = g(r) \ . \qquad (5.25)$$

where,

$$f(r) = f_1(r) = V_e \qquad (0 \le r < a) \qquad (5.26)$$

$$= f_3(r) = V_g \qquad (b < r < c) \qquad (5.27)$$

$$g(r) = g_2(r) = 0 \qquad (a < r < b) \qquad (5.28)$$

$$= g_4(r) = 0 \qquad (c < r < \infty) \ . \qquad (5.29)$$

These are analogous to Eqs. (3.5)-(3.12). The quadruple integral equations analogous to Eqs. (3.13)-(3.16) that can be solved by the methods of Chapters III and IV are

$$\int_0^\infty \frac{D(u)}{u} [1 + h(u)]J_0(ur)du = f_1(r) \qquad (0 \le r < a) \qquad (5.30)$$

$$\int_0^\infty D(u)J_0(ur)du = 0 = g_2(r) \qquad (a < r < b) \qquad (5.31)$$

$$\int_0^\infty \frac{D(u)}{u} [1 + h(u)]J_0(ur)du = f_3(r) \qquad (b < r < c) \qquad (5.32)$$

$$\int_0^\infty D(u)J_0(ur)du = 0 = g_4(r) \qquad (c < r < \infty) \qquad (5.33)$$

and $h(u)$ is given by Eq. (5.23).

Let

$$\frac{\sigma_2}{\sigma_1} = k \ . \qquad (5.34)$$

From Eq. (5.23)

$$h(u) = \left[\frac{(1+k)e^{ud} + (1-k)e^{ud - 2u\ell} + (k-1)e^{-ud + 2u\ell} - (k+1)e^{-ud}}{(k+1)e^{ud} + (k-1)e^{ud - 2u\ell} + (k-1)e^{-ud + 2u\ell} + (k+1)e^{-ud}}\right] - 1$$

$$= \frac{2(1-k)e^{ud - 2u\ell} - 2(k+1)e^{-ud}}{(k+1)e^{ud} + (k-1)e^{ud - 2u\ell} + (k-1)e^{-ud + 2u\ell} + (k+1)e^{-ud}}$$

$$= \frac{e^{-ud}}{e^{ud}}\left[\frac{2(1-k)e^{2ud - 2u\ell} - 2(1+k)}{(k+1) + (k-1)e^{-2u\ell} + (k-1)e^{-2ud + 2u\ell} + (k+1)e^{-2ud}}\right]$$

$$= e^{-2ud}\left[\frac{2(1-k)e^{2ud - 2u\ell} - 2(1+k)}{(k+1) + (k-1)e^{-2u\ell} + (k-1)e^{-2ud + 2u\ell} + (k+1)e^{-2ud}}\right] \quad . \quad (5.35)$$

Again using the transformation of Eq. (4.51) yields

$$h(u)du \equiv \frac{e^{-x}}{d}\left[\frac{(1-k)e^{x - x\ell/d} - (1+k)}{(1+k) + (k-1)e^{-x\ell/d} + (k-1)e^{-x + x\ell/d} + (1+k)e^{-x}}\right] dx \quad .$$

$$(5.36)$$

Hence, in computing the kernels given by Eqs. (4.53)-(4.56) instead of the

term $e^{-x}\left(\dfrac{-1}{d(1+e^{-x})}\right)$, Eq. (5.36) is used. Now the Fredholm integral Eqs.

(4.43) and (4.44) are solved for $G_1(s)$ and $H(\theta)$ by the computer program in

Appendix D with the new $h(u)$ function.

By Eq. (4.78) the current from the center electrode is

$$I_{eN} = \frac{I_e}{\sigma_1} = 4\int_0^a G_1(s)ds \qquad (5.37)$$

and by Eq. (4.83) the current supplied by the guard ring is

$$I_{gN} = \frac{I_g}{\sigma_1} = 4b\int_0^{\sec^{-1}(c/b)} H(\theta)d\theta \quad . \qquad (5.38)$$

Analogous to Eqs. (4.91) and (4.92) and by comparing Eqs. (3.13)-(3.16) with

Eqs. (5.30)-(5.33)

$$\frac{D(u)}{u} = \frac{2}{\pi} \int_0^a G_1(t)\cos(tu)dt + \frac{2b}{\pi} \int_0^{\sec^{-1}(c/b)} H(\theta)F(\theta,u)d\theta \qquad (5.39)$$

and

$$\frac{D(\frac{x}{2d})}{x} = \frac{1}{2d} \left\{ \frac{2}{\pi} \int_0^a G_1(t)\cos\left(\frac{tx}{2d}\right)dt + \frac{2b}{\pi} \int_0^{\sec^{-1}(c/b)} H(\theta)F(\theta,\frac{x}{2d})d\theta \right\} . \qquad (5.40)$$

From Eq. (5.19)

$$A(u) = \frac{D(u)\cosh ud}{\sinh u(d-\ell)\sinh u\ell + k \cosh u(d-\ell)\cosh u\ell} . \qquad (5.41)$$

By using the same transformation x = 2ud as before

$$\frac{A(\frac{x}{2d})}{x} = \frac{D(\frac{x}{2d})}{x} \left[\frac{\cosh \frac{x}{2}}{\sinh \frac{x}{2d}(d-\ell)\sinh \frac{x\ell}{2d} + k \cosh \frac{x}{2d}(d-\ell)\cosh \frac{x\ell}{2d}} \right] . \qquad (5.42)$$

By Eq. (4.86) $\partial V/\partial z$ is required to obtain the current in any plane. For the current in the first layer $\partial V_1(r,z)/\partial z$ is required and for the second layer $\partial V_2(r,z)/\partial z$.

Relationships to calculate the current at any plane z=z are now derived. The current flowing within a radius R in the first layer is given by

$$I_{z1} = -\sigma_1 2\pi \int_0^R r \frac{\partial V_1(r,z)}{\partial z} dr \qquad (5.43)$$

and the current flowing within a radius R in the second layer is given by

$$I_{z2} = -\sigma_2 2\pi \int_0^R r \frac{\partial V_2(r,z)}{\partial z} dr . \qquad (5.44)$$

By Eq. (5.16)

$$\frac{\partial V_1(r,z)}{\partial z} = \int_0^\infty \frac{A(u)}{2(e^{ud} + e^{-ud})} \left[(1-k)e^{ud+uz-2u\ell} - (1+k)e^{ud-uz} - (1+k)e^{-ud+uz} \right.$$
$$\left. + (1-k)e^{-ud-uz+2u\ell} \right] J_0(ur)du$$

$$\frac{\partial V_1(r,z)}{\partial z} = \int_0^\infty \frac{e^{-2ud}\,A(u)}{2(1+e^{-2ud})} \left[(1-k)e^{2ud+uz-2u\ell} - (1+k)e^{2ud-uz} - (1+k)e^{uz} \right.$$

$$\left. + (1-k)e^{-uz+2u\ell} \right] J_0(ur)\,du \quad .$$

Again using the transformation of Eq. (4.51)

$$\frac{\partial V_1(r,z)}{\partial z} = \int_0^\infty \frac{e^{-x}\,A(\frac{x}{2d})}{4d(1+e^{-x})} \left[(1-k)e^{x+\frac{xz}{2d}-\frac{x\ell}{d}} - (1+k)e^{x-\frac{xz}{2d}} \right.$$

$$\left. - (1+k)e^{\frac{xz}{2d}} + (1-k)e^{-\frac{xz}{2d}+\frac{x\ell}{d}} \right] J_0(\frac{xr}{2d})\,dx \quad . \tag{5.45}$$

Substituting Eq. (5.45) into Eq. (5.43) and following the steps of Eqs. (4.93)-(4.95) results in an equation analogous to Eq. (4.95)

$$I_{z1} = -\sigma_1 \pi R \int_0^\infty e^{-x} \left\{ \frac{A(\frac{x}{2d})}{x} \cdot \frac{1}{(1+e^{-x})} \left[(1-k)e^{x+\frac{xz}{2d}-\frac{x\ell}{d}} - (1+k)e^{x-\frac{xz}{2d}} \right. \right.$$

$$\left. \left. - (1+k)e^{\frac{xz}{2d}} + (1-k)e^{-\frac{xz}{2d}+\frac{x\ell}{d}} \right] J_1(\frac{xR}{2d}) \right\}\,dx \quad . \tag{5.46}$$

The normalized current flowing through a radius R in any plane z=z in the first layer is

$$I_{z_{1N}} = \frac{I_{z1}}{\sigma_1} = -\pi R \int_0^\infty e^{-x} \left\{ \frac{A(\frac{x}{2d})}{x} \cdot \frac{1}{(1+e^{-x})} \left[(1-k)e^{x+\frac{xz}{2d}-\frac{x\ell}{d}} - (1+k)e^{x-\frac{xz}{2d}} \right. \right.$$

$$\left. \left. - (1+k)e^{\frac{xz}{2d}} + (1-k)e^{-\frac{xz}{2d}+\frac{x\ell}{d}} \right] J_1(\frac{xR}{2d}) \right\}\,dx \quad . \tag{5.47}$$

Comparing Eq. (5.8) with Eq. (4.87) and following the steps that lead to Eq. (4.95) yields,

$$I_{z2} = 2\pi\,\sigma_2 R \int_0^\infty e^{-x} \left\{ \frac{A(\frac{x}{2d})}{x} \frac{(e^{x-\frac{xz}{2d}} + e^{\frac{xz}{2d}})}{(1+e^{-x})} J_1(\frac{xR}{2d}) \right\}\,dx \quad . \tag{5.48}$$

Normalizing again with respect to σ_1, the total normalized current flowing

through a radius R in any plane z=z in the second layer is

$$I_{z_2N} = \frac{I_{z_2}}{\sigma_1} = 2\pi kR \int_0^\infty e^{-x} \left\{ \frac{A(\frac{x}{2d})}{x} \frac{(e^{x-\frac{xz}{2d}} + e^{\frac{xz}{2d}})}{(1+e^{-x})} J_1(\frac{xR}{2d}) \right\} dx \ . \qquad (5.49)$$

Equations (5.47) and (5.49) are incorporated in the computer program of

Appendix D, the $(0,\infty)$ integrals being evaluated by the 24-point Laguerre-

Gauss formula.

The function $A(\frac{x}{2d})/x$ is evaluated from Eqs. (5.40) and (5.42). All the

current distributions can now be obtained for the two-layer model. Results

and conclusions of both models are discussed in Chapter VI.

VI. RESULTS AND CONCLUSIONS

Using the formulations for the guard ring model several computer runs were made. The effects of variations in a selected set of parameters of the system were studied. The main parameters under study were the design of the guard ring and the relative potentials between the center electrode and the guard ring. The radius of the center electrode "a" was always kept at 1 cm and the potential on the center electrode was one volt for ease of comparison. With respect to the design of the guard ring, the effect of the gap between the center electrode and the guard ring and the effect of the width of the guard ring were studied. The potential on the guard ring was varied with respect to that on the center electrode and its effect on the flow of current from the center electrode was observed.

In the Introduction it was mentioned that the impedance pneumograph described by Schmalzel et al (3) injects a constant current through the central electrode. This current flowing through the impedance of its path develops a potential between the central electrode and the reference electrode. This potential is sensed and its value divided by the constant injected current is a measure of the impedance of the current pathway. The sensed potential is buffered and fed to a variable gain amplifier which drives the guard ring. The schematic is shown in Fig. 6.1.

Upon an initial observation it seems that the analysis of this research effort differs from the principle that is followed in practice. The analysis maintains a constant potential of one volt on the center electrode rather than maintaining a constant current flowing from the center electrode. This approach is just for mathematical convenience! As the path of the current flow varies the impedance varies, too. Therefore, if the potential
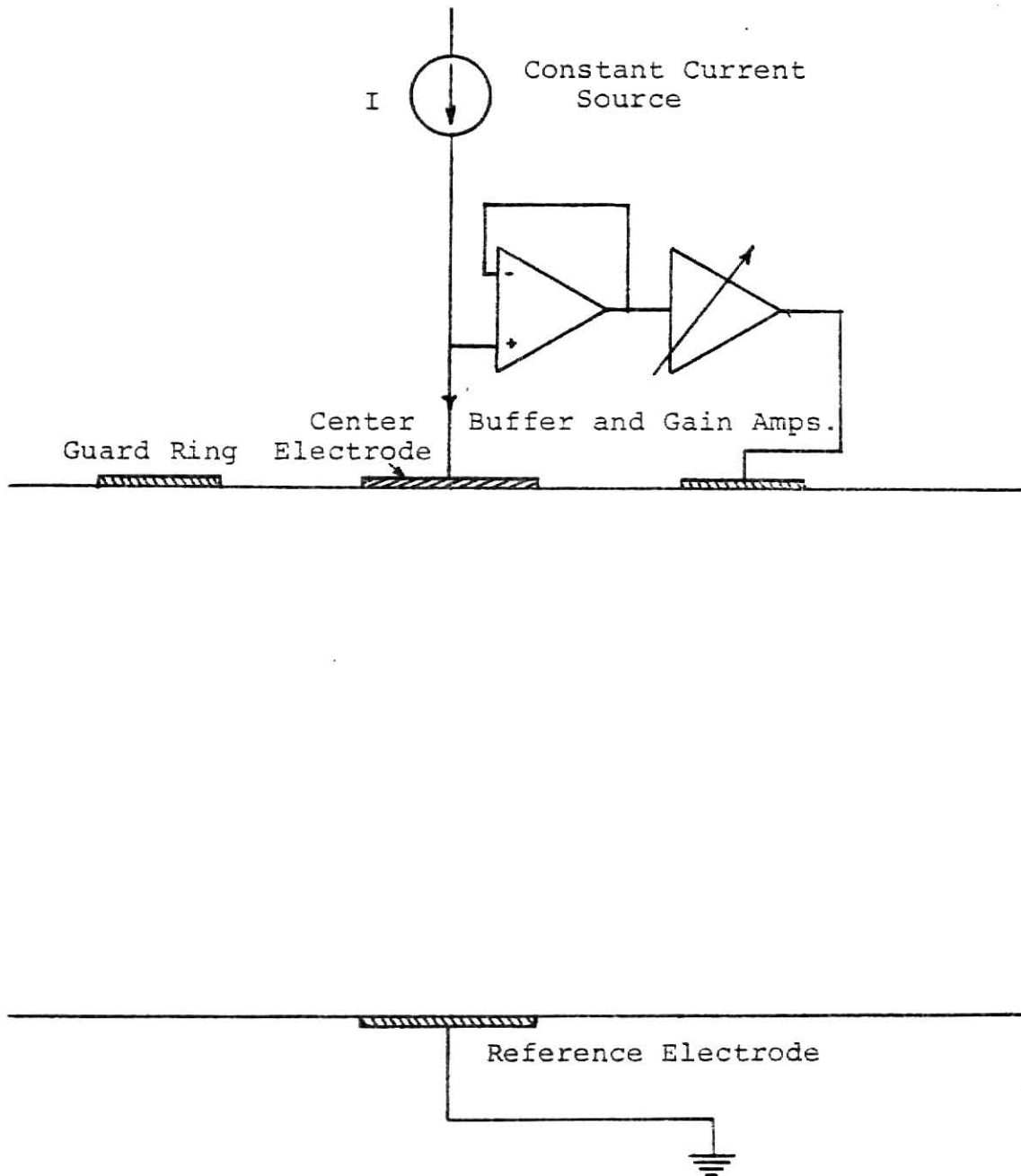
Figure 6.1. Schematic of Guard Ring Drive.

is kept constant then the current flowing from the central electrode
increases or decreases as the impedance decreases or increases respectively.
However, the problem is completely linear; therefore, the current can be
restored to a chosen value simply by increasing or decreasing the center
electrode potential without disturbing its pathway. This point will be
further explained after studying a few computer runs.

6.1 Single-Layer Model: Case One

The first case investigated is one with a relatively large gap between
the center electrode and the guard ring for the single-layer model. For
this design of the guard ring and the electrode the current flow for dif-
ferent potentials on the guard ring is observed. The results are tabulated
in Table 6.1.

Table 6.1. Single-Layer: Case 1

$a = 1$ cm, $b = 3.0$ cm, $c = 4.5$ cm, $d = 20$ cm, $V_e = 1.0V$,

gap $= b - a = 2$ cm, width of guard ring $= c - b = 1.5$ cm.

V_g Volts	$\Delta V = V_g - V_e$ Volts	Gain $= \dfrac{V_g}{V_e}$	Center Electrode Current I_{eN} Amps ohm cm	Impedance $Z_N = \dfrac{V_e}{I_{eN}}$ cm^{-1}	Guard ring Current I_{gN} Amps ohm cm
1.00	0.00	1.00	1.444	0.692	17.851
1.20	0.20	1.20	0.809	1.236	22.056
1.40	0.40	1.40	0.174	5.735	26.261
1.44	0.44	1.44	0.047	21.120	27.102
1.48	0.48	1.48	-0.080	-ve	27.943

From Table 6.1 it can be seen that as the potential on the guard ring is
increased the current from the central electrode, I_{eN}, decreases and cor-
respondingly the impedance increases. A plot of the center electrode

current versus the difference in potential between the center electrode and guard ring is shown in Fig. 6.2. It can be seen that a pinch-off potential occurs. This occurs when the potential on the guard ring is increased to the point where current flows directly from the guard ring to the center electrode. All the current flow in the medium is then between the guard ring and the ground plane with none between the central electrode and the ground plane. Figure 6.3a shows a plot of the unknown function $(A(x/2d))/x$ versus x for the same potential on the center electrode and guard ring. A very interesting explanation for this phenomenon of decreasing current or increasing impedance with increasing guard ring potential can be obtained from the plot of Fig. 6.3b. This is a plot of the contours of the current from the center electrode throughout the medium with the difference in potential, $\Delta V = V_g - V_e$, as a parameter.

First, if the center electrode had no guard ring the current would spread out to an infinite distance at the ground plane. It can be seen that the presence of the guard ring with the same potential as on the center electrode ($\Delta V = 0$) confines the current to a finite region about the axis. Hence the guard ring does channel the current from the central impedance measuring electrode so that the measurement of the impedance can be restricted to only a central core of tissue. What is more interesting is that increasing the potential on the guard ring results in a focusing effect, i.e., narrowing the width of the current beam. It is precisely this effect that produces the decreasing current and increasing impedance since the narrower central core has a greater impedance.

The infinite ground plane is a worst case condition of a finite size reference electrode. With the reference electrode being of a finite size
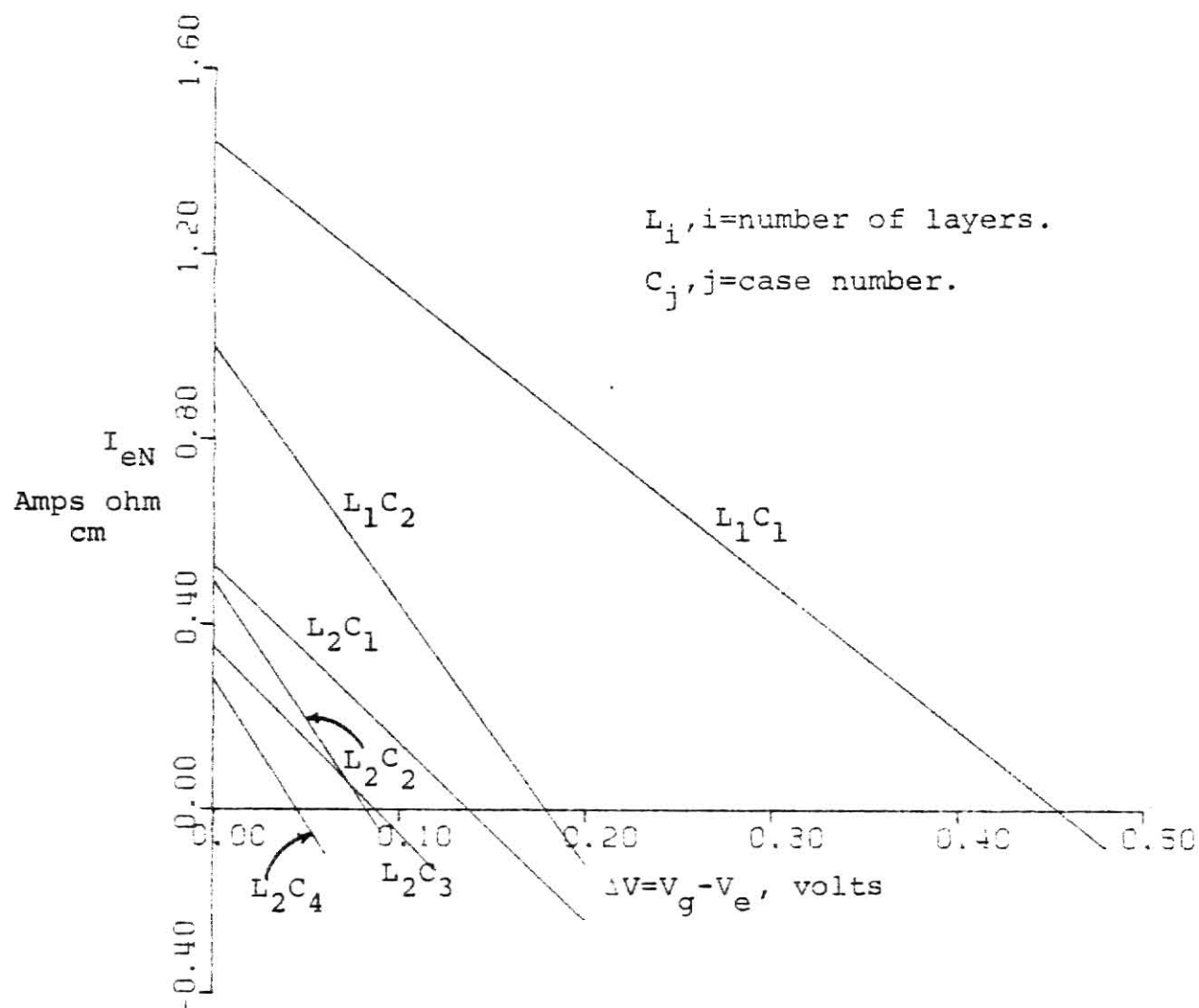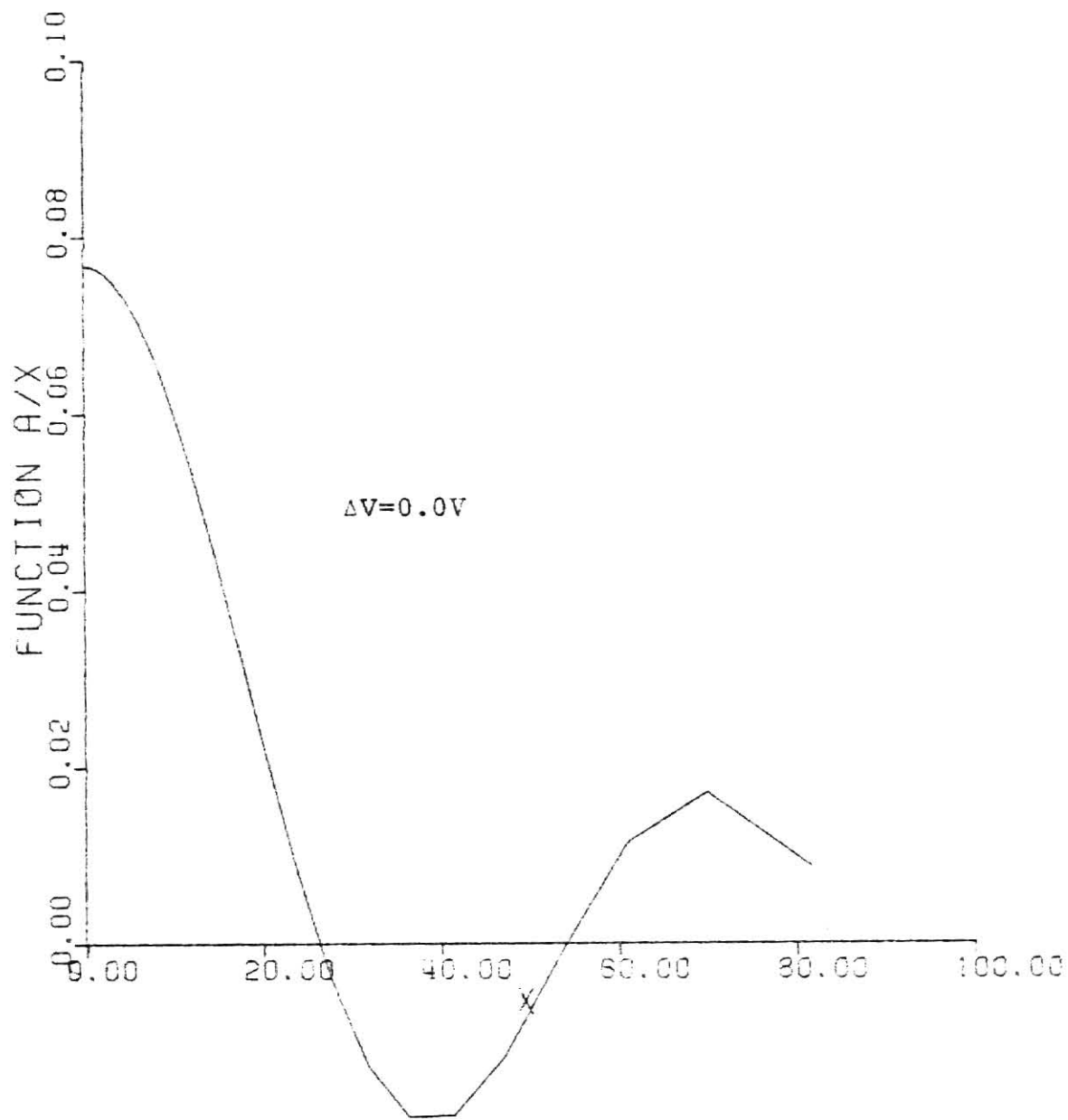
Figure 6.2. Plot of Center Electrode Current I_{eN} versus the Difference in Potential $\Delta V = V_g - V_e$.

(a)

Plot of A(x/2d) versus x.
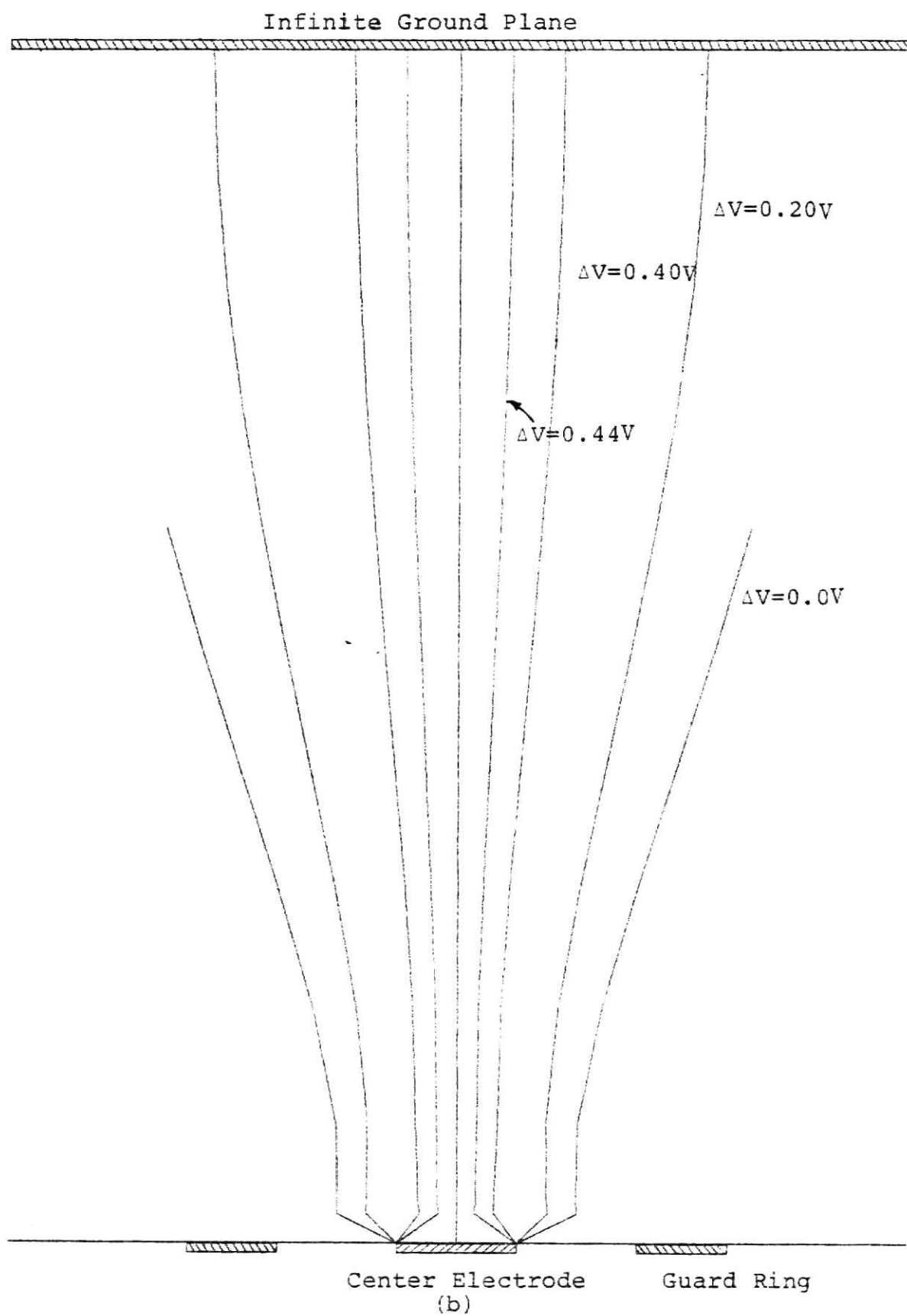
Figure 6.3. Single-Layer: Case 1.

Infinite Ground Plane

$\Delta V=0.20V$

$\Delta V=0.40V$

$\Delta V=0.44V$

$\Delta V=0.0V$

Center Electrode   Guard Ring
(b)

Constant Current Contours.

Figure 6.3.   Single-Layer: Case 1.

all current lines would have to terminate on it and the beam width would
then be narrower than what it is with an infinite ground plane.

Confirmation of the argument that the current can be kept constant
without changing its pathway by merely increasing the potential on the
center electrode is now made. Consider the case when $\Delta V = 0.44V$. From
Table 6.1 with $\Delta V = 0$ the center electrode current is $I_{eN} = 1.444$ units.
The assumption to keep the current constant at 1.444 units is made even for
a $\Delta V = 0.44V$. Now, the impedance for $\Delta V = 0.44V$ is 21.120 units. Hence if
the current of 1.444 units flows through this impedance the potential on
the center electrode should be $V_e = 1.444 \times 21.120 = 30.497$ units. $\Delta V =$
0.44 means that the gain is 1.44 or $V_g = 1.44 \, V_e$. Now if V_e is increased
by a factor of 30.497 then V_g is increased by the same factor. This is
equivalent to multiplying both sides of the simultaneous Eqs. (4.58) and
(4.59) by the same factor 30.497. If the coefficients of the unknowns,
$G_1(s_i)$ and $H(\theta_i)$, are fixed then $G_1(s_i)$ and $H(\theta_i)$ are each multiplied by
the same factor 30.497. By Eq. (4.97), $(A(x/2d))/x$ will increase by the
same factor 30.497 and by Eq. (4.98) the current in any plane at any radius
will increase by the same factor 30.497. Since the increase in current is
independent of the z plane or the radius, the current pathway will remain
the same. The same argument holds for the 2-layer model when it is applied
to the relevant equations. The pair of Fredholm integral equations (4.43)
and (4.44) are solved using this value of V_e while keeping the gain the
same at 1.44, i.e., $V_g = 1.44 \, V_e$. The current contour is shown in Fig.
6.4. The impedance of the path is the same at 21.120 and if this contour
is compared with the one in Fig. 6.3b for $\Delta V = 0.44V$ it can be seen that the

Infinite Ground Plane

$\Delta V = 0.44V$

Center Electrode   Guard Ring
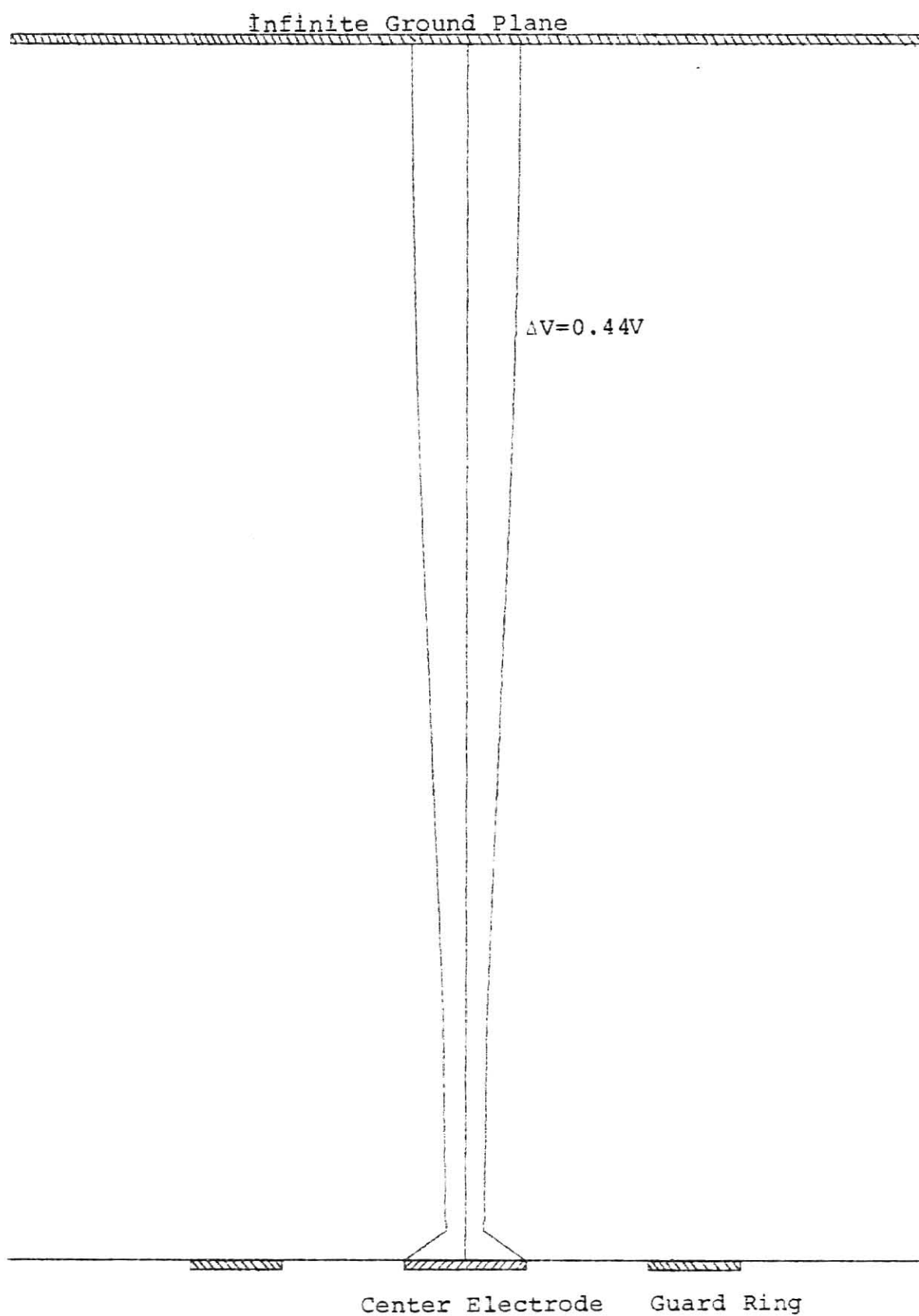
Figure 6.4. Single-Layer: Case 1
Constant Current Contour Confirming
Constant Potential Hypothesis.

two overlap. Hence the analytic technique of using a constant potential on the center electrode is equivalent to the constant current injection technique.

Having observed the focusing effect, different designs of the guard ring were studied.

6.2 Single-Layer Model: Case Two

The second case for the single layer model consists of a narrow gap guard ring of the same width as Case 1.

The results are tabulated in Table 6.2.

Table 6.2: Single-Layer: Case 2
$a = 1.0$ cm, $b = 1.25$ cm, $c = 2.75$ cm, $d = 20$ cm, $V_e = 1.0$V,
gap $= b - a = 0.25$ cm,   width of guard ring $= c - b = 1.5$ cm.

V_g Volts	$\Delta V = V_g - V_e$ Volts	Gain $= \dfrac{V_g}{V_e}$	Center Electrode Current I_{eN} Amps ohm cm	Impedance $Z_N = \dfrac{V_e}{I_{eN}}$ cm^{-1}	Guard ring Current I_{gN} Amps ohm cm
1.00	0.00	1.00	1.000	1.000	10.695
1.05	0.05	1.05	0.721	1.387	11.508
1.10	0.10	1.10	0.442	2.264	12.322
1.15	0.15	1.15	0.162	6.154	13.136
1.16	0.16	1.16	0.107	9.376	13.299
1.17	0.17	1.17	0.051	19.680	13.462
1.20	0.20	1.20	-0.117	-ve	13.950

Again, a plot of the center electrode current versus the difference in potential ΔV is shown in Fig. 6.2. Figure 6.5a shows a plot of the unknown function $(A(x/2d))/x$ versus x. The current contours are shown in Fig. 6.5b with ΔV as a parameter. It can be seen that for the narrower gap case (gap = 0.25 cm) the pinch-off potential occurs at a lower value of ΔV than

(a)
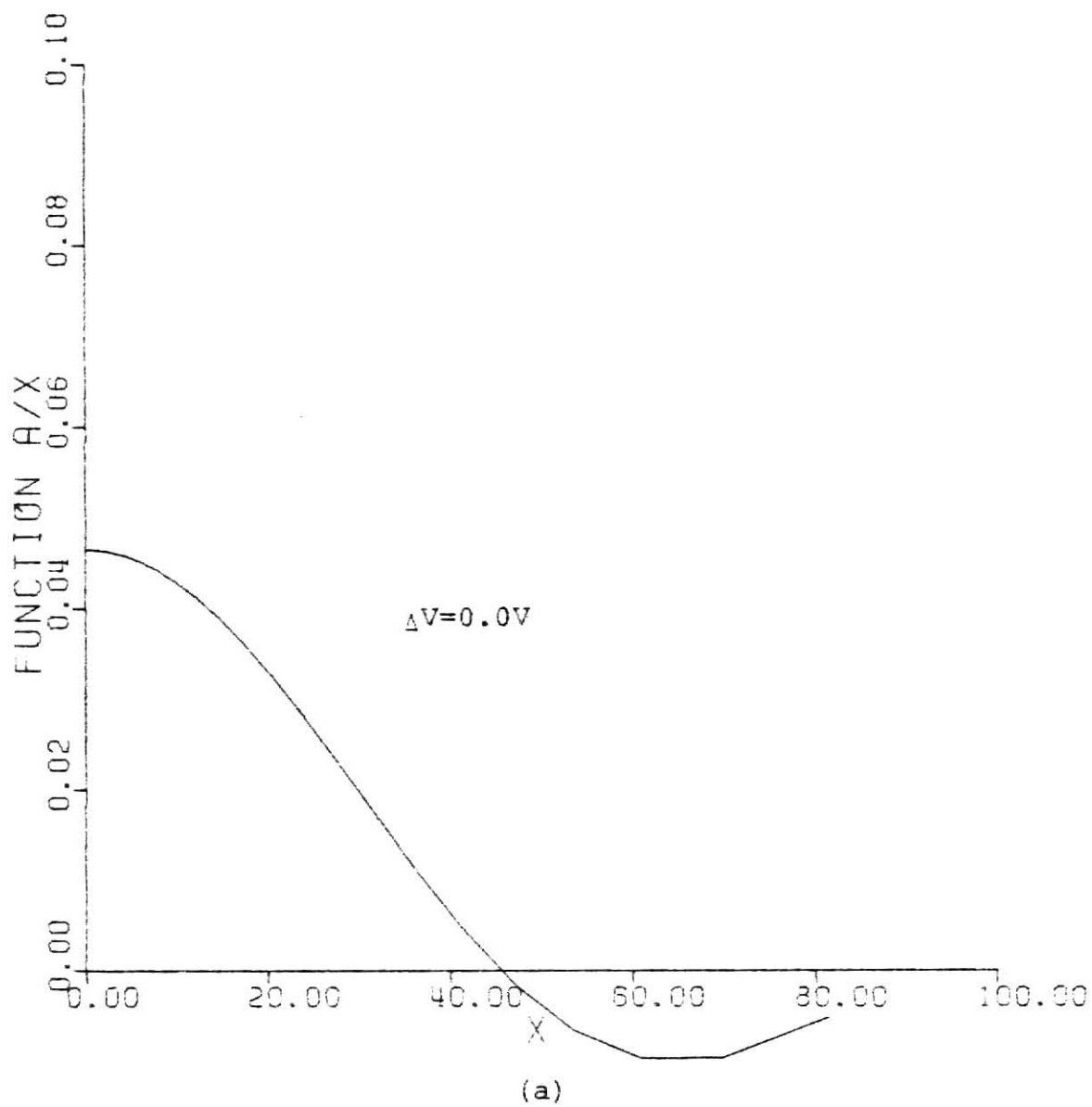
Plot of A(x/2d) versus x.

Figure 6.5.   Single-Layer: Case 2.

Infinite Ground Plane

ΔV=0.10V

ΔV=0.15V

ΔV=0.16V

ΔV=0.17v

ΔV=0.05V

ΔV=0.0V

Guard Ring

Center Electrode

(b)

Constant Current Contours.

Figure 6.5.   Single-Layer: Case 2.

for Case 1. The focusing effect is more pronounced near the center electrode but some spreading occurs at the far end near the ground plane.

6.3 Two-Layer Model: Case One

The following discussion relates to the two-layer model with different guard ring designs. The Two-Layer: Case 1 uses a guard ring of the same design as the Single-Layer: Case 1. The results of this case are shown in Table 6.3.

The conductivities used are σ_1 = 1/400 ohm^{-1} cm^{-1}, σ_2 = 1/2000 ohm^{-1} cm^{-1} [17]

Table 6.3. Two-Layer: Case 1.

a = 1.0 cm, b = 3.0 cm, c = 4.5 cm, d = 20 cm, V_e = 1.0 V, k = 0.2, ℓ = 2 cm, gap = $b - a$ = 2 cm,   width of guard ring = $c - b$ = 1.5 cm.
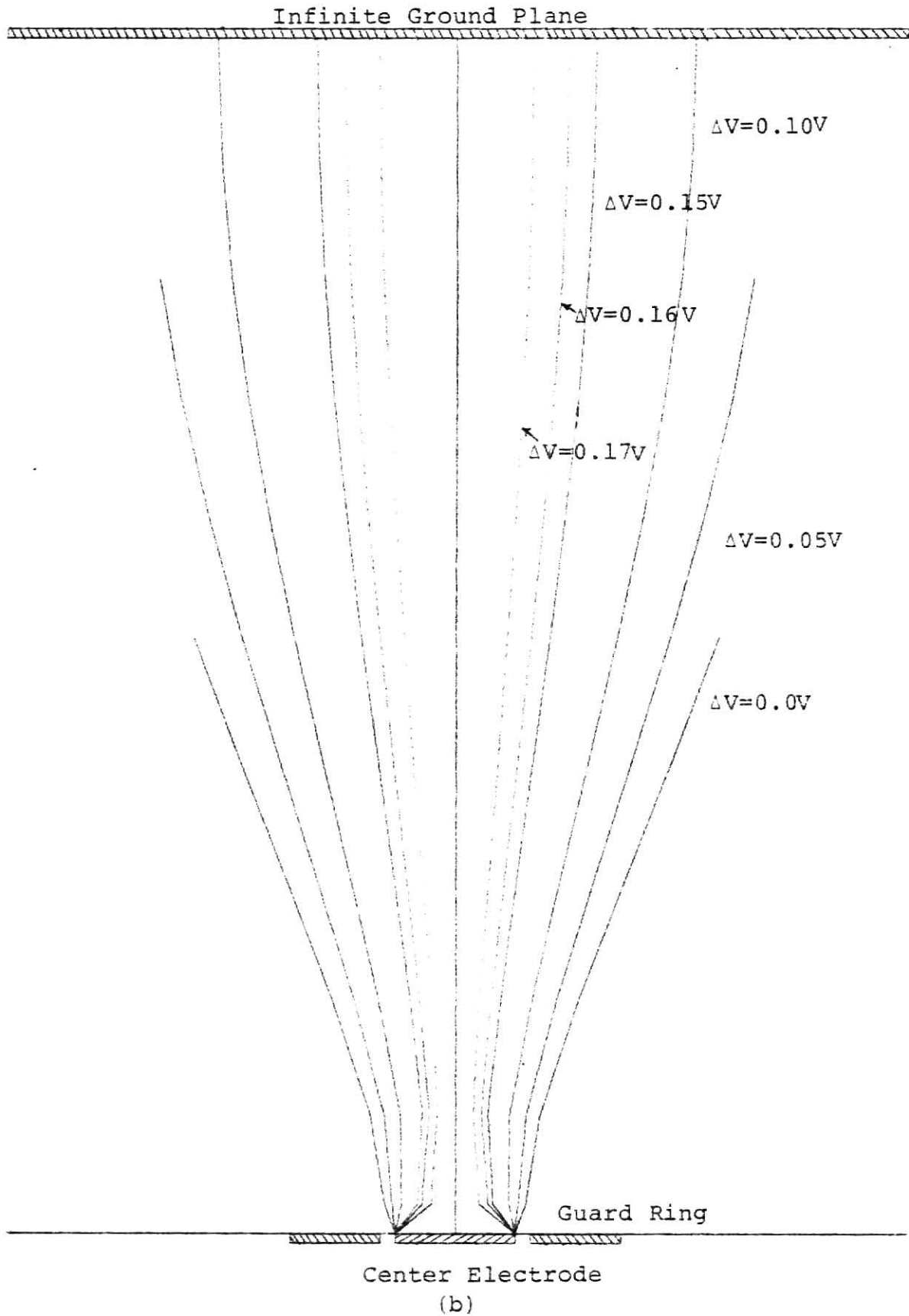
V_g Volts	$\Delta V = V_g - V_e$ Volts	Gain = $\frac{V_g}{V_e}$	Center electrode Current I_{eN} Amps ohm cm	Impedance $Z_N = \frac{V_e}{I_{eN}}$ cm^{-1}	Guard ring Current I_{gN} Amps ohm cm
1.0	0.0	1.0	0.530	1.888	9.313
1.1	0.1	1.1	0.146	6.852	10.628
1.2	0.2	1.2	-0.238	-ve	11.943

A plot of the center electrode current versus the difference in potential ΔV is shown in Fig. 6.2. The pinch-off potential occurs between a guard ring potential of 1.1 and 1.2 volts. Figure 6.6a shows a plot of the unknown function $(A(x/2d))/x$ versus x. The current contours are shown in Fig. 6.6b. Once again the channeling of the current through a central core of tissue is apparent with increasing potentials on the guard ring.

FUNCTION A/X

ΔV=0.0V

X

(a)
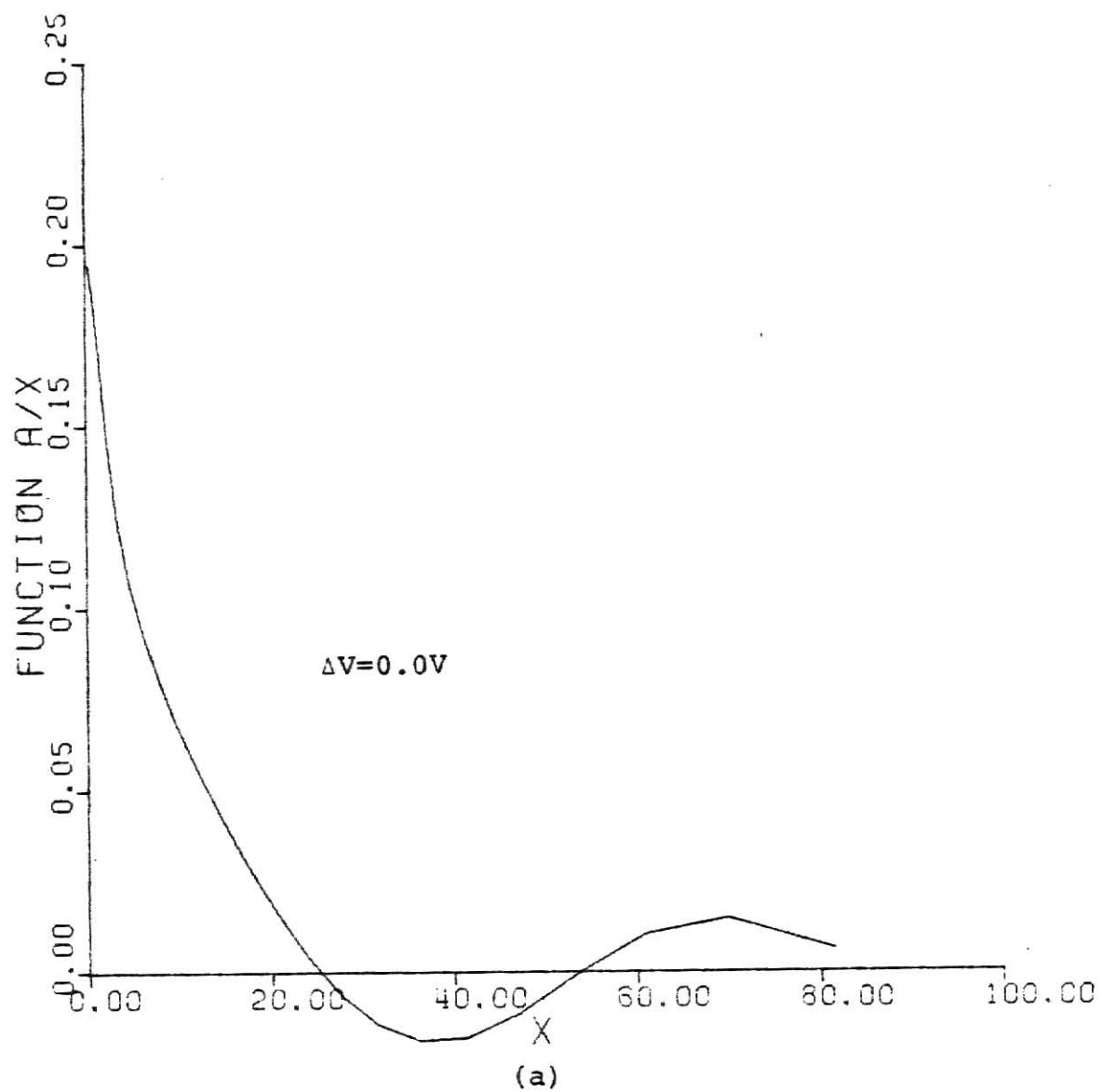
Plot of A(x/2d) versus x.

Figure 6.6.   Two-Layer: Case 1.

Infinite Ground Plane

$\Delta V=0.1V$

$\Delta V=0.0V$

σ_2

σ_1

Center Electrode   Guard Ring

(b)

Constant Current Contours.

Figure 6.6.   Two-Layer: Case 1.

6.4 Two-Layer Model: Case Two

This case is associated with a model which possesses a narrow gap between the central electrode and the guard ring. The design of the guard ring is the same as the one in the Single-Layer: Case 2. The results are shown in Table 6.4.

Table 6.4. Two-Layer: Case 2

$a = 1.0$ cm, $b = 1.25$ cm, $c = 2.75$ cm, $d = 20$ cm, $V_e = 1.0V$, $k = 0.2$, $\ell = 2$ cm, gap $= b - a = 0.25$ cm, width of guard ring $= c - b = 1.5$ cm.

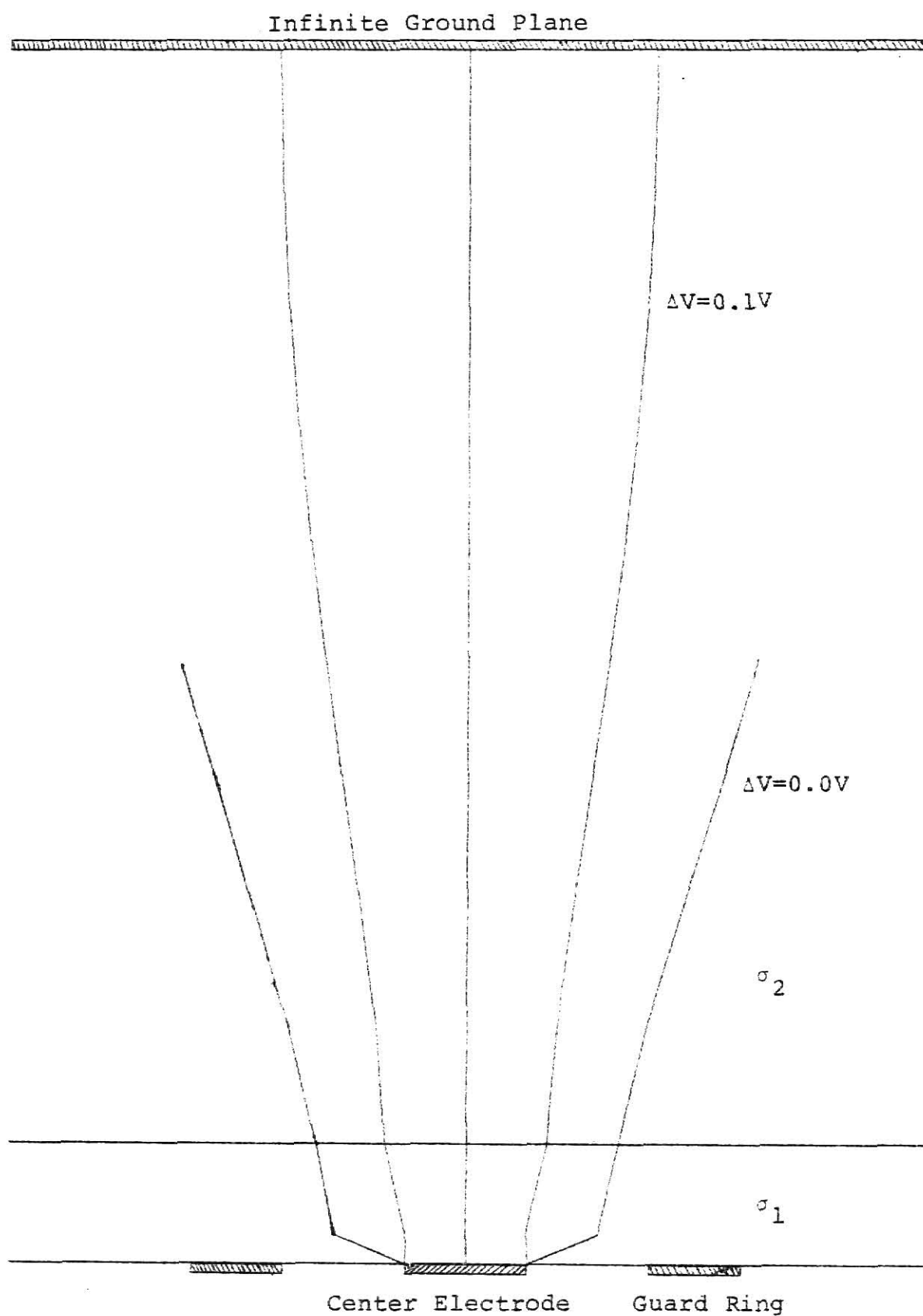| V_g Volts	$\Delta V = V_g - V_e$ Volts	Gain $= \frac{V_g}{V_e}$	Center electrode Current I_{eN} Amps ohm cm	Impedance $Z_N = \frac{V_e}{I_{eN}}$ cm^{-1}	Guard ring Current I_{gN} Amps ohm cm
1.00	0.00	1.00	0.493	2.028	6.378
1.03	0.03	1.03	0.313	3.196	6.749
1.06	0.06	1.06	0.133	7.535	7.121
1.09	0.09	1.09	-0.047	-ve	7.492

A plot of the center electrode current versus the difference in potential ΔV is shown in Fig. 6.2. The value of the pinch-off potential in this case is seen to occur at a lower value of guard ring potential than in the Two-Layer: Case 1. Figure 6.7a shows a plot of the unknown function $(A(x/2d))/x$ versus x. The current contours are shown in Fig. 6.7b.

Similar to the Single-Layer: Case 2, there appears to be an increased focusing effect near the central electrode and a slight spread at the far end near the ground plane. The two cases for the two-layer model studied thus far view the two desirable extremes, i.e., a large gap and a narrow gap. The results show that cases between these two extremes will also have

Plot of A(x/2d) versus x.

Figure 6.7.   Two-Layer: Case 2.

Infinite Ground Plane

$\Delta V=0.06V$

$\Delta V=0.03V$

$\Delta V=0.0V$

σ_2

σ_1

Guard Ring

Center Electrode

(b)
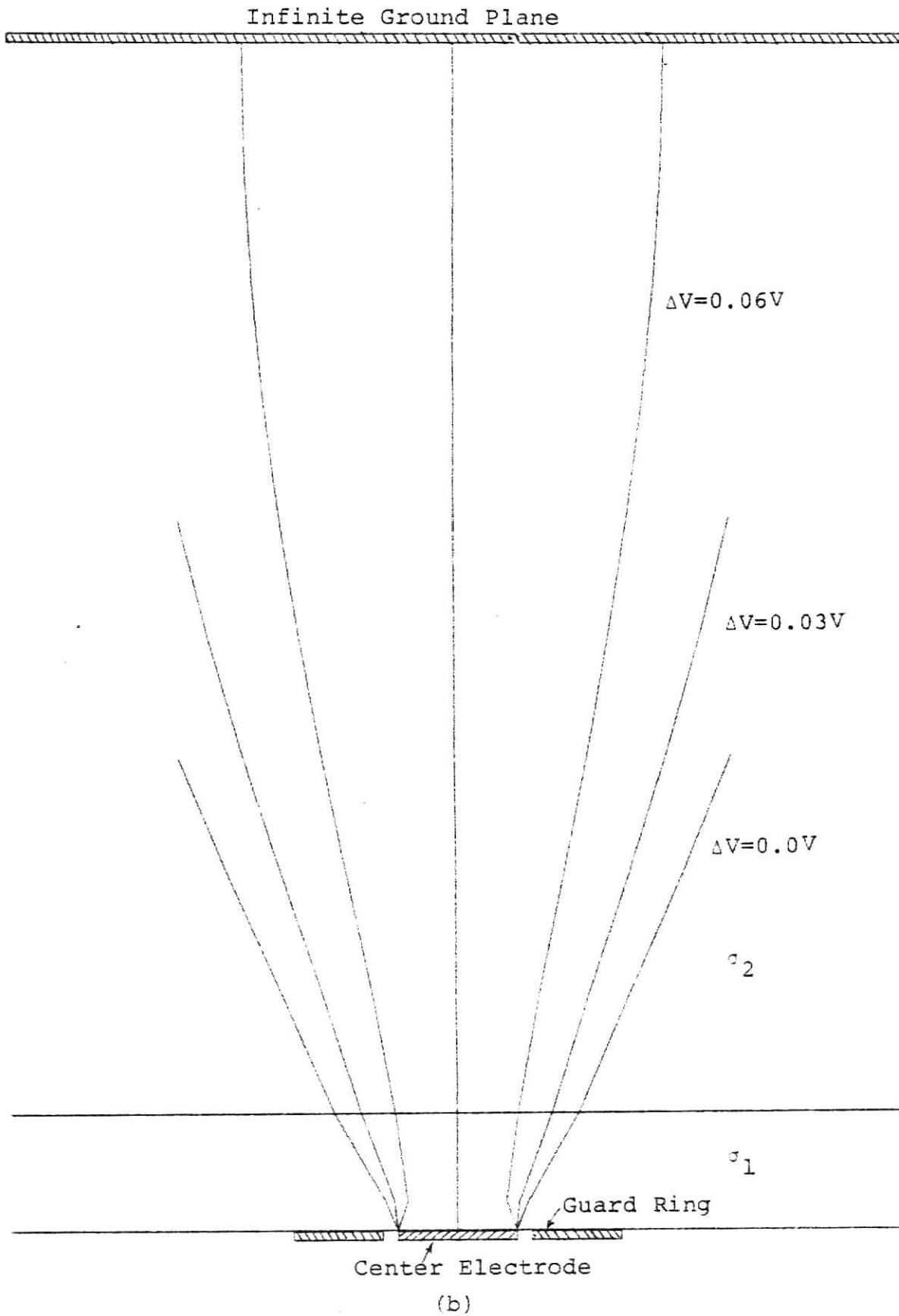
Constant Current Contours.

Figure 6.7.   Two-Layer: Case 2.

a focusing effect somewhere between that shown by the two cases; the degree
of which depends upon the relative size of the gap.

6.5 Two-Layer Model: Cases Three and Four.

Another aspect of the guard ring design that was analyzed was the
effect of the width of the guard ring on the current contours for variations
in the guard ring potential. A broader guard ring is used for these cases.
Plots are given of the current contours for a large gap (Case Three) and for
a small gap (Case Four). Case 3 deals with a wide guard ring and a large
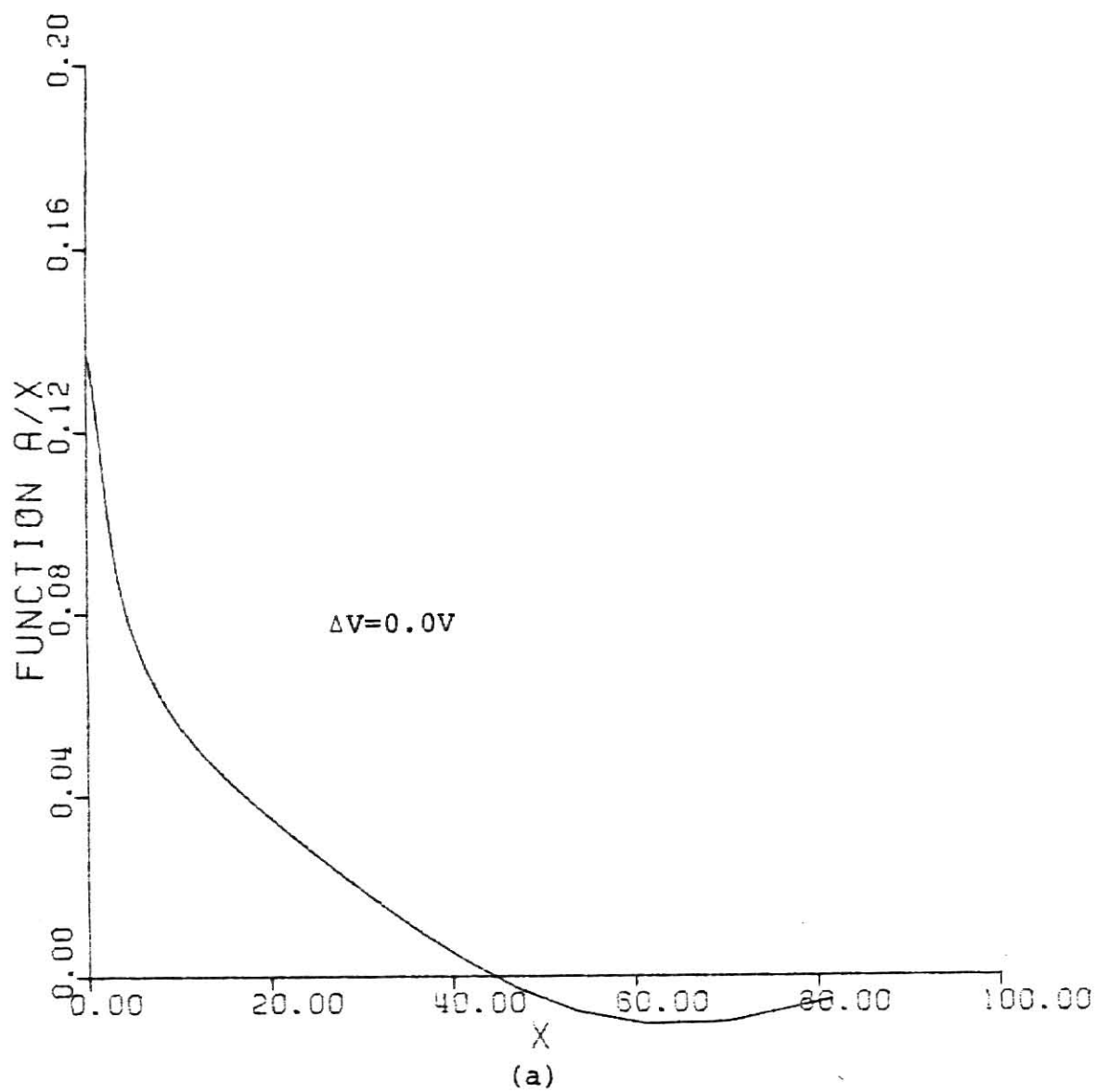gap. The results of Case 3 are tabulated in Table 6.5.

Table 6.5. Two-Layer: Case 3

$a = 1.0$ cm, $b = 3.0$ cm, $c = 5.5$ cm, $d = 20$ cm, $V_e = 1.0$ V, $k = 0.2$, $\ell = 2$ cm,

gap $= b - a = 2$ cm, width of guard ring $= c - b = 2.5$ cm.

| V_g Volts	$\Delta V = V_g - V_e$ Volts	Gain $= \dfrac{V_g}{V_e}$	Center electrode Current I_{eN} Amps ohm cm	Impedance $Z_N = \dfrac{V_e}{I_{eN}}$ cm^{-1}	Guard ring Current I_{gN} Amps ohm cm
1.00	0.00	1.00	0.352	2.835	11.252
1.08	0.08	1.08	0.030	33.226	12.475
1.12	0.12	1.12	-0.131	-ve	13.086

A plot of the center electrode current versus the difference in potential ΔV
is shown in Fig. 6.2. Comparing Tables 6.3 and 6.5 which are both for the
large gap case and from Fig. 6.2, it can be seen that pinch off with the
wider guard ring (Table 6.5) occurs for a smaller value of guard ring
potential that for the narrower ring case. Figure 6.8a shows a plot of
the unknown function $(A(x/2d))/x$ versus x. The current contours of Fig.
6.8b indicate that the focusing effect near the central electrode is similar
to the Two-Layer: Case 2 (narrower gap) but does not have the undesirable

(a)
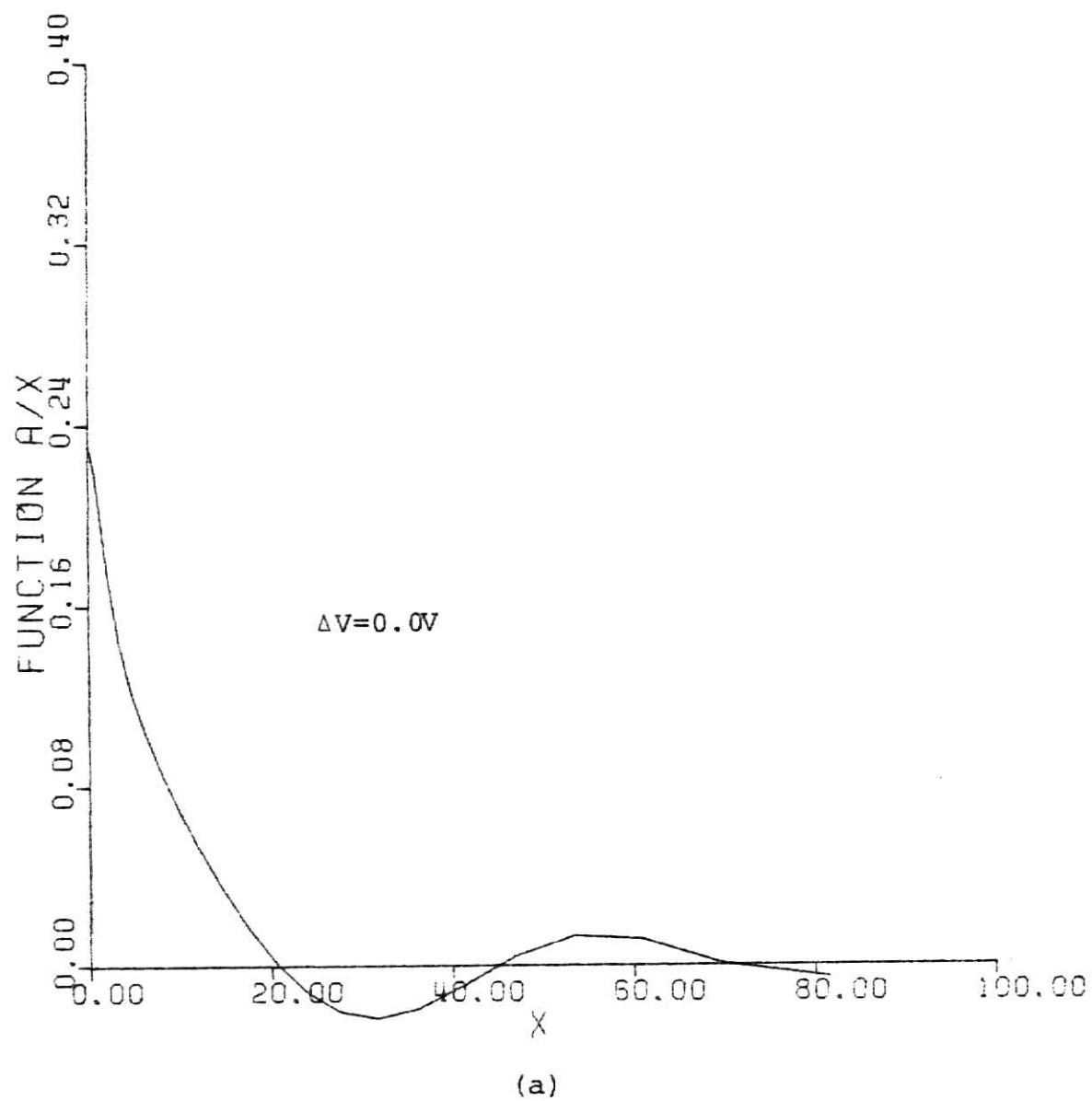
Plot of A(x/2d) versus x.

Figure 6.8.   Two-Layer: Case 3.

Constant Current Contours.

Figure 6.8. Two-Layer: Case 3.

spread near the ground plane of the Two-Layer: Case 2. The last case (Case Four) that was analyzed used the same width of the guard ring as in Case 3 above but with a narrow gap like the Two-Layer: Case 2. The results of Case 4 are shown in Table 6.6.

Table 6.6. Two-Layer: Case 4

$a = 1.0$ cm, $b = 1.25$ cm, $c = 3.75$ cm, $d = 20$ cm, $V_e = 1.0$ V, $k = 0.2$, $\ell = 2$ cm, gap $= b - a = 0.25$ cm, width of guard ring $= c - b = 2.5$ cm.
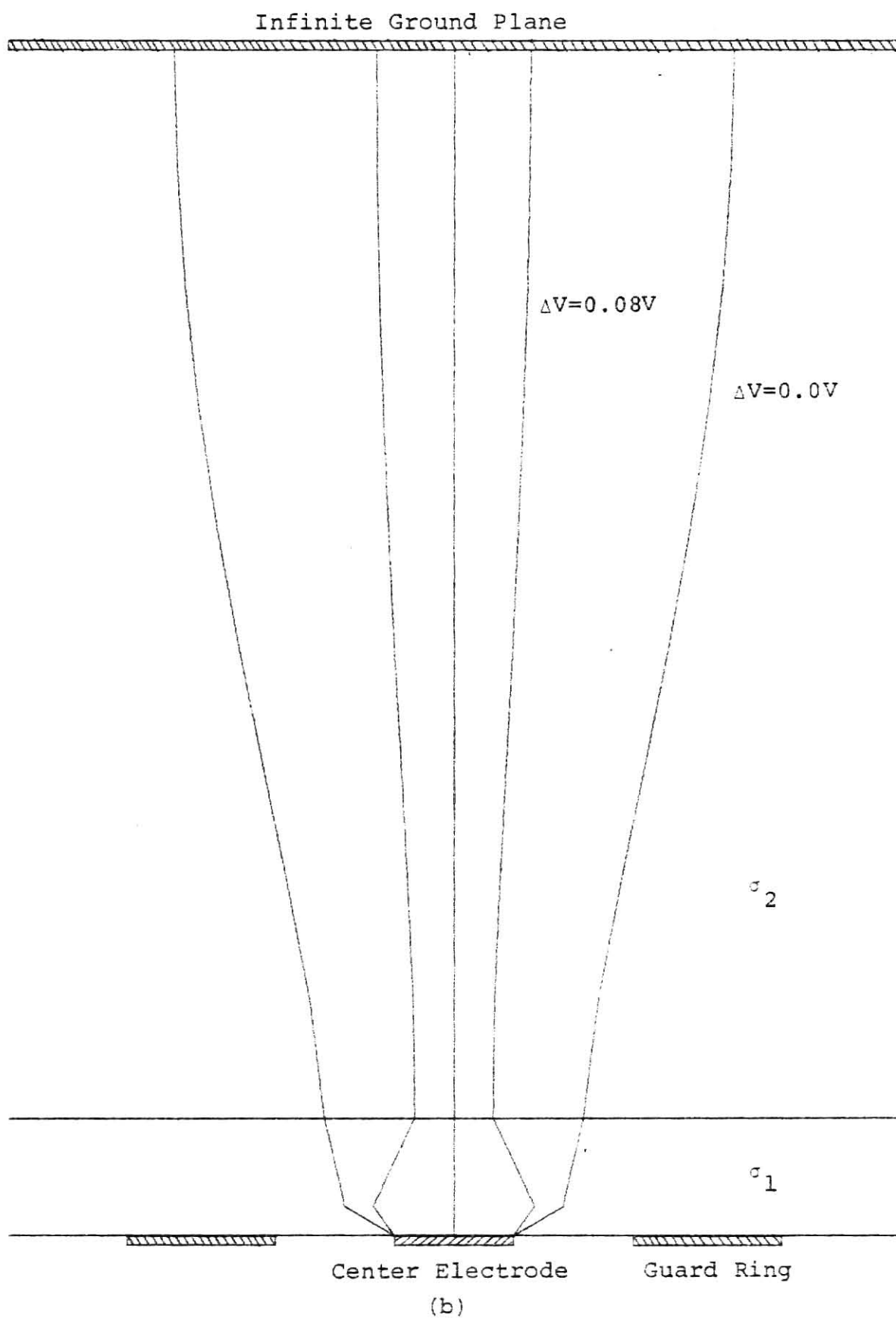
V_g Volts	$\Delta V = V_g - V_e$ Volts	Gain $= \dfrac{V_g}{V_e}$	Center electrode Current I_{eN} Amps ohm cm	Impedance $Z_N = \dfrac{V_e}{I_{eN}}$ cm^{-1}	Guard ring Current I_{gN} Amps ohm cm
1.00	0.00	1.00	0.280	3.572	8.372
1.02	0.02	1.02	0.155	6.448	8.664
1.04	0.04	1.04	0.030	33.150	8.956
1.06	0.06	1.06	-0.095	-ve	9.249

A plot of the center electrode current versus the difference in potential ΔV is shown in Fig. 6.2. It can be seen that pinch-off occurs at a value of guard ring potential that is smaller than that for any other case for the two-layer model. Figure 6.9a shows a plot of the unknown function $(A(x/2d))/x$ versus x. A plot of the current contours is shown in Fig. 6.9b. The focusing effect near the central electrode is quite pronounced and there isn't an undesirable spread near the ground plane. From the four cases for the two layer model it seems that the gap between the central electrode and the guard ring affects the focusing in planes close to the central electrode where as the width of the guard ring affects the focusing near the ground plane. From all the cases discussed this far the Two-Layer: Case 4 seems to show the best channeling of the central impedance

(a)
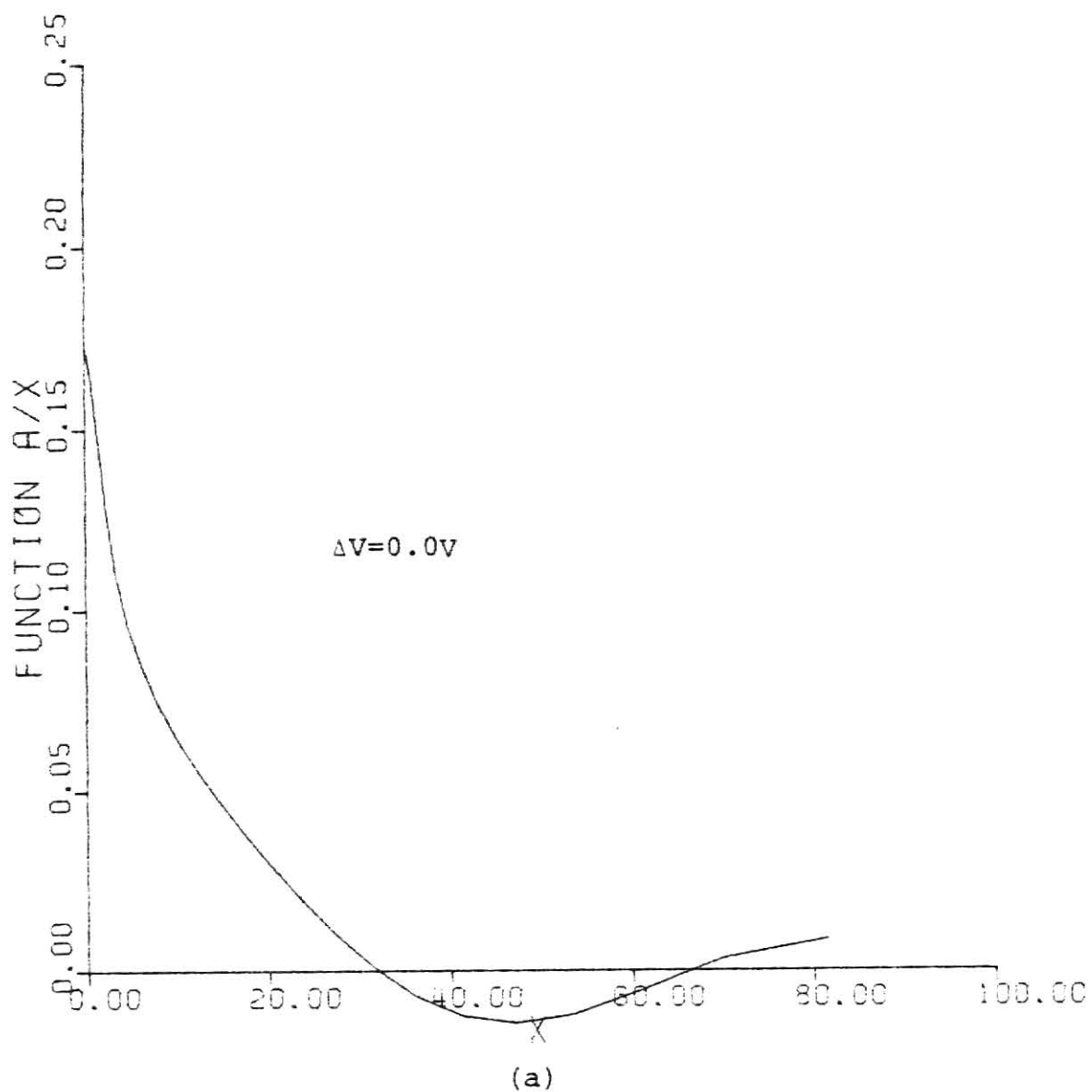
Plot of A(x/2d) versus x.

Figure 6.9.   Two-Layer: Case 4.

Infinite Ground Plane

ΔV=0.0V

ΔV=0.02V

ΔV=0.04V

σ_2

σ_1

Guard Ring

Center Electrode

(b)
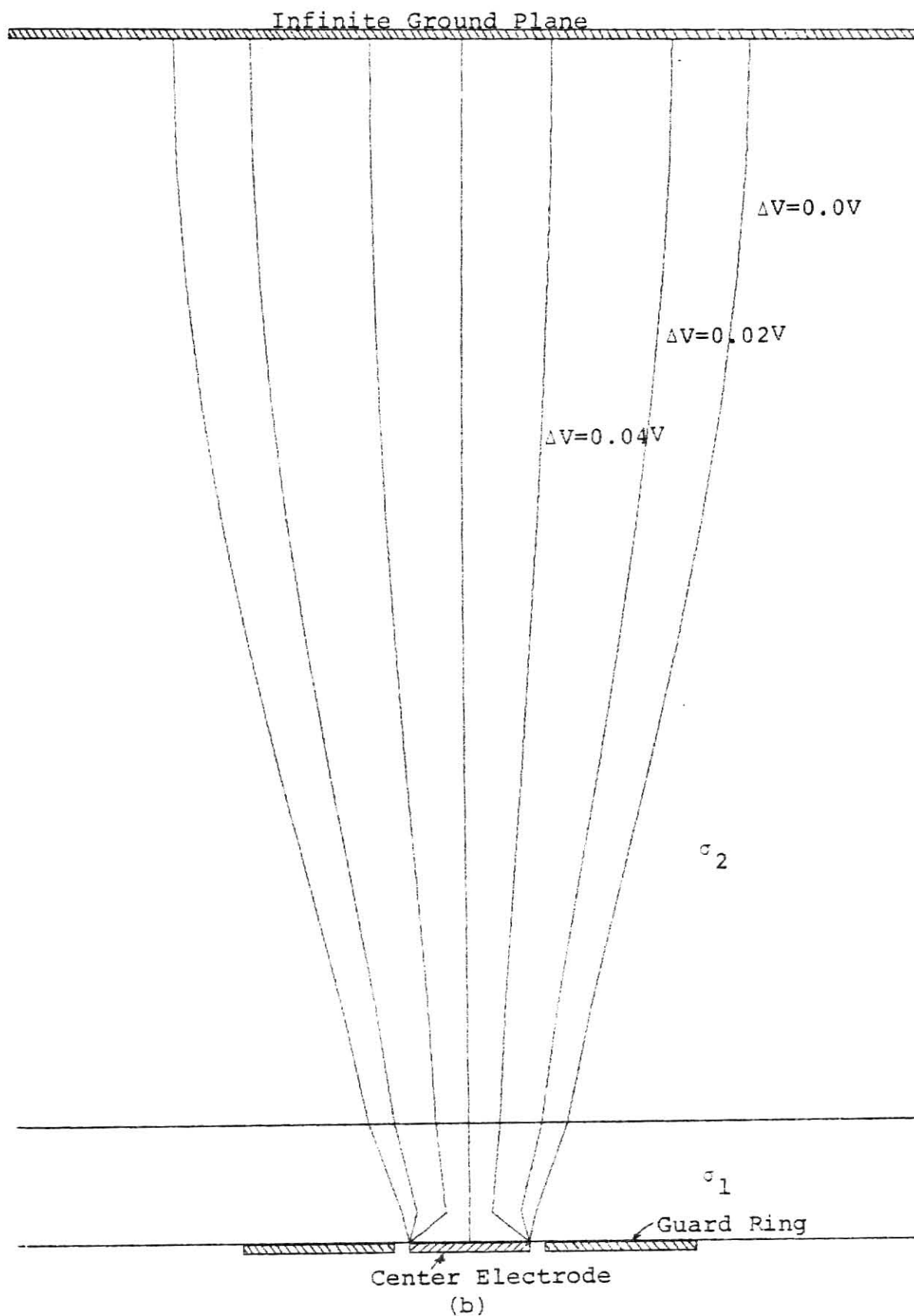
Constant Current Contours.

Figure 6.9. Two-Layer: Case 4.

measuring electrode current so that the measurement of impedance is restricted to only a central core. However, some practical difficulties might be encountered.

6.6 Practical Aspects Associated with the Guard-Ring System

There are a few points to be discussed with respect to the practical feasibility of the guard ring technique. As the current is focused the impedance of its pathway increases. If the constant current impedance pneumograph is used this means that the potential on the center electrode that is sensed increases and the guard ring driven by the amplifier with the adjusted gain also has an increased potential. Depending on the value of the injected constant current and the impedance of the pathway, this sensed and amplified potential can drive the amplifiers to saturation. Cases with very low pinch-off potentials have a very small range over which the guard ring amplifier gain can be varied. The best way to focus the current is to vary the gain while observing the impedance signal. The gain ought to be set for the maximum achievable impedance signal. Concurrent experimental research on dogs at Kansas State University has confirmed the presence of the focusing effect as is shown in the tracings of Figs. 6.10. A constant current impedance pneumograph is being used in the experimental effort. The tracings with the larger impedance signals are those with gains (V_g/V_e) greater than unity.

A difficulty encountered in using a narrow gap between the center electrode and guard ring is application of the electrodes. Conductive gel has to be used to apply the guard ring and electrode and often the gel spreads out to form a conductive path between the electrode and the ring on the surface of the skin.
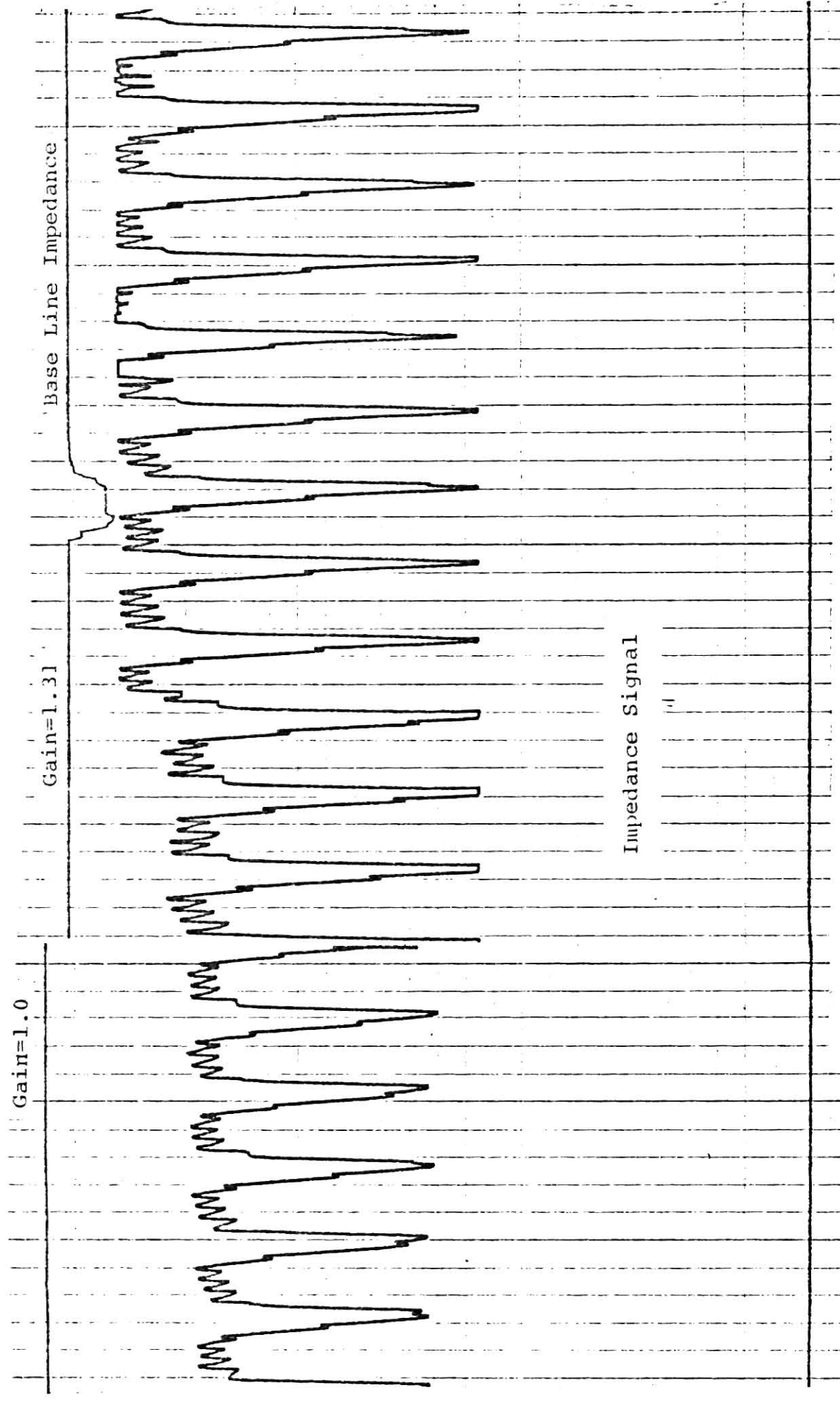
Figure 6.10. Focusing Effect of Increased Potential on Guard Ring.

The analysis carried out in this research effort pertains to a static system. During breathing the conductivity of the lung tissue is changing. This means that the current pathway does not remain the same during inspiration and expiration. As a result, the impedance signal observed will not pertain to a fixed narrow central core. A question that needs to be investigated is if the impedance signal can be fed back to increase the guard ring potential and thus increase focusing when the current spreads out due to a change in conductivity of the medium and vice versa.

This research effort has established a method for solving the encountered equations. Other models can be developed by including inhomogeneities in the media to represent other anatomical structures (e.g., heart and lungs). A bounded medium of cylindrical, hexagonal or trapezoidal shape could also be used to represent a more realistic model of the thorax instead of the semi-infinite model. There is in fact an endless number of models that could be developed; however, the mathematical complexity and required computer time to study more complicated models could be abominable.

VII.   BIBLIOGRAPHY

1. Cooley, W. L., The Parameters of Transthoracic Electrical Conduction, Annals New York Academy of Sciences, 1968-69, 702-712.

2. Cooley, W. L. and R. L. Longini, A New Design for an Impedance Pneumograph, Journal of Applied Physiology, 25(4), 1968, 429-432.

3. Schmalzel, J. L., R. R. Gallagher, and J. M. Barquest, An Impedance Pneumograph Utilizing Microprocessor-Based Instrumentation, Proceedings of the Fourteenth Annual Rocky Mountain Bioengineering Symposium, Vol. 13, April 1977, 63-68.

4. Abramowitz, M. and I. Stegun, Handbook of Mathematical Functions, Dover Publications, Inc., New York, 1965.

5. Kreyszig, E., Advanced Engineering Mathematics, 2nd Edition, John Wiley and Sons, Inc., New York, 1967.

6. Ramo, S., J. R. Whinnery and T. V. Duzer, Fields and Waves in Communication Electronics, John Wiley and Sons, Inc., New York, 1965.

7. Sneddon, I. N., Mixed Boundary Value Problems in Potential Theory, North-Holland, Amsterdam, 1966.

8. Kiyono, T. and M. Shimasaki, On a Generalized Problem of Disc Electrodes, II, Memoirs of the Faculty of Engineering, Kyoto Univ., Japan, 31, 1969, 548-563.

9. Cooke, J. C., The Solution of Triple and Quadruple Integral Equations and Fourier-Bessel Series, Quarterly Journal of Mechanics and Applied Mathematics, Vol. 25, Pt 2, 1972, 247-263.

10. Hochstadt, H., Integral Equations, John Wiley & Sons, Inc., New York, 1973.

11. Noble, B., Certain Dual Integral Equations, Journal of Mathematics and Physics, 37, 1958, 128-136.

12. Srivastav, R. P., Proceedings of the Edinburgh Mathematical Society (ii) 13, 1963a, 271.

13. Cooke, J. C., Triple Integral Equation, Quarterly Journal of Mechanics and Applied Mathematics, Vol. 16, p. 12, 1963, 193-203.

14. Watson, G. N., Theory of Bessel Functions, Cambridge, 1940.

15. Krylov, V. I., Approximate Calculation of Integrals, Macmillan, New York, 1962.

16. Stroud, A. H. and D. Secrest, Gaussian Quadrature Formulas, Prentice-Hall, Inc., New Jersey, 1966.

17. Geddes, L. A. and L. E. Baker, The Specific Resistance of Biological Material -- A Compendium of Data for the Biomedical Engineer and Physiologist, Medical and Biological Engineering, Vol. 5, 1967, 271-293.

VIII. APPENDICES

APPENDIX A

This treatment on the preliminaries of Integral Equations is taken from Sneddon [7] pgs. 40-42.

Many integral equations encountered are of the form

$$\int_a^x \frac{f(t)dt}{[h(x)-h(t)]^r} = g(x) \qquad (a < x < b) \tag{A.1}$$

where $0 < r < 1$ and $h(t)$ is a strictly monotonic increasing function in (a,b).

Consider the integral

$$\int_a^x \frac{h'(u)g(u)du}{[h(x)-h(u)]^{1-r}} . \tag{A.2}$$

Substituting (A.1) for $g(u)$ and interchanging the order of integration, the integral is equal to

$$\int_a^x f(t)dt \int_t^x \frac{h'(u)du}{[h(u)-h(t)]^r[h(x)-h(u)]^{1-r}} . \tag{A.3}$$

From standard tables the inner integral has the value $B(r,1-r)=\pi\cosec(\pi r)$ where B is the Incomplete Beta Function. Therefore

$$\int_a^x \frac{h'(u)g(u)du}{[h(x)-h(u)]^{1-r}} = \pi\cosec(\pi r) \int_a^x f(t)dt . \tag{A.4}$$

Differentiating (A.4) the solution of the integral equation (A.1) is

$$f(t) = \frac{\sin\pi r}{\pi} \frac{d}{dt} \int_a^t \frac{h'(u)g(u)du}{[h(t)-h(u)]^{1-r}} \qquad (a < t < b). \tag{A.5}$$

By a similar method it can be shown that the integral equation

$$\int_x^b \frac{f(t)dt}{[h(t)-h(x)]^r} = g(x) \qquad (a < x < b) \tag{A.6}$$

where $0 < r < 1$ and $h(t)$ is strictly monotonic increasing in (a,b), has

the solution

$$f(t) = -\frac{\sin\pi r}{\pi} \frac{d}{dt} \int_t^b \frac{h(u)g(u)du}{[h(u)-h(t)]^{1-r}} \qquad (a < t < b), \qquad (A.7)$$

Consider the particular case $h(u)=u^2$ and $r=1/2$. Substituting in (A.1)

and (A.5) the integral equation

$$\int_a^x \frac{f(t)dt}{(x^2-t^2)^{1/2}} = g(x) \qquad (a < x < b) \qquad (A.8)$$

has the solution

$$f(t) = \frac{2}{\pi} \frac{d}{dt} \int_a^t \frac{ug(u)du}{(t^2-u^2)^{1/2}} \qquad (a < t < b) . \qquad (A.9)$$

Substituting $h(u)=u^2$ and $r=1/2$ in (A.6) and (A.7) the integral equation

$$\int_x^b \frac{f(t)dt}{(t^2-x^2)^{1/2}} = g(x) \qquad (a < x < b) \qquad (A.10)$$

has the solution

$$f(t) = -\frac{2}{\pi} \frac{d}{dt} \int_t^b \frac{ug(u)du}{(u^2-t^2)^{1/2}} \qquad (a < t < b). \qquad (A.11)$$

APPENDIX B

Consider the integral

$$I = \frac{d}{ds} \int_b^s \frac{r \, dr}{(s^2-r^2)^{1/2}(r^2-t^2)^{1/2}} \, .$$

Let $r^2=u$, therefore $rdr=du/2$. Now

$$I = \frac{1}{2} \frac{d}{ds} \int_{b^2}^{s^2} \frac{du}{(-u^2+u(s^2+t^2)-s^2t^2)^{1/2}} \, .$$

From standard tables

$$I = \frac{1}{2} \frac{d}{ds} \left[-\sin^{-1}\left(\frac{-2u+s^2+t^2}{s^2-t^2}\right) \right]_{b^2}^{s^2}$$

$$= \frac{1}{2} \frac{d}{ds} \left[\sin^{-1}\left(\frac{-2b^2+s^2+t^2}{s^2-t^2}\right) \right]$$

$$= \frac{s(b^2-t^2)^{1/2}}{(s^2-t^2)(s^2-b^2)^{1/2}} \, . \tag{B.1}$$

Consider the integral

$$R = \int_b^c \frac{1}{(y^2-s^2)^{1/2}} \left[-\frac{2}{\pi} \frac{d}{dy} \int_y^c \frac{tG_3(t)dt}{(t^2-y^2)^{1/2}} \right] dy \, . \tag{B.2}$$

Let

$$\int_y^c \frac{tG_3(t)dt}{(t^2-y^2)^{1/2}} = P(y) \, .$$

Then

$$\frac{d}{dy} \int_y^c \frac{tG_3(t)dt}{(t^2-y^2)^{1/2}} = P'(y) \, . \tag{B.3}$$

Substituting in (B.2)

$$R = -\frac{2}{\pi} \int_b^c P'(y) \frac{dy}{(y^2-s^2)^{1/2}} \, .$$

On integrating by parts we have,

$$R = -\frac{2}{\pi} \left[\frac{P(y)}{(y^2-s^2)^{1/2}}\right]_b^c - \frac{2}{\pi} \int_b^c \frac{yP(y)dy}{(y^2-s^2)^{3/2}}$$

$$= -\frac{2}{\pi} \left[\frac{1}{(y^2-s^2)^{1/2}} \int_y^c \frac{tG_3(t)dt}{(t^2-y^2)^{1/2}}\right]_b^c - \frac{2}{\pi} \int_b^c \frac{ydy}{(y^2-s^2)^{3/2}} \int_y^c \frac{tG_3(t)dt}{(t^2-y^2)^{1/2}} \; .$$

Interchanging the order of integration for the second term

$$R = \frac{2}{\pi} \frac{1}{(b^2-s^2)^{1/2}} \int_b^c \frac{tG_3(t)dt}{(t^2-b^2)^{1/2}}$$

$$- \frac{2}{\pi} \int_b^c tG_3(t)dt \int_b^t \frac{ydy}{(y^2-s^2)^{3/2}(t^2-y^2)^{1/2}} \; . \qquad (B.4)$$

From standard tables

$$\int_b^t \frac{ydy}{(y^2-s^2)^{3/2}(t^2-y^2)^{1/2}} = \frac{(t^2-b^2)^{1/2}}{(t^2-s^2)(b^2-s^2)^{1/2}} \; . \qquad (B.5)$$

Substituting (B.5) into (B.4) we have,

$$R = \frac{2}{\pi} \frac{1}{(b^2-s^2)^{1/2}} \int_b^c \frac{tG_3(t)}{(t^2-b^2)^{1/2}} \left[1 - \frac{(t^2-b^2)}{t^2-s^2}\right]dt$$

$$= \frac{2}{\pi} \int_b^c \frac{t(b^2-s^2)^{1/2}G_3(t)dt}{(t^2-s^2)(t^2-b^2)^{1/2}} \; . \qquad (B.6)$$

Now consider the integral

$$J = \frac{d}{ds} \int_b^s \frac{rdr}{(s^2-r^2)^{1/2}} \int_0^b \frac{dt}{(r^2-t^2)^{1/2}} \int_b^c \frac{yg_3(y)dy}{(y^2-t^2)^{1/2}} \; . \qquad (B.7)$$

Changing the variable t to x,

$$J = \frac{d}{ds} \int_b^s \frac{rdr}{(s^2-r^2)^{1/2}} \int_0^b \frac{dx}{(r^2-x^2)^{1/2}} \int_b^c \frac{yg_3(y)dy}{(y^2-x^2)^{1/2}} \; . \qquad (B.8)$$

Using Eq. (3.35) and interchanging the order of differentiation and integration,

$$J = \int_0^b dx \cdot \frac{d}{ds} \int_b^s \frac{rdr}{(s^2-r^2)^{1/2}(r^2-x^2)^{1/2}} \cdot \int_b^c \frac{dy}{(y^2-x^2)^{1/2}} \left[-\frac{2}{\pi} \frac{d}{dy} \int_y^c \frac{tG_3(t)dt}{(t^2-y^2)^{1/2}}\right] \cdot$$

$$(B.9)$$

By Eqs. (B.1) and (B.6), Eq. (B.9) becomes

$$J = \int_0^b \frac{s(b^2-x^2)^{1/2} dx}{(s^2-x^2)(s^2-b^2)^{1/2}} \cdot \frac{2}{\pi} \int_b^c \frac{t(b^2-x^2)^{1/2} G_3(t)dt}{(t^2-x^2)(t^2-b^2)^{1/2}}$$

$$= \frac{2}{\pi} \int_b^c G_3(t)dt \frac{ts}{(t^2-b^2)^{1/2}(s^2-b^2)^{1/2}} \int_0^b \frac{b^2-x^2}{(t^2-x^2)(s^2-x^2)} dx \cdot \qquad (B.10)$$

APPENDIX C

Consider the integral

$$L = \int_b^t \frac{y J_0(yu) dy}{(t^2 - y^2)^{1/2}} \, . \tag{C.1}$$

Let
$$p = J_0(yu) \qquad\qquad dq = \frac{ydy}{(t^2-y^2)^{1/2}}$$

$$dp = -u J_1(yu) dy \qquad\qquad q = -(t^2-y^2)^{1/2} \, .$$

Integrating (C.1) by parts

$$L = -(t^2-y^2)^{1/2} J_0(yu) \Big]_b^t - u\int_b^t J_1(yu) \, (t^2-y^2)^{1/2} dy$$

$$= (t^2-b^2)^{1/2} J_0(yu) - u\int_b^t J_1(yu)(t^2-y^2)^{1/2} dy \, . \tag{C.2}$$

Now
$$I(t,u,b) = \frac{d}{dt} \int_b^t \frac{y J_0(yu) dy}{(t^2-y^2)^{1/2}} \, .$$

$$\therefore \quad I(t,u,b) = \frac{dL}{dt} = \frac{t}{(t^2-b^2)^{1/2}} J_0(bu) - u \int_b^t J_1(yu) \, \frac{tdy}{(t^2-y^2)^{1/2}} \, . \tag{C.3}$$

Now
$$F(\theta,u) = \sin\theta \, I(b\sec\theta,u,b) \, .$$

Let
$$t = b\sec\theta \quad \text{in Eq. (C.3).}$$

$$\therefore \quad F(\theta,u) = J_0(bu) - \sin\theta \, u \int_b^{b\sec\theta} J_1(yu) \, \frac{b\sec\theta dy}{(b^2\sec^2\theta - y^2)^{1/2}} \, . \tag{C.4}$$

Now let $y = b\sec\theta\cos\emptyset$, with a new variable $\emptyset$ defined.

Then $dy = -b\sec\theta\sin\emptyset d\emptyset$.

Substituting in Eq. (C.4)

$$F(\theta,u) = J_0(bu) + \sin\theta \, u \int_\theta^0 J_1(bu \, \sec\theta\cos\emptyset) b\sec\theta d\emptyset$$

$$= J_0(bu) - bu \tan\theta \int_0^\theta J_1(bu \, \sec\theta\cos\emptyset) d\emptyset \, . \tag{C.5}$$

```
C      ***********************************************************
C      *                                                         *
C      *   COMPUTER PROGRAM TO SOLVE THE PAIR OF FREDHOLM         *
C      *   INTEGRAL EQUATIONS SET UP AS A SET OF 35 SIMULTANEOUS  *
C      *   EQUATIONS  FX=CNST                                     *
C      *                                                         *
C      ***********************************************************

       DIMENSION F(35,35),CNST(35),XL(20),AL(20),SL(20),DU(24),
      1T13(20,15),THETA(15),CL(15),T33(15,15),XG(24),BESO(24),
      2BL(15),YL(15),AU(30),CURR(12,11,25),R1(23),Z(11),
      3COEF(35,35),VG(12),ECUR(12),F1(15,24),X1(24),R(24),DL(24),
      4IBUF(8000)

C         OPEN PLOT LIBRARY AND FIX ORIGIN

       CALL PLOTS(IBUF,8000)
       CALL PLOT(0.0,-11.0,3)
       CALL PLOT(2.25,-7.5,-3)
   10 FORMAT ('0',I4)
   20 FORMAT (1F10.5)
   25 FORMAT (I4)
   30 FORMAT (1E13.7)
   40 FORMAT (1E14.7)
   50 FORMAT (5E15.5)

C         READ VALUES OF CENTER ELECTRODE RADIUS A, INNER
C         RADIUS OF GUARD-RING B, OUTER RADIUS C, TOTAL
C         THICKNESS D,NUMBER OF LAYERS LAYR, THICKNESS OF
C         LAYER 1 FOR 2-LAYER CASE D1, CENTER ELECTRODE
C         VOLTAGE VE, GUARD-RING VOLTAGE VG,CONDUCTIVITY RATIO
C         CON (CON=1. FOR 1 LAYER), RADII R1 AND PLANES Z=Z

       READ 25,LAYR
       READ 20,A,B,C,D,D1,VE,CON
       READ 20,(VG(I),I=1,12)
       READ 20,(R1(I),I=1,23)
       READ 20,(Z(I),I=1,11)
       PHI=ARCOS(B/C)
       PI=4.*ATAN(1.)

C         READ VALUES OF NODES XL,YL,XG AND WEIGHTS AL,BL,DL
C         OF THE 20-POINT AND 15-POINT LEGENDRE-GAUSS FORMULAE
C         AND THE 24-POINT LAGUERRE-GAUSS FORMULA RESPECTIVELY

       READ 40,(XL(I),I=1,20)
       READ 30,(AL(I),I=1,20)
       READ 30,(YL(I),I=1,15)
       READ 30,(BL(I),I=1,15)
       READ 30,(XG(I),I=1,24)
       READ 30,(DL(I),I=1,24)

C         OBTAIN NODES SL TRANSFORMED FROM THE (-1,+1) TO THE
C         (0,A) INTERVAL AND NODES THETA AND WEIGHTS CL
C         TRANSFORMED FROM THE (-1,+1) TO THE (0,PHI) INTERVAL

       DO 60 I=1,20
   60 SL(I)=A*(1.+XL(I))/2.
```

```
      DO 70 I=1,15
      THETA(I)=PHI*(1.+YL(I))/2.
   70 CL(I)=PHI*BL(I)/2.

C         OBTAIN BESSEL FUNCTIONS TO COMPUTE THE FUNCTION F
C         AND COMPUTE FUNCTION H(U) DENOTED BY R HERE

      DO 100 I=1,24
      X1(I)=(B*XG(I))/(2.*D)
      IF (LAYR.EQ.2) GO TO 80
      R(I)=-1./(D*(1.+EXP(-XG(I))))
      GO TO 90
   80 R(I)=((1.-CON)*EXP(XG(I)-XG(I)*D1/D)-(1.+CON))/(D*((1.+CON)
     1+(CON-1.)*EXP(-XG(I)*D1/D)+(CON-1.)*EXP(-XG(I)+XG(I)*D1/D)
     2+(1.+CON)*EXP(-XG(I))))
   90 IF (ABS(X1(I)).LE.3.) GO TO 95
      CALL BEL0(X1(I),BES0(I))
      GO TO 100
   95 CALL BEL3(X1(I),BES0(I))
  100 CONTINUE

C         LOOP TO COMPUTE FIRST 20 ROWS AND FIRST 20 COLUMNS
C         OF THE MATRIX F (THE KERNEL K11)

      DO 150 I=1,20
      S=SL(I)
      DO 120 J=1,20
      T=SL(J)
      Y=0
      DO 110 K=1,24
  110 Y=Y+R(K)*COS(S*X1(K)/B)*COS(T*X1(K)/B)*DL(K)
      Y=(2./PI)*Y
  120 F(I,J)=Y*AL(J)*A/2.
  150 F(I,I)=1.+F(I,I)
  155 FORMAT ('0',10E13.5/' ',10E13.5/' ',4E13.5)

C         LOOP TO COMPUTE THE FUNCTION F DENOTED HERE AS F1

      DO 200 I=1,15
      P1=THETA(I)
      DO 200 J=1,24
      P2=X1(J)
      VAL=BES0(J)
      SUM=0
      DO 180 K=1,15
      ARG=(P2/COS(P1))*COS(P1*(1.+YL(K))/2.)
      IF (ABS(ARG).LE.3.) GO TO 170
      CALL BEL1(ARG,BES1)
      GO TO 180
  170 CALL BEL3(ARG,BES1)
  180 SUM=SUM+P1*(BL(K)/2.)*BES1
  200 F1(I,J)=VAL-P2*(TAN(P1))*SUM

C         LOOP FOR THE FIRST 20 ROWS AND COLUMNS 21 TO 35
C         OF THE F MATRIX

      DO 300 K=1,20
      S=SL(K)
      DO 300 I=1,15
      T1=0
```

```
      DO 250 J=1,24
  250 T1=T1+DL(J)*(2./PI)*R(J)*F1(I,J)*COS(S*X1(J)/B)
      T13(K,I)=((2./PI)*SQRT(B*B-S*S))/(((B*B)/(COS(THETA(I))
     1*COS(THETA(I)))-S*S))+T1
  300 F(K,I+20)=B*CL(I)*T13(K,I)

C          LOOP FOR ROWS 21 TO 35 AND FIRST 20 COLUMNS OF
C          THE F MATRIX

      DO 310 J=1,15
      DO 310 I=1,20
  310 F(J+20,I)=T13(I,J)*A*AL(I)/2.

C          LOOP FOR ROWS 21 TO 35 AND COLUMNS 21 TO 35 OF MATRIX F

      DO 400 I=1,15
      VAL1=THETA(I)
      DO 400 J=1,15
      VAL2=THETA(J)
      T2=0
      DO 320 K=1,24
  320 T2=T2+(2./PI)*B*DL(K)*R(K)*F1(I,K)*F1(J,K)
      IF (I.EQ.J) GO TO 330
      T33(I,J)=(4./(PI*PI))*(SIN(VAL2)*TAN(VAL2)*ALOG(TAN(VAL2/2.)
     1)-SIN(VAL1)*TAN(VAL1)*ALOG(TAN(VAL1/2.)))/((1./(COS(VAL1)
     2*COS(VAL1)))-(1./(COS(VAL2)*COS(VAL2))))+T2
      F(I+20,J+20)=CL(J)*T33(I,J)
      GO TO 400
  330 T33(I,J)=(-4./(PI*PI))*(1.-0.5*SIN(VAL1)*SIN(VAL1))
     1*(COS(VAL1)*ALOG(TAN(VAL1/2.)))-(2./(PI*PI))*COS(VAL1)
     2*COS(VAL1)+T2
      F(I+20,J+20)=CL(J)*T33(I,J)+SIN(VAL1)*COS(VAL1)*COS(VAL1)
  400 CONTINUE

C          LOOP TO SOLVE THE 35 SIMULTANEOUS EQUATIONS FOR
C          THE DIFFERENT VALUES OF VG

      DO 700 L=1,12
      M=L
      PRINT 10,L
      DO 410 I=1,20
  410 CNST(I)=VE
      DO 420 I=21,35
  420 CNST(I)=VG(L)
      DO 430 I=1,35
      DO 430 J=1,35
  430 COEF(I,J)=F(I,J)
      CALL GELG(CNST,COEF,35,1,0.001,IER)
      IF (IER.NE.0) GO TO 820
  440 FORMAT ('0',10E13.5/' ',10E13.5/' ',10E13.5/' ',5E13.5)
  450 FORMAT ('0',E20.10)

C          THE SOLUTION OF THE 35 SIMULTANEOUS EQUATIONS IS
C          RETURNED IN THE CNST MATRIX

      PRINT 440,(CNST(I),I=1,35)

C          LOOP TO CALCULATE THE CENTER ELECTRODE CURRENT ECUR

      SUM=0
```

```
          DO 460 I=1,20
    460 SUM=SUM+A*AL(I)*CNST(I)/2.
          ECUR(L)=4.*SUM
          PRINT 450,ECUR(L)

C          LOOP TO CALCULATE THE GUARD-RING CURRENT GCUR

          SUM1=C
          DO 470 I=1,15
    470 SUM1=SUM1+CL(I)*CNST(I+20)
          GCUR=4.*B*SUM1
          PRINT 450,GCUR
          RO=VE/ECUR(L)
          PRINT 450,RO

C          LOOPS TO CALCULATE THE UNKNOWN FUNCTIONS A(U)&D(U)

          DO 520 J=1,24
          SUM=0
          SUM1=0
          DO 480 I=1,20
          T=A*(1.+XL(I))/2.
    480 SUM=SUM+A*AL(I)*CNST(I)*(COS(T*X1(J)/B))/2.
          SUM=(2./PI)*SUM
          DO 490 I=1,15
    490 SUM1=SUM1+CL(I)*CNST(I+20)*F1(I,J)
          SUM1=(2.*B/PI)*SUM1
          IF (LAYR.EQ.2) GO TO 510
          AU(J)=(1./(2.*D))*(SUM+SUM1)
          GO TO 520
    510 DU(J)=(1./(2.*D))*(SUM+SUM1)
          UP=COSH(XG(J)/2.)
          ARG1=X1(J)*(D-D1)/B
          ARG2=D1*X1(J)/B
          DOWN=SINH(ARG1)*SINH(ARG2)+CON*COSH(ARG1)*COSH(ARG2)
          AU(J)=DU(J)*UP/DOWN
    520 CONTINUE
          PRINT 155,(AU(I),I=1,24)

C          LOOP TO CALCULATE THE CURRENT AT DIFFERENT RADII R1,
C          AT DIFFERENT PLANES Z=Z

          DO 600 J=1,11
          DO 590 I=1,23
          TOT=0
          DO 580 K=1,24
          IF (LAYR.EQ.2) GO TO 540
          UP=EXP(XG(K)-X1(K)*Z(J)/B)+EXP(X1(K)*Z(J)/B)
          GO TO 560
    540 IF (J.GT.1) GO TO 550
          UP=(1.-CON)*EXP(XG(K)+X1(K)*Z(J)/B-D1*XG(K)/D)
        1-(1.+CON)*EXP(XG(K)-X1(K)*Z(J)/B)
          UP=UP-(1.+CON)*EXP(X1(K)*Z(J)/B)+(1.-CON)*EXP(-X1(K)*Z(J)
        1/B+D1*XG(K)/D)
          GO TO 560
    550 UP=EXP(XG(K)-X1(K)*Z(J)/B)+EXP(X1(K)*Z(J)/B)
    560 DOWN=1.+EXP(-XG(K))
          ARG=X1(K)*R1(I)/B
          IF (ARG.LE.3.) GO TO 570
          CALL BEL1(ARG,BES)
```

```
      GO TO 580
570 CALL BE13(ARG,BES)
580 TOT=TOT+AU(K)*UP*BES*DL(K)/DOWN
      IF (LAYR.EQ.2) GO TO 582
      CURR(L,J,I)=2.*PI*R1(I)*TOT
      GO TO 590
582 IF (J.GT.1) GO TO 585
      CURR(L,J,I)=-PI*R1(I)*TOT
      GO TO 590
585 CURR(L,J,I)=CON*2.*PI*R1(I)*TOT
590 CONTINUE
      PRINT 155,(CURR(L,J,I),I=1,23)
      PUNCH 50,(CURR(L,J,I),I=1,23)
600 CONTINUE
      IF (ECUR(L).LT.0.) GO TO 710

C        PLOT OF THE FUNCTION A(U) VS U

      FIRSTV=0.0
      DELTAV=20.0
      CALL AXIS(0.0,0.0,'X',-1,5.0,0.0,FIRSTV,DELTAV)
      CALL SCALE(AU,5.0,24,1)
      FIRST=0.0
      DELTA=AU(26)
      CALL AXIS(0.0,0.0,'FUNCTION A/X',12,5.0,90.0,FIRST,DELTA)

C        XG(1) IS THE LARGEST NODE XG(24) IS THE SMALLEST ON
C        THE INFINITE INTERVAL

      YO=AU(24)/DELTA
      XO=XG(24)/DELTAV
      CALL PLOT(XO,YO,3)
      DO 640 I=1,24
      YO=AU(25-I)/DELTA
      XO=XG(25-I)/DELTAV
640 CALL PLOT(XO,YO,2)
      CALL PLOT(10.0,0.0,-3)
700 CONTINUE

C        PLOT THE CONSTANT CURRENT CONTOURS

710 CALL PLOT(10.0,-1.75,-3)
      CALL PLOT(-3.0,0.0,3)
      CALL PLOT(3.0,0.0,2)
      CALL PLOT(0.0,0.0,3)
      CALL PLOT(0.0,8.0,2)
      WIDTH=2.*A/2.5
      XO=A/2.5
      CALL RECT(-XO,-0.0625,0.0625,WIDTH,0.0,3)
      XO=C/2.5
      WIDE=(C-B)/2.5
      CALL RECT(-XO,-0.0625,0.0625,WIDE,0.0,3)
      XO=B/2.5
      CALL RECT(XO,-0.0625,0.0625,WIDE,0.0,3)
      CALL RECT(-3.0,8.0,0.0625,6.0,0.0,3)
      M1=M-1
      DO 808 L=1,M1
      XO=A/2.5
      CALL PLOT(XO,0.0,3)
      DO 800 I=1,11
```

```
      DO 790 J=1,23
      IF (CURR(L,I,J).GT.ECUR(L)) GO TO 720
      GO TO 790
  720 IF (J.EQ.1) GO TO 770
      XR=(CURR(L,I,J)-CURR(L,I,J-1))/(R1(J)-R1(J-1))
      XDIF=ECUR(L)-CURR(L,I,J-1)
      XO=XDIF/XR
      XLEN=R1(J-1)+XO
      XCORD=XLEN/2.5
      CNST(I)=-XCORD
      YORD=Z(I)/2.5
      GO TO 780
  770 XCORD=0.
      CNST(I)=-XCORD
      YORD=Z(I)/2.5
  780 CALL PLOT(XCORD,YORD,2)
      N1=I
      GO TO 800
  790 CONTINUE
  800 CONTINUE
      XO=A/2.5
      CALL PLOT(-XO,0.0,3)
      DO 805 I=1,N1
      YORD=Z(I)/2.5
  805 CALL PLOT(CNST(I),YORD,2)
  808 CONTINUE
      IF (LAYR.NE.2) GO TO 830
      YO=D1/2.5
      CALL PLOT(-3.0,YO,3)
      CALL PLOT(3.0,YO,2)
      GO TO 830
  810 FORMAT (' ',4HIER=,I4)
  820 PRINT 810,IER
  830 CALL PLOT(0.0,0.0,999)
      STOP
      END


C     *************************************************************
C     *                                                           *
C     *   SUBROUTINE TO COMPUTE THE ZERO ORDER BESSEL             *
C     *   FUNCTION JO(X) FOR (X.LE.3.)                            *
C     *                                                           *
C     *************************************************************

      SUBROUTINE BEL3(X,BESO)
      A=X/3.
      BESO=1.-2.2499997*A*A+1.2656208*(A**4.)-.3163866*(A**6.)
      BESO=BESO+.0444479*(A**8.)-.003944*(A**10.)+.0002100*(A**12.)
      RETURN
      END


C     *************************************************************
C     *                                                           *
C     *   SUBROUTINE TO COMPUTE THE ZERO ORDER BESSEL             *
C     *   FUNCTION JO(X) FOR (X.GT.3.)                            *
C     *                                                           *
C     *************************************************************

      SUBROUTINE BELJ(X,BESO)
      A=3./X
```

```
      FO=.79788456-(.77E-06)*A-(.552740E-02)*A*A-(.9512E-04)*A*A*A
      FO=FO+(.137237E-02)*(A**4.)-(.72305E-03)*(A**5.)
      FO=FO+(.14476E-03)*(A**6.)
      SO=X-.78539816-(.4166397E-01)*A-(.3954E-04)*A*A
      SO=SO+(.262573E-02)*A*A*A-(.54125E-03)*(A**4.)
      SO=SO-(.29333E-03)*(A**5.)+(.13558E-03)*(A**6.)
      BESO=FO*CCS(SO)/SQRT(X)
      RETURN
      END


C     ********************************************************************
C     *                                                                  *
C     *    SUBROUTINE TO COMPUTE THE FIRST ORDER BESSEL                   *
C     *    FUNCTION J1(X) FOR (X.LE.3.)                                   *
C     *                                                                  *
C     ********************************************************************

      SUBROUTINE BE13(X,BES1)
      A=X/3.
      BES1=.5-.56249985*A*A+.21093573*(A**4.)-(.3954289E-01)
     1*(A**6.)
      BES1=BES1+(.443319E-02)*(A**8.)-(.31761E-03)*(A**10.)
      BES1=BES1+(.1109E-04)*(A**12.)
      BES1=X*BES1
      RETURN
      END


C     ********************************************************************
C     *                                                                  *
C     *    SUBROUTINE TO COMPUTE THE FIRST ORDER BESSEL                   *
C     *    FUNCTION J1(X) (X.GT.3.)                                       *
C     *                                                                  *
C     ********************************************************************

      SUBROUTINE BEL1(X,BES1)
      A=3./X
      F1=.79788456+(.156E-05)*A+(.1659667E-01)*A*A+(.17105E-03)*A
     1*A*A
      F1=F1-(.249511E-02)*(A**4.)+(.113653E-02)*(A**5.)
      F1=F1-(.20033E-03)*(A**6.)
      S1=X-2.35619449+.12499612*A+(.5650E-04)*A*A-(.637879E-02)*A
     1*A*A
      S1=S1+(.74348E-03)*(A**4.)+(.79824E-03)*(A**5.)
      S1=S1-(.29166E-03)*(A**6.)
      BES1=F1*COS(S1)/SQRT(X)
      RETURN
      END
```

ACKNOWLEDGEMENTS

THEORETICAL ANALYSIS OF THE GUARD RING
TECHNIQUE IN IMPEDANCE PNEUMOGRAPHY

by

LIONEL J. D'LUNA

B. Tech, Indian Institute of Technology, Bombay, INDIA, 1973

———————————

AN ABSTRACT OF A MASTER'S THESIS

submitted in partial fulfillment of the

requirements for the degree

MASTER OF SCIENCE

Department of Electrical Engineering

KANSAS STATE UNIVERSITY
Manhattan, Kansas

1977

ABSTRACT

A simple modeling approach is investigated for the study of the guard ring electrode system in impedance pneumography. Initially the thorax is modeled as a semi-infinite layer with a guarded electrode on one surface and an infinite ground plane on the other. The field equations are formulated as quadruple integral equations. The solution of these equations defines the current pathways in the medium.

The model is then extended to a two-layered medium which represents the thoracic wall and the remaining thoracic tissue. The current pathways through the media are investigated for different designs of the specialized guard ring electrode system.